Epilepsie mehr als nur Anfälle

Moderne Bildgebungsverfahren ermöglichen uns einen Einblick in das Gehirn: Mittels Magnetresonanztomografie können wir nicht nur den äusseren Aufbau (die anatomische Struktur) darstellen, sondern auch Einblicke in den Aufbau von Netzwerk-Strukturen und die Zusammensetzung von Botenstoffen im Gehirn erhalten und damit Funktionsstörungen direkt untersuchen.

Die idiopathische Epilepsie ist eine der häufigsten chronischen neurologischen Erkrankungen des Hundes und betrifft schätzungsweise zwischen 0.6 -0.75 % aller Hunde. Bei einigen Rassen wie zum Beispiel beim Grossen Schweizer Sennenhund und beim Border Collie scheinen überdurchschnittlich viele Hunde betroffen zu sein. Nicht selten leiden diese Hunde auch an besonders schweren Formen der Epilepsie.

Idiopathische Epilepsie, was ist das?

Bei der idiopathischen Epilepsie kommt es zu spontanen, wiederkehrenden epileptischen Anfällen, die ohne äussere Einflüsse auftreten. Diese spontanen Anfälle stellen eine Art Fehlfunktion zwischen den hemmenden und den erregenden Einflüssen im Gehirn dar. Der derzeitige Goldstandard zur Diagnose der idiopathischen Epilepsie beinhaltend vornehmlich Untersuchungen, die dem Ausschluss von organischen Ursachen dienen. Dabei werden unter anderem auch **Magnetresonanztomografie (MRT)**-Bilder des Gehirns erstellt. Diese können zwar mit grosser Genauigkeit strukturelle Ursachen, wie Tumore, Entzündungen oder auch Missbildungen ausschliessen, aber sie geben keine Information über die Funktion des Gehirns.

Moderne Bildgebungsverfahren geben Einblick in die Hirnfunktion.

Einen solchen Rückschluss auf die Funktion des Gehirns erlauben modernere, fortschrittlichere Bildgebungsverfahren. Viele solcher Verfahren werden beim Menschen zur Erforschung aber auch zur Diagnose und Therapieanpassung bei Epilepsie bereits erfolgreich angewendet. Beim Hund sind diese Verfahren bisher weder etabliert noch eingesetzt worden.
Im Rahmen von dieser, von der Albert Heim Stiftung unterstützen, Studie konnten wir erfolgreich neue Bildgebungsverfahren beim Grossen Schweizer Sennhund und Border Collie mit Epilepsie anwenden und mit den Ergebnissen gesunder Hunde vergleichen. Zwei solcher Beispiele sind die funktionelle Magnetresonanztomographie (f-MRT) und die Magnetresonanz Spektroskopie:

Bei der Magnetresonanz Spektroskopie wird kein Bild, sondern eine Kurve, ein so genanntes Spektrum erzeugt. Mit Hilfe eines solchen Spektrums können Konzentrationen von bestimmten Stoffen, wie hemmenden oder erregenden Botenstoffen, aber auch von anderen Metaboliten gemessen werden. So kann man mittels Spektroskopie nicht nur einen Einblick in die Verteilung von hemmenden oder erregenden Botenstoffen erhalten, sondern auch Hinweise auf die Funktionsfähigkeit von Nervenzellen erhalten.

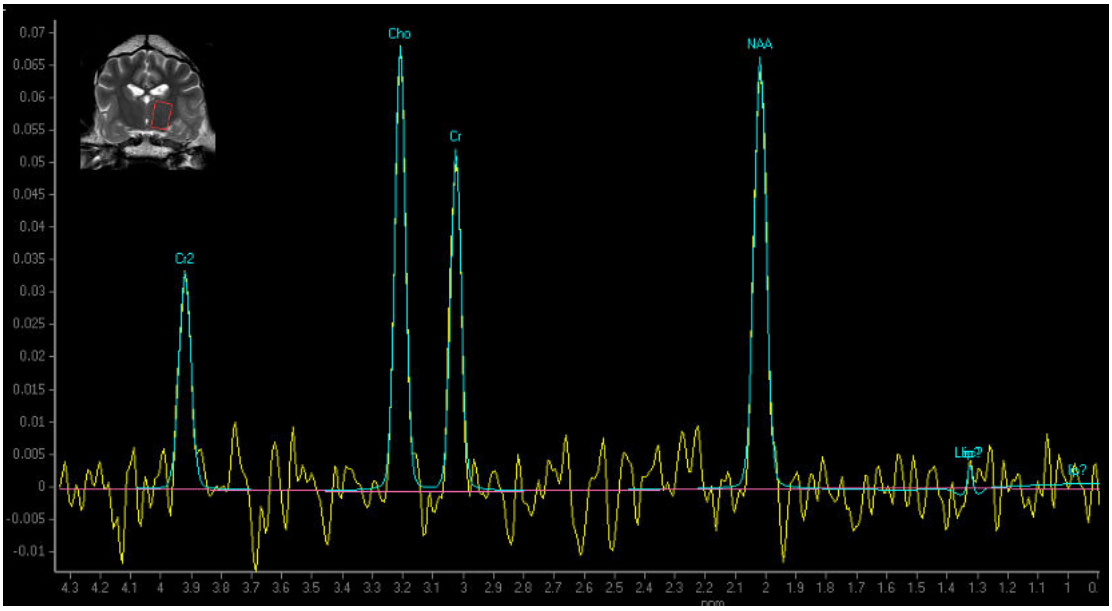

Die Abbildung zeigt ein Spektrum, das auf Höhe des Zwischenhirns gemessen wurde. Mittels dieses Spektrums können Rückschlüsse auf Konzentrationen von Metaboliten gezogen werden.

Unsere Studie hat gezeigt, dass die Konzentration des Metaboliten N-Acetylaspartat bei Hunden mit idiopathischer Epilepsie unter Therapie mit Antiepileptika deutlich geringer war als bei den gesunden Kontrollhunden. Dieser Metabolit wird als Marker für Nervenzellen angesehen. Eine verminderte Konzentration dieses Metaboliten im betroffenen Gehirnbereich, auch zwischen den epileptischen Anfällen, ist ein Hinweis auf eine reduzierte Funktion der Nervenzellen.

Funktionelle Magnetresonanztomographie (f-MRT) im Ruhezustand

Beim f-MRT im Ruhezustand handelt es sich um ein bildgebendes Verfahren bei dem Netzwerkstrukturen des Gehirns dargestellt werden können. Netzwerke bilden die Basis der Organisation im Gehirn und beruhen auf der Verknüpfung von verschiedenen Hirnarealen. Mittels f-MRT konnten beim Menschen neuronale Fehlverknüpfungen bei Epilepsie aber auch bei anderen Erkrankungen wie Depressionen, Angststörungen oder Demenz nachgewiesen werden.

Bei den Hunden mit idiopathischer Epilepsie in unsere Studie konnte eine solche Fehlverknüpfung im Bereich des so genannten Ruhenetzwerks («Default mode») dargestellt werden. Das Default-mode Netzwerk ist von besonderem Interesse, weil es in viele wichtige Prozesse wie Emotionen eingebunden ist.

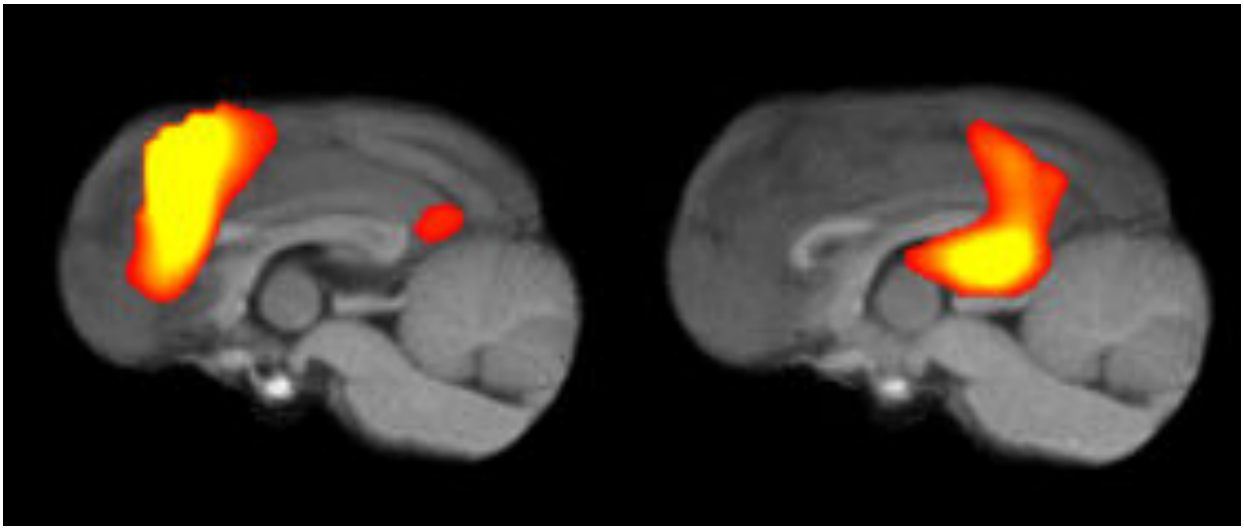

Die Abbildung zeigt 2 Netzwerke beim Hund, die den Bereichen des Default Mode Netzwerks beim Menschen entsprechen. Das linke Bild zeigt dabei den entsprechenden Bereich im vorderen Anteil und das rechte Bild das zum hinteren Anteil. Anders als beim Menschen sind diese Netzwerke beim Hund weniger stark verknüpft.

Eine solche Fehlverbindung könnte der Schlüssel auch zu sogenannten Begleiterkrankungen bei Epilepsie beim Hund sein. In den letzten Jahren haben verscheiden Studien gezeigt, dass zum Beispiel Angststörungen und Hyperaktivität bei Hunden mit Epilepsie gehäuft auftreten. Diese Begleiterkrankungen beeinträchtigen zusammen mit den Abbauprodukten und den Nebenwirkungen der Medikamente unter Umständen zusätzlich die Lebensqualität betroffener Hunde und deren Besitzer.

Zusammenfassung:

Moderne Bildgebungsverfahren, wie die f-MRT Untersuchung, geben uns einen Einblick in die Hirnfunktion bei Hunden mit Epilepsie. Dadurch stehen uns auch beim Hund neue Möglichkeiten zur Verfügung, um die idiopathische Epilepsie zu diagnostizieren, neue Therapieformen zu entwickeln und zu verstehen, warum bisherige Therapien nicht anschlagen. Die Resultate unserer Studie bestätigen, dass Epilepsie eine Gehirnerkrankung ist, die über die Anfälle hinaus geht. In Hinblick auf die Lebensqualität betroffener Hunde und deren Halter sollte unbedingt mögliche Begleiterkrankungen (Angststörungen, Hyperaktivität, o.ä.) geachtet werden.

Unser besonderer Dank gilt allen Hunden und deren Besitzern, die an der Studie teilgenommen haben, insbesondere dem Klub für Grosse Schweizer Sennenhunde und den Border Collie Clubs der Schweiz, ohne deren breite Unterstützung das Projekt nicht möglich gewesen wäre.

Albert-Heim-Stiftung
der Schweizerischen Kynologischen Gesellschaft

Abschlussbericht

„Erforschung von Hirnveränderungen bei Hunden mit idiopathischer Epilepsie mittels anatomischer und funktioneller Magnetresonanztomographie“

K. Beckmann, H. Richter, F. Steffen, M. Dennler, I. Carrera, P. Kircher

Gerne möchten wir Ihnen hiermit den Abschlussbericht zu unserem Projekt Erforschung von Hirnveränderungen bei Hunden mit idiopathischer Epilepsie vorlegen.

Im Anhang finden Sie auch unsere für Laien verständlichen deutschsprachige Zusammenfassung für die allfällige Veröffentlichung in einer Fachzeitschrift der Schweizerischen Kynologischen Gesellschaft SKG

Wir möchten uns für die Untersetzung und das Vertrauen der Albert-Heim Stiftung herzlichst bedanken. Dank der finanziellen Unterstützung konnten wir insgesamt neue Erkenntnisse zur funktionellen Bildgebung des Hundes und insbesondere zur Epilepsie des Hundes gewinnen. Unser Forschungsergebnis wurde in 4 Veröffentlichungen in verschieden interanationalen Fachzeitschriften veröffentlich und in 4 Vorträgen auf internationalen Kongressen vorgestellt. Eine kurze Zusammenfassung finden sie im nachfolgenden Abschnitt, alle Publikationen finden sie separat im Anhang.

Vorstudie:

1) Resting state networks of the canine brain under sevoflurane anaesthesia[1]

Zum ersten Mal konnten beim Hund so genannte resting state networks in Anästhesie dargestellt werden. Sie Ergebnisse zeigen eine weitgehende Übereinstimmung mit den wichtigsten Netzwerken beim Menschen und auch mit Netzwerken, die beim wachen Hund mit der gleichen Methode nachgewiesen wurden.

Die Resultate wurden auf dem 32.ECVN-Kongress in Wrocław im September 2019 vorgestellt (oral presentation).

Hauptstudie:

2) Increased resting state connectivity in the anterior default mode network of idiopathic epileptic dogs[2]

Bei der Analyse der „Resting State Networks“ epileptischer Hunde im Vergleich zu gesunden Kontrollen konnte eine erhöhte Konnektivität im Bereich des anterioren Default mode Netzwerks festgestellt werden. Das Default mode Netzwerk ist eines der wichtigsten resting state Networks und wurde als eines der ersten beim Hund nachgewiesen. In der Humanmedizin konnte abnormale Konnektivität im Bereich des

Default mode Netzwerks bei verschiedenen Erkrankungen wie zum Beispiel Epilepsie, Cognitive Dysfunktion aber auch Angststörungen gefunden werden. Dies ist das erste Mal, das „Resting State Networks“ bei Hirnerkrankungen beim Hund untersucht wurden und abnormale Befunde bei caninen idiopathischer Epilepsie eröffnet die die Möglichkeit diese nicht invasive Technik auch bei anderen Hirnerkrankungen einzusetzen. Weiter Untersuchungen müssen zeigen in der Tiermedizin möglicherweise auch als Biomarker eingesetzt werden.

Ergebnisse dieser Studie wurden auf dem 33. ECVN-Symposium vorgestellt.

3) **Single-Voxel Proton Magnetic Resonance Spectroscopy of the Thalamus in Idiopathic Epileptic Dogs and in Healthy Control Dogs[3]**

Wir konnten nun zeigen, dass Hunde unter Therapie mit Antiepileptika ein signifikant reduziertes Verhältnis von N-acethyl aspartat zu Kreatin und von Gutamat/Glutamin (GLX) zu Kreatin haben (Abbildung2). N-acethyl aspartat (NAA) gilt hierbei als Marker für Neuronen-Funktion. Bei Menschen wurden solche reduzierten N-acethyl aspartat Verhältnisse vor allem bei steigender Anzahl der Anfälle, bei therapieresitenten Epileptikern und nach langer Erkrankungsdauer festgestellt, Faktoren, die auch auf die Patienten in unserer Studie eingetroffen sind. Vermindertes Glutamat wird als frühes Zeichen von Neuro-Degeneration gesehen und ist auch beim Menschen mit kognitiver Dysfunktion unter Antiepileptika Therapie korreliert.

Ergebnisse dieser Studie wurden auf dem 33. ECVN-Symposium vorgestellt.

4) **Ketamine administration in idiopathic epileptic and healthy control dogs: Can we detect differences in brain metabolite response with spectroscopy?[4]**

Mittels MRS konnten wir, nach intravenöser Verabreichung von 1 mg/kg Ketamin bei Hunden Veränderungen im Metaboliten/Kreatin-Verhältnis nachzuweisen und diese Wirkung unterschied sich bei gesunden Hunden und solchen mit idiopathischer Epilepsie die unter Therapie waren mit Antiepileptika. Die Ergebnisse dieser Forschung legen nahe, dass die Wirkung von Ketamin auf die Gehirnmetaboliten von den Konzentrationen der Gehirnmetaboliten vor der Verabreichung abhängen könnte.

Sollten Sie weiter Fragen zu unserer Forschung haben, stehen wir selbstverständlich jeder Zeit zur Verfügung.

Vielen Dank für Ihre Unterstützung.

Katrin Beckmann, Dr. med. vet., Dipl. ECVN

K. Beckmann

1. Beckmann KM, Wang-Leandro A, Dennler M, Carrera I, Richter H, Bektas RN, Steiner A, Haller S: **Resting state networks of the canine brain under sevoflurane anaesthesia**. *PloS one* 2020, **15**(4):e0231955.
2. Beckmann KM, Wang-Leandro A, Richter H, Bektas RN, Steffen F, Dennler M, Carrera I, Haller S: **Increased resting state connectivity in the anterior default mode network of idiopathic epileptic dogs**. *Scientific reports* 2021, **11**(1):23854.
3. Mauri N, Richter H, Steffen F, Zölch N, Beckmann KM: **Single-Voxel Proton Magnetic Resonance Spectroscopy of the Thalamus in Idiopathic Epileptic Dogs and in Healthy Control Dogs**. *Frontiers in veterinary science* 2022, **9**.
4. Wieser M, Beckmann KM, Kutter APN, Mauri N, Richter H, Zölch N, Bektas RN: **Ketamine administration in idiopathic epileptic and healthy control dogs: Can we detect differences in brain metabolite response with spectroscopy?** *Frontiers in veterinary science* 2023, **9**.

PLOS ONE

RESEARCH ARTICLE

Resting state networks of the canine brain under sevoflurane anaesthesia

Katrin M. Beckmann[1☯]*, Adriano Wang-Leandro[2☯], Matthias Dennler[2], Ines Carrera[3], Henning Richter[2], Rima N. Bektas[4], Aline Steiner[4], Sven Haller[5,6]

1 Neurology Department, Clinic of Small Animal Surgery, Vetsuisse Faculty Zurich, Zurich, Switzerland, **2** Department of Diagnostics and Clinical Services, Clinic for Diagnostic Imaging, Vetsuisse-Faculty Zurich, Zurich, Switzerland, **3** Willows Veterinary Centre and Referral Service, Shirley, United Kingdom, **4** Department of Diagnostics and Clinical Services, Section of Anaesthesiology, Vetsuisse Faculty, University of Zurich, Zurich, Switzerland, **5** Department of Surgical Sciences, Radiology, Uppsala University, Uppsala, Sweden, **6** Faculty of Medicine of the University of Geneva, Geneva, Switzerland

☯ These authors contributed equally to this work.
* kbeckmann@vetclinics.uzh.ch

Citation: Beckmann KM, Wang-Leandro A, Dennler M, Carrera I, Richter H, Bektas RN, et al. (2020) Resting state networks of the canine brain under sevoflurane anaesthesia. PLoS ONE 15(4): e0231955. https://doi.org/10.1371/journal.pone.0231955

Editor: Xi Chen, McLean Hospital, UNITED STATES

Received: August 8, 2019

Accepted: April 5, 2020

Published: April 17, 2020

Data Availability Statement: All relevant data are within the paper and its Supporting Information files.

Funding: The study was partly supported by the "Albert-Heim-Stiftung" and the "Stiftung für Kleintiere der Vetsuisse-Fakultät Universität Zürich" to KMB. The funders had no role in study design, data collection and analysis, decision to publish, or preparation of the manuscript.

Competing interests: The authors have declared that no competing interests exist.

Abstract

Resting-state functional Magnetic Resonance Imaging (rs-fMRI) has become an established technique in humans and reliably determines several resting state networks (RSNs) simultaneously. Limited data exist about RSN in dogs. The aim of this study was to investigate the RSNs in 10 healthy beagle dogs using a 3 tesla MRI scanner and subsequently perform group-level independent component analysis (ICA) to identify functionally connected brain networks. Rs-fMRI sequences were performed under steady state sevoflurane inhalation anaesthesia. Anaesthetic depth was titrated to the minimum level needed for immobilisation and mechanical ventilation of the patient. This required a sevoflurane MAC between 0.8 to 1.2. Group-level ICA dimensionality of 20 components revealed distributed sensory, motor and higher-order networks in the dogs' brain. We identified in total 7 RSNs (default mode, primary and higher order visual, auditory, two putative motor-somatosensory and one putative somatosensory), which are common to other mammals including humans. Identified RSN are remarkably similar to those identified in awake dogs. This study proves the feasibility of rs-fMRI in anesthetized dogs and describes several RSNs, which may set the basis for investigating pathophysiological characteristics of various canine brain diseases.

Introduction

Spontaneous fluctuations in activity in different parts of the brain can be used to study functional brain networks [1]. Increased neuronal activity leads to increased energy consumption. This energy is produced locally from glucose and oxygen supplied by blood vessels, leading to an increased oxygen consumption [2]. Blood oxygenation level-dependent (BOLD) functional magnetic resonance imagining (fMRI) technique takes advantage of the fact that oxyhaemoglobin is diamagnetic, and de-oxyhaemoglobin is paramagnetic which leads to an increased

signal intensity in activated brain areas [3]. Resting-state fMRI (rs-fMRI) is based on spontaneous low frequency fluctuations (0.1 Hz) in the BOLD signal when the brain is at rest (not performing any specific task). Studying correlations between variations of the BOLD signal can identify anatomically distinct regions, which activate synchronously with each other, these regions are called "resting state networks" [4]. Resting state networks (RSN) have been identified in many species including rodents [5–7], ferrets [8], monkeys [9, 10] and humans [11, 12] and have been extensively used in cognitive neuroscience research [13].

BOLD task-fMRI has been used successfully to compare dogs' and humans' brain function under physiological [14] and pathological [15] conditions, but little is known about the rs-fMRI in dogs. To date two studies have been performed in healthy dogs. The first study identified one component of the RSN, the default mode network (DMN), in awake and anaesthetized dogs [16]. A very recent study found multiple, spatially distributed RSNs in awake dogs [17].

Increasing evidence from clinical rs-fMRI studies in humans has indicated that rs-fMRI may be a promising tool for investigating pathophysiological characteristics of RSNs associated with epilepsy and neurodegenerative diseases. Alterations in RSNs, correlating with the progression and severity of the diseases, can be found in the absence of structural lesions indicating the sensitivity of this method [18]. The role of the dog as an established large animal translational model has been increasingly recognized in multiple research fields of neuroscience including mental disorders [19, 20], aging [21] and naturally occurring neurological diseases such as epilepsy [22, 23]. Many questions are open regarding similarities and differences between these diseases in humans and dogs. Rs-fMRI, as a non-invasive method would allow investigation of alteration in the brain function of aging dogs or dogs suffering from epilepsy. It could be used to measure natural disease progression or response to new therapeutics, but it is necessary to collect a sufficient number of dogs to reflect variation within the population and to enable generalization of specific results from the examined dog. Previously published fMRI data from dogs are collected from small number of dogs. This is mainly because of the huge effort to train the dog for awake fMRI in order to get high quality data [19]. Idiopathic epilepsy for example is one of the most common chronic neurological diseases in dogs with an estimated prevalence of 0.6–0.75% in the general dog population [24, 25]. To take advantage of this considerably high number of dogs suffering from these diseases it is essential to find a more feasible approach than months of training for rs-fMRI. General anaesthesia is such an approach, especially because companion animals are routinely examined under anaesthesia for diagnostic purposes. From an animal welfare point of view this means data could be collected with minimal additional physical strain for the animals, but this requires the ability to reliably identify RSNs under routine general anaesthesia. It is well known that general aesthesia has an effect on detection of RSN [26–29]. And also, in human medicine awake rs-fMRI is preferred method, it has been suggested, that for those patients that cannot be scanned awake, rs-fMRI under general anaesthesia can add significant information [30–32]. For further investigations in dogs it is necessary to prove that RSNs can be detected under common aesthetic protocols in dogs.

The aim of this study was to investigate the RSNs in dogs using a standardized anaesthetic protocol. We hypothesize that not only the DMN, but also other higher order networks will be identified.

Material and methods

Animals

A total of 10 adult purpose-bred research Beagles were included in the study. Four dogs were females and six were males. All dogs were sexually intact. Age ranged from 2–6 years (mean

age 4.8 years). The bodyweight was between 9.6 and 18.6 kg (mean weight 15.22 kg). For inclusion, clinical and neurological examination as well as blood biochemical analysis and haematology had to be within reference limits. The study was approved by the Cantonal Veterinary Office of Zurich (animal license number ZH272/16).

Animal preparation

Dogs were pre-medicated with butorphanol (0.1–0.2mg/kg IM, depending on the temperament of the dog) prior to catheter placement. An IV catheter was placed in the cephalic vein using aseptic technique. Anaesthesia was induced with Propofol 1% (MCT Fresenius Kabi, Oberdorf, Switzerland) IV, given to effect. All dogs were oro-tracheally intubated following induction of anaesthesia. Anaesthesia was maintained with sevoflurane vaporized in oxygen and medical air. Vaporizer settings were adjusted depending on the depth of anaesthesia (0.8–1.2 mean alveolar concentration (MAC)). End tidal concentration of sevoflurane, heart rate (HR), respiratory rate (RR), non-invasive mean blood pressure, percutaneous arterial oxygen saturation (SpO2) and end tidal partial pressure of carbon dioxide (EtCO2) were monitored using medical monitor (DatexOhmeda) and recorded every 5 minutes. Normocapnia (EtCO2 between 35 and 38 mmHg) was maintained using a ventilator (tidal volume 10-15ml/kg). FiO2 was kept between 55–65%. Blood pressures were maintained stable within physiological values under general anaesthesia (Mean arterial blood pressure (MAP) $>$ 60mmHg) using RiAc infusion.

MAP under 60mmHg was treated first with fluid/RiAc challenges of 3ml/kg IV administered over 5–10 minutes. After 3 fluid challenges of RiAc, a dobutamine constant rate infusion (1-5mcg/kg/min) was started to maintain MAP over 60mmHg.

fMRI protocol

All MRI data were acquired with a 3 Tesla scanner (Philips Ingenia, Philips AG, Zurich, Switzerland) using a 16-channel receive-transmit head coil (dStream HeadSpine coil solution, Philips AG). For anatomical evaluation, a 3D T1-weighted (T1W; TR 13 ms; TE 6 ms; FOV 130 mm; slice thickness 0.6 mm; flip angle 8˚) sequence was acquired. After the anatomical scans were obtained, around 1 h after induction of anaesthesia, rs-fMRI scans were acquired in all dogs.

BOLD functional resting state scans were acquired with gradient-echo planar imaging (EPI) sequence using the following protocol: TR = 2.0 s; TE = 30 ms; field of view (FOV) = 236 mm; slice thickness = 3 mm; acquisition time of 12.07 minutes.

MR data pre-processing

DICOM images were converted to 4D NIFTI formatted-images using an open-source conversion software (dcm2nii, University of South Carolina, South Carolina, U.S). Further pre-processing was performed using the open source software FSL (FMRIB Software Library v6.0, Oxford, UK).

Orientation of the images was set according to neurological convention. T1W images were cropped in order to remove as much of the extra-calvarial structures such as skin and muscles, taking care of including all parts of the brain. In the next step the brain was extracted using automated method the brain extraction tool of FSL-BET [33] with parameters set at -f 0.15 and -g 0.

A study specific T1-template was created by registering all T1W images to the T1W image of one of the study dogs. In a second step the output images were averaged together using the FLIRT and fslmaths of the above mentioned software [34, 35] (S1 Fig).

For correction of motion artefacts and high pass temporal filtering with sigma = 50.0 s, fMRI data underwent intra-modal motion correction (MCFLIRT [34]): the time series are in its entirety loaded and the middle volume represents the initial template image. A course 8-mm search for the motion parameters is then carried out using the cost function specified followed by two subsequent searches at 4 mm using increasingly tighter tolerances. All optimisations use tri-linear interpolation. In the second phase, an identity transformation is assumed between the middle volume and the adjacent volume. The transformation found in this first search is then used as the estimate for the transformation between the middle volume and the volume beyond the adjacent one [34]. Full width at half-maximum (FWHM) spatial smoothing was applied at the default 5mm [34]. FSL-BET tool was applied for brain extraction with parameters set at -f 0.35 and -g 0. Afterwards, registration of individual fMRI data was performed to the matching main structural image of this dog (3D-T1W sequence) and to a standard space (anatomical T1W template) using a linear approach with 12 degrees of freedom. The resampling resolution was set at 2mm (Fig 1).

Independent component analysis

RSNs were generated by means of a multivariate data-driven ICA approach. As data quality control, different output independent components were initially assessed: 17, 20, 25 and 30. Individual ICs were visually compared and 20 components were selected by consensus of three authors (K.B, A.W-L, and S.H).

Criteria for selection of RSNs in the different components were the following: consisted of relatively large continuous regions of increased BOLD signal, 2) were largely bilateral and/or 3) could be referred to anatomical landmarks comparable to well-known structures in existing literature of dogs [14–16, 36–39].

For identification of brain regions within gICA connectivity maps were thresholded with red-yellow color encoding using a 3.5< Z-score, main foci were defined as regions that exhibited high BOLD signal (labelled in yellow) and satisfied the above criteria.

For statistical analysis, one sample t-test after dual regression analysis of the data was performed. Specifically, a set of spatial maps from the group-average analysis was used to generate subject-specific versions of the spatial maps, and associated time series, using dual regression [40]. First, for each subject, the group-average set of spatial maps is regressed (as spatial regressors in a multiple regression) into the subject's 4D space-time dataset. This results in a set of subject-specific time series, one per group-level spatial map. Afterwards, those time series are regressed (as temporal regressors, again in a multiple regression) into the same 4D dataset, resulting in a set of subject-specific spatial maps, one per group-level spatial map. Finally, one sample t-test was performed using FSL's randomize permutation-testing tool [41]. Clusters of increased BOLD signal within the RSNs were confirmed using a significance level of $p<0.05$.

Results

Image acquisition and pre-processing

Anaesthesia was uneventful in all dogs. Mean deviation time series of six affine parameters (three translations and three rotations) were plotted to check whether there was significant head movement during the functional scan.

HR varied during rs-fMRI between 78-150/min (median HR: 98/min; mean HR: 105/min. RR varied during rs-fMRI between 10-21/min (median RR: 15/min, mean RR: 15/min)

The motion was minimal in all dogs during the scan with a mean relative displacement of 0.05 mm (0.04–0.08mm) and a mean absolute displacement of 0.06 mm (0.03–0.09 mm; Fig 1).

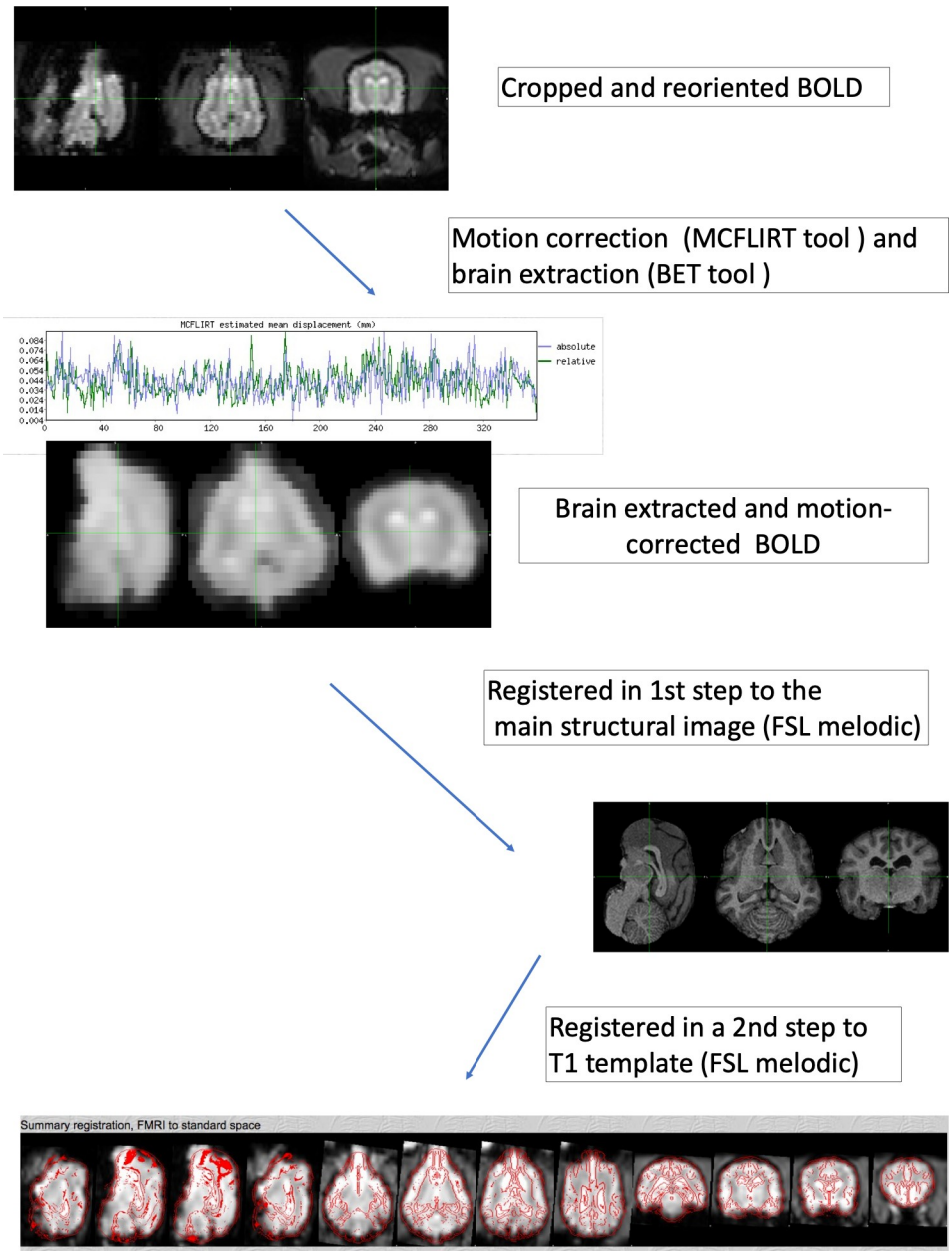

Fig 1. Schematic representation of the pre-processing of fMRI data. The first two steps (converting DICOM to NIFTI-files, reorienting and cropping are identical to the pre-processing of the anatomical images and not shown in this figure).

https://doi.org/10.1371/journal.pone.0231955.g001

Identification of RSN

We used ICA to derive RSNs in the dogs' brain. The components or putative networks were visually inspected and those not meeting the established inclusion criteria (n = 12) were excluded and the remaining components (n = 8) were further evaluated. Excluded components are shown in the S2 Fig. Excluded components were either localised completely (#1 & #2) or partially outside the brain (#3) or were clearly not overlaying grey matter (#4–12) and therefore originate most likely from non-neural physiological fluctuation [12].

The remaining components were topological consistent with 7 RSNs observed in other species and included auditory(3), primary visual(4) higher order visual(2), DMN; 1a [anterior] & 1b [posterior], motor/somatosensory(6 and 7), and somatosensory(5) (Fig 2).

1a anterior DMN 1b posterior DMN, 2 higher order visual, 3 auditory, 4 primary visual, 5 somatosensory, 6 & 7 sensory-motor.

The main foci of each of functional (bolded) and anatomical structures are listed as follows:

We labelled the network 1a as **anterior DMN** as it was composed of main foci in medial prefrontal cortex. Additionally, network 1b was deemed **posterior DMN** as it composed of main foci in posterior parietal cortex and posterior cingulate cortex.

Main connectivity foci of the **auditory (network 3)** included peri-sylvian regions, including the Sylvian gyri along the Sylvian and the ecto-sylvian gyri along the ecto-sylvian sulcus and extending dorsally to the supra-sylvian sulcus.

The **primary visual (network 4)** included the primary visual cortex [42]: posterior, midline structure adjacent to the inter-hemispheric fissure. A second, **higher order visual (network 2)** was identified within the more laterally located in the caudal ecto-marginal and supra-sylvian areas.

Three further networks were identified in the parietal cortex: one putative **motor/somatosensory (network 7)** includes the pre- and post-cruciate gyrus, the rostral supra-sylvian gyrus, the rostral endo-marginal gyrus, rostral marginal, the rostral ecto-sylvian gyrus and the middle cingulate gyrus. The second putative **motor/somatosensory** network includes only the pre- and post-cruciate gyrus adjacent to the inter-hemispheric fissure and the rostral endo-marginal, marginal and ecto-marginal gyrus. A third putative **somatosensory** network only includes the rostral splenial gyrus, parts of the marginal and ecto-marginal gyrus.

One sample t-test maps of the identified RSNs, thresholded at $P<0.05$ are shown in S3 Fig.

Discussion

This study proves the feasibility of rs-fMRI in anesthetized healthy beagle dogs and documents several brain RSNs, such as DMN, primary and higher order visual, auditory, somatosensory and sensory-motor.

In the past fMRI in dogs has been used mainly in specifically trained awake, healthy dogs to investigate aspects of canine cognition [43]. This approach requires months of training for each dog and is not feasible in a clinical setting. A further possible disadvantage of scanning dogs awake is movement during scanning and less motion was found in anaesthetised dogs compared to well-trained awake dogs in one study [16]. Performing fMRI under general anaesthesia therefore has clear benefits in dogs, but the influence of anaesthesia must be considered when interpreting the data. Before implementing rs-fMRI in a clinical setting, the presence of not only DMN, but also other networks has to be proven and reliably recognised under standardised anaesthesia regime, including standardised patient monitoring as it is routinely used for our daily clinical patients. Based on knowledge from literature, the standardised anaesthesia protocol was adjusted to minimise influence on the fMRI signal [44].

FMRI sequences were performed after the standard anatomical sequences, approximately one hour after induction of anaesthesia, allowing steady-state sevoflurane inhalation anaesthesia and minimising the influence of the medication used for induction. Anaesthetic depth was titrated to the minimum level needed for immobilisation and mechanical ventilation of the patient. This required a sevoflurane MAC between 0.8 to 1.2. The influence of anaesthesia on RSN has been investigate in humans [26], monkeys [27] and in rodents [28]. Not all networks are equally affected by anaesthetic agents. Higher-order networks linked to cognition are more severely affected than lower-order, such as basic sensorimotor networks [28]. Every

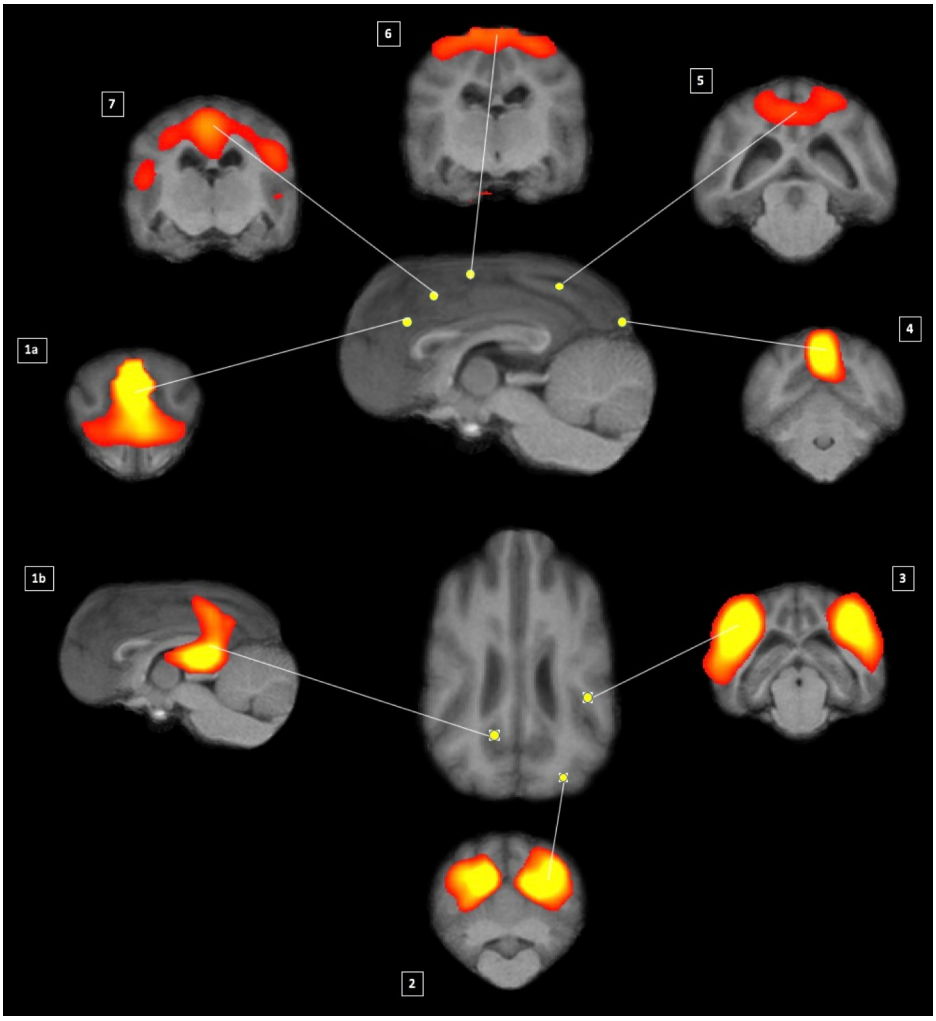

Fig 2. Maps of healthy beagle dog obtained by means of group independent component analysis and registered on T1 group-specific template with red-yellow color encoding using a 3.5< Z-score threshold: 1a and 2–7 transverse and 1b sagittal. Centre of the networks shown in the sagittal and dorsal view in the middle.

https://doi.org/10.1371/journal.pone.0231955.g002

anaesthetic drug uniquely modulates resting state connectivity [28]. Sevoflurane for example is associated with selectively reduced functional connectivity within cortical networks associated with consciousness [29]. Little is known about the influence of anaesthesia on RSN in dogs. The only study investigating the DMN in dogs found no significant differences DMN in dogs anaesthetised with Ketamine/Xylazine and awake dogs [16], but significantly greater connectivity of the posterior cingulate seed with voxels in the posterior regions of the brain was found in anaesthetised compared to awake dogs [16]. Therefore, comparing results from anaesthetised animals with those of awake ones bears the risk of anaesthesia related confounders. All these findings highlight the need of performing highly standardised and uniform studies either awake or under the same anaesthetic conditions, which enables to compare results between different groups. It is beyond the scope of this paper to discuss the best anaesthetic protocol for performing rs-fMRI. We have consequently used a standard protocol for this study, which is also applied for routine MRI examinations of clinical patients. This enables further investigation of RSN alterations in different canine diseases such as idiopathic epilepsy, cognitive dysfunction and behavioural diseases in the future. General anaesthesia was necessary for this

study as clinical conditions do not allow training patients for awake and unrestrained fMRI examination.

The influence of changes in partial pressure of carbon dioxide and partial pressure of oxygen levels under sevoflurane anaesthesia on the fMRI signal has been shown in dogs [45]. To limit these influence EtCO2 was kept in physiological range between 35–38 mm/Hg and FiO2 between 55–65%.

Blood pressure was maintained within a physiological range in all patients as well as sudden changes were avoided to preclude influence of blood-pressure changes on fMRI signal [46].

Due to the ability of acquiring data from animals and humans in the same manner, rs-fMRI has emerged as a translational method for bridging experimental animal and human studies. In conjunction with data-driven gICA analysis, rs-fMRI has proven to be a robust approach to identify and characterise similar brain networks across species [5, 8, 9, 16, 47, 48].

Little is known about RSNs in dogs and for this reason a data driven approach was used to identify the RSN in our study. While gICA needs little assumption beforehand and results are easily reproducible within and in-between subjects, even using different number of components [12], one of the challenges is the correct labelling of the RSN. They can be labelled by macroscopic anatomy, cyto-architecture or function [49]. Stereotactic atlases exist for the human brain allowing localisation of the peak coordinates within a standardised space. These atlases are providing anatomical and cyto-architectonic labels, which give conclusion about the function of this area. Although stereotactic atlases exist in dogs, no functional correlation for these coordinates exists [50]. To overcome this issue, we used cross anatomy to identify functional areas previously localised in dogs in rs-fMRI and task-fMRI. This study compared the presented results with previously published RSNs in humans and other animals, for those canine functional areas without a reported correlate in fMRI. To enable cross anatomical comparison, results were registered to a high quality and study-specific T1 template that allows identification of anatomical structures easily.

We report the presence of seven RSN in the anaesthetised dogs similar to those previously shown in human and other animal data.

The DMN is involved in states of self-reference and has been extensively characterised in several other animals and humans. It is of particular interest due to its involvement and its relevance to mental disorders [51, 52]. In dogs DMN has been identified in anaesthetised and awake dogs and was found to be dissociated in an anterior and posterior component [16]. In the above-mentioned study, results were relatively consistent in all dogs, only minor differences were found between both groups with increased connectivity in the anaesthetised versus awake dogs. Highlighting reproducibility of rs-fMRI, the two components of DMN were also clearly identified in the present study, although different anaesthetic protocol and the different number of IC were chosen. Recently, anterior and posterior components of DMN were described in ferrets by means of ICA as well [8].

Weaker connectivity between the anterior and posterior component in dogs has been supported using diffusion tensor tractography, which only identified white matter tracts connecting medial prefrontal cortex/anterior cingulate cortex to the posterior cingulate cortex in 9/23 dogs [53], while in humans these tracts were identified in 22/23 subjects [54]. This was also reflected by a significantly lower group fractional anisotropy in dogs in this area compared to humans [53]. Dissociation of the DMN has been found in children and in patients with Alzheimer‘s diseases and may reflect a lower level cognitive processing [52]. Strikingly, the components of the DMN could not be clearly identified in the study of Szabó et al. [17]. In contrast to our study anterior-posterior connectedness was found, but the component included also areas not included in the human DMN [17].

Analogy between canine and human visual and auditory cortex functions have been shown by previous task-fMRI. Therefore, it was expected to find correspondence also in the RSNs.

We found two visual networks reflecting primary and higher-order separations seen in the human and animal studies, including awake dogs [9, 17, 55]. Furthermore, this primary visual network was in consistency with results from task-fMRI in awake and anaesthetised healthy dogs after visual stimulation [15, 37]. In these studies, a second response was also noticed reflecting higher order visual networks (for face processing, only on the right side and suspected motion perception, on both sides) overlapping with the higher order visual network identified in our study.

The auditory network identified in our study corresponds with the primary auditory cortex in dogs and auditory RSN identified in awake dogs [17]. Activation of this area by sound has been shown in previous studies in awake unrestrained dogs [14, 56]. While Andics and colleagues showed common functions in dog and human voice processing [14], Prichard et al. reported that most dogs were able to discriminated pseudo-words from trained words [56]. Interestingly, in anaesthetised dogs, Bach and colleagues found only subcortical but no cortical response to auditory stimuli [36]. The authors discuss the possibility of anaesthesia precluding activation of cortical areas. The effect of anaesthesia on fMRI signal is well known and cortical response to auditory stimuli has been identified in anaesthetised cats [57] and rats [58] using different anaesthesia protocols.

RSNs found in the parietal and temporal cortex were analysed in the context of previous human studies and this finding should be therefore carefully interpreted. While the primary motor and sensory cortex is well defined in dogs [59], precise organisation of higher order networks is not well known. Two of the these RSN (networks 6 and 7) include primary motor cortex areas in the pre- and post-cruciate gyrus and the primary sensory cortex areas in the post-cruciate and supra-sylvian gyrus. These two RSN appear similar to the RSN labelled "Primary sensorimotoric, premotoric and supplementer motoric regions" and "Primary and associative sensory cortical areas" by Szabó and colleagues [17].

Regarding network 5, neither primary motor nor primary sensory cortex areas are included and for this reason the function of this network can only be speculated. This is similar to a corresponding RSN in humans in the superior parietal lobule which was associated with action and somesthesis [60]. This network is overlapping with the RSN labeled "External limbic circle (mid cingulate cortex)" by Szabó and colleagues in their IC_{15} [17].

In summary, RSN in dogs are anatomically similar to networks found in humans (Fig 3) and other animals [5, 8, 9, 47, 48, 61]. Our results are in general agreement with the recent rs-fMRI study in awake dogs, with 6 out of 7 of our RSNs matching in both studies [17]. Only one RSN, the DMN, does not match in both studies. While our results correspond to the results of Kyathanahally et al. [16], that showed dissociated DMN in dogs in rs-fMRI as well as in DTI [53], this could not be reproduced by Szabó and colleagues [17].

Fig 3 illustrates similarities by comparing our results to RSNs previously published in humans [12, 60].

An important limitation of the present study is the lack of corresponding electrophysiological examinations of the brain. The RSNs have been positively correlated with alpha activity seen in electroencepahlography in humans [62, 63]. Further research, including simultaneous electroencephalographic recordings, would be helpful to better define the functional cortical organisation of the canine brain and to characterise these networks.

Furthermore, no direct comparison has been performed with awake dogs or dogs under a different anaesthetic protocols to demonstrate the influence of anaesthesia on detection of RSN.

Even if task-fMRI has been performed in anaesthesia before and results match to RSN in our study, a direct intra-individual comparison is missing. Performing task-fMRI under the

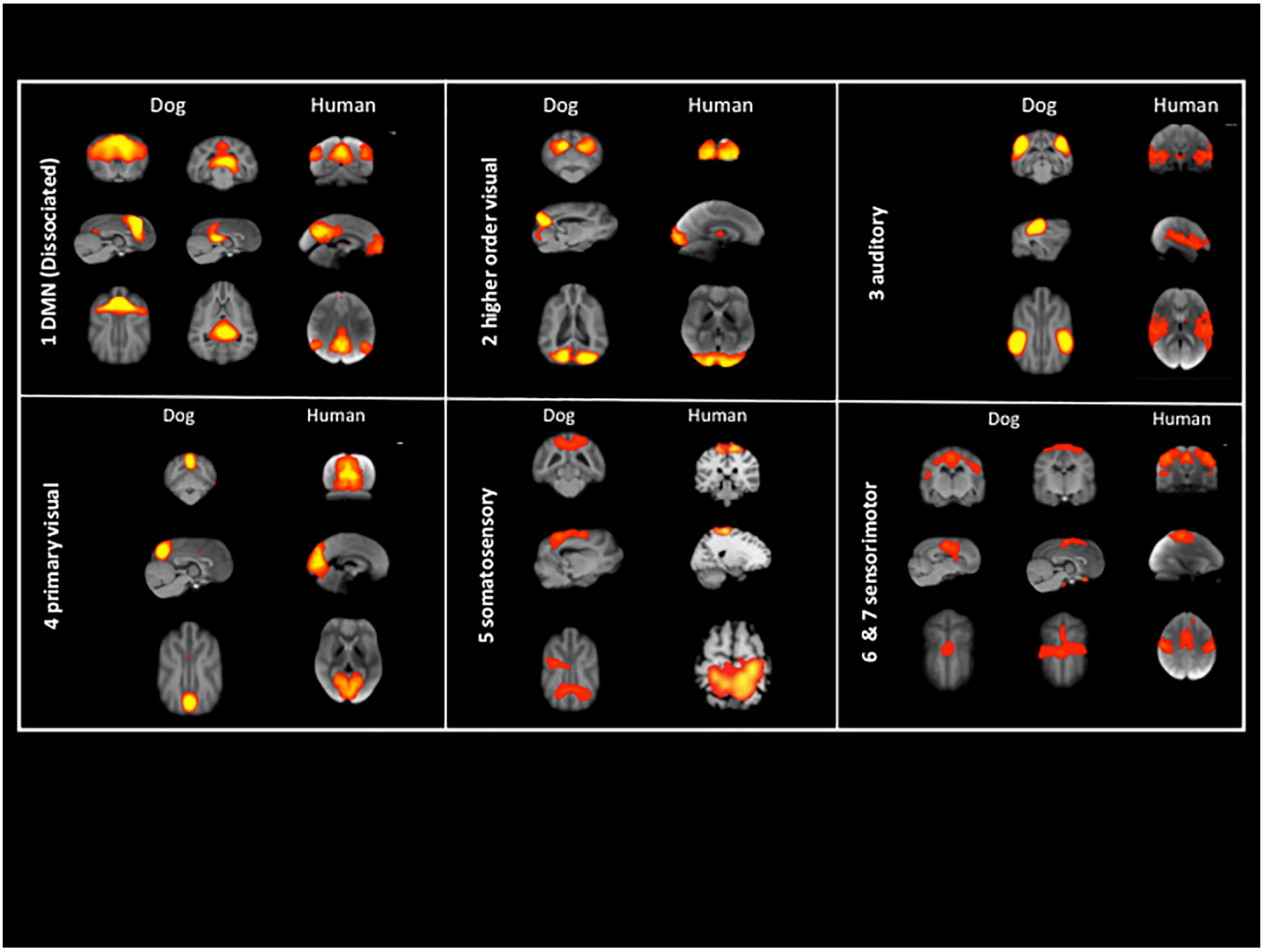

Fig 3. Comparison of generated RSNs of the present study with published RSNs in humans, both registered to T1W anatomical templates. RSN 1: DMN; RSN 2: higher order visual; RSN 3: auditory; RSN 4: primary visual; RSN 5: somatosensory; RSN 6 and 7: sensorimotor. Images from human RSNs adapted from Smith et al., 2009 (RSNs 1–4 and 6–7) and Laird et al., 2013 (RSN 5).

https://doi.org/10.1371/journal.pone.0231955.g003

current conditions would have supported the resting state results and supported the choice of anaesthesia protocol.

Identifying RSN in dogs under standardised general anaesthesia opens the door to investigate pathophysiological changes in brain diseases under clinical settings. This may play a major role when no structural abnormalities are found during examination. Since MRI as a non-invasive technique, is routinely performed in dogs with brain disease, it allows to investigate naturally occurring diseases as translational large animal model.

Conclusion

Using ICA method, we identified 7 RSNs common to those of awake dogs and to other mammals including humans. This study sets a basis for investigating pathophysiological characteristics of various canine brain diseases.

Supporting information

S1 Fig. Pre-processing of the anatomical images. This figure shows how the raw-data were first converted into a FMRIB Software Library v6.0 compatible format and then further pre-processed using this software.
(TIFF)

S2 Fig. Artefactual components from the 20-component ICA decomposition of the resting fMRI data. The RS components do not lie within grey matter and are caused most likely by confound factors such as variations in subjects' head sizes, head motion, and non-neural physiological fluctuations.
(TIFF)

S3 Fig. One sample t-test maps of the anterior and posterior DMN, the auditory network, the primary and higher order visual network, the somatosensory, and the two putative sensory motor networks identified. Maps are thresholded at $p<0.05$.
(TIFF)

Acknowledgments

We are grateful to Erika Bruellmann for her technical advice regarding acquisition protocols and to Eilin Thieme for her assistance in the conduction of the study.

Author Contributions

Conceptualization: Katrin M. Beckmann, Adriano Wang-Leandro, Matthias Dennler, Ines Carrera, Rima N. Bektas, Sven Haller.

Data curation: Katrin M. Beckmann, Adriano Wang-Leandro, Matthias Dennler, Sven Haller.

Formal analysis: Katrin M. Beckmann, Adriano Wang-Leandro.

Funding acquisition: Katrin M. Beckmann.

Investigation: Katrin M. Beckmann, Adriano Wang-Leandro, Sven Haller.

Methodology: Katrin M. Beckmann, Adriano Wang-Leandro, Matthias Dennler, Ines Carrera, Rima N. Bektas, Sven Haller.

Project administration: Katrin M. Beckmann, Matthias Dennler, Ines Carrera, Henning Richter, Rima N. Bektas.

Resources: Katrin M. Beckmann.

Supervision: Sven Haller.

Validation: Sven Haller.

Visualization: Katrin M. Beckmann, Adriano Wang-Leandro, Sven Haller.

Writing – original draft: Katrin M. Beckmann, Adriano Wang-Leandro, Rima N. Bektas, Aline Steiner.

Writing – review & editing: Katrin M. Beckmann, Adriano Wang-Leandro, Matthias Dennler, Ines Carrera, Henning Richter, Rima N. Bektas, Aline Steiner, Sven Haller.

References

1. Deco G, Jirsa VK, McIntosh AR. Emerging concepts for the dynamical organization of resting-state activity in the brain. Nature reviews Neuroscience. 2011; 12(1):43–56. https://doi.org/10.1038/nrn2961 PMID: 21170073
2. Huneau C, Benali H, Chabriat H. Investigating Human Neurovascular Coupling Using Functional Neuroimaging: A Critical Review of Dynamic Models. Frontiers in neuroscience. 2015; 9:467. https://doi.org/10.3389/fnins.2015.00467 PMID: 26733782
3. Kwong KK, Belliveau JW, Chesler DA, Goldberg IE, Weisskoff RM, Poncelet BP, et al. Dynamic magnetic resonance imaging of human brain activity during primary sensory stimulation. Proceedings of the National Academy of Sciences of the United States of America. 1992; 89(12):5675–9. https://doi.org/10.1073/pnas.89.12.5675 PMID: 1608978
4. Brown GG, Perthen JE, Liu TT, Buxton RB. A primer on functional magnetic resonance imaging. Neuropsychology review. 2007; 17(2):107–25. https://doi.org/10.1007/s11065-007-9028-8 PMID: 17468956
5. Lu H, Zou Q, Gu H, Raichle ME, Stein EA, Yang Y. Rat brains also have a default mode network. Proceedings of the National Academy of Sciences of the United States of America. 2012; 109(10):3979–84. https://doi.org/10.1073/pnas.1200506109 PMID: 22355129
6. Mechling AE, Hubner NS, Lee HL, Hennig J, von Elverfeldt D, Harsan LA. Fine-grained mapping of mouse brain functional connectivity with resting-state fMRI. NeuroImage. 2014; 96:203–15. https://doi.org/10.1016/j.neuroimage.2014.03.078 PMID: 24718287
7. Stafford JM, Jarrett BR, Miranda-Dominguez O, Mills BD, Cain N, Mihalas S, et al. Large-scale topology and the default mode network in the mouse connectome. Proceedings of the National Academy of Sciences of the United States of America. 2014; 111(52):18745–50. https://doi.org/10.1073/pnas.1404346111 PMID: 25512496
8. Zhou ZC, Salzwedel AP, Radtke-Schuller S, Li Y, Sellers KK, Gilmore JH, et al. Resting state network topology of the ferret brain. NeuroImage. 2016; 143:70–81. https://doi.org/10.1016/j.neuroimage.2016.09.003 PMID: 27596024
9. Belcher AM, Yen CC, Stepp H, Gu H, Lu H, Yang Y, et al. Large-scale brain networks in the awake, truly resting marmoset monkey. The Journal of neuroscience: the official journal of the Society for Neuroscience. 2013; 33(42):16796–804.
10. Vincent JL, Patel GH, Fox MD, Snyder AZ, Baker JT, Van Essen DC, et al. Intrinsic functional architecture in the anaesthetized monkey brain. Nature. 2007; 447(7140):83–6. https://doi.org/10.1038/nature05758 PMID: 17476267
11. Damoiseaux JS, Rombouts SA, Barkhof F, Scheltens P, Stam CJ, Smith SM, et al. Consistent resting-state networks across healthy subjects. Proceedings of the National Academy of Sciences of the United States of America. 2006; 103(37):13848–53. https://doi.org/10.1073/pnas.0601417103 PMID: 16945915
12. Smith SM, Fox PT, Miller KL, Glahn DC, Fox PM, Mackay CE, et al. Correspondence of the brain's functional architecture during activation and rest. Proceedings of the National Academy of Sciences of the United States of America. 2009; 106(31):13040–5. https://doi.org/10.1073/pnas.0905267106 PMID: 19620724
13. Smitha KA, Akhil Raja K, Arun KM, Rajesh PG, Thomas B, Kapilamoorthy TR, et al. Resting state fMRI: A review on methods in resting state connectivity analysis and resting state networks. The neuroradiology journal. 2017; 30(4):305–17. https://doi.org/10.1177/1971400917697342 PMID: 28353416
14. Andics A, Gacsi M, Farago T, Kis A, Miklosi A. Voice-sensitive regions in the dog and human brain are revealed by comparative fMRI. Current biology: CB. 2014; 24(5):574–8. https://doi.org/10.1016/j.cub.2014.01.058 PMID: 24560578
15. Aguirre GK, Komaromy AM, Cideciyan AV, Brainard DH, Aleman TS, Roman AJ, et al. Canine and human visual cortex intact and responsive despite early retinal blindness from RPE65 mutation. Plos Medicine. 2007; 4(6):1117–28.
16. Kyathanahally SP, Jia H, Pustovyy OM, Waggoner P, Beyers R, Schumacher J, et al. Anterior-posterior dissociation of the default mode network in dogs. Brain structure & function. 2015; 220(2):1063–76.
17. Szabó D, Czeibert K, Kettinger Á, Gácsi M, Andics A, Miklósi Á, et al. Resting-state fMRI data of awake dogs (Canis familiaris) via group-level independent component analysis reveal multiple, spatially distributed resting-state networks. Scientific reports. 2019; 9(1):15270. https://doi.org/10.1038/s41598-019-51752-2 PMID: 31649271
18. Barkhof F, Haller S, Rombouts SA. Resting-state functional MR imaging: a new window to the brain. Radiology. 2014; 272(1):29–49. https://doi.org/10.1148/radiol.14132388 PMID: 24956047

19. Bunford N, Andics A, Kis A, Miklosi A, Gacsi M. Canis familiaris As a Model for Non-Invasive Comparative Neuroscience. Trends in neurosciences. 2017; 40(7):438–52. https://doi.org/10.1016/j.tins.2017.05.003 PMID: 28571614

20. Danek M, Danek J, Araszkiewicz A. Large animals as potential models of human mental and behavioral disorders. Psychiatr Pol. 2017; 51(6):1009–27. https://doi.org/10.12740/PP/74304 PMID: 29432500

21. Mazzatenta A, Carluccio A, Robbe D, Giulio CD, Cellerino A. The companion dog as a unique translational model for aging. Seminars in cell & developmental biology. 2017; 70:141–53.

22. Potschka H, Fischer A, von Ruden EL, Hulsmeyer V, Baumgartner W. Canine epilepsy as a translational model? Epilepsia. 2013; 54(4):571–9. https://doi.org/10.1111/epi.12138 PMID: 23506100

23. Patterson EE. Canine epilepsy: an underutilized model. ILAR journal / National Research Council, Institute of Laboratory Animal Resources. 2014; 55(1):182–6.

24. Heske L, Nødtvedt A, Jäderlund KH, Berendt M, Egenvall A. A cohort study of epilepsy among 665,000 insured dogs: incidence, mortality and survival after diagnosis. Veterinary journal (London, England: 1997). 2014; 202(3):471–6.

25. Kearsley-Fleet L, O'Neill DG, Volk HA, Church DB, Brodbelt DC. Prevalence and risk factors for canine epilepsy of unknown origin in the UK. The Veterinary record. 2013; 172(13):338–. https://doi.org/10.1136/vr.101133 PMID: 23300065

26. Ramani R. Connectivity. Curr Opin Anaesthesiol. 2015; 28(5):498–504. https://doi.org/10.1097/ACO.0000000000000237 PMID: 26270569

27. Moeller S, Nallasamy N, Tsao DY, Freiwald WA. Functional connectivity of the macaque brain across stimulus and arousal states. The Journal of neuroscience: the official journal of the Society for Neuroscience. 2009; 29(18):5897–909.

28. Paasonen J, Stenroos P, Salo RA, Kiviniemi V, Gröhn O. Functional connectivity under six anesthesia protocols and the awake condition in rat brain. NeuroImage. 2018; 172:9–20. https://doi.org/10.1016/j.neuroimage.2018.01.014 PMID: 29414498

29. Palanca BJA, Mitra A, Larson-Prior L, Snyder AZ, Avidan MS, Raichle ME. Resting-state Functional Magnetic Resonance Imaging Correlates of Sevoflurane-induced Unconsciousness. Anesthesiology. 2015; 123(2):346–56. https://doi.org/10.1097/ALN.0000000000000731 PMID: 26057259

30. Roland JL, Griffin N, Hacker CD, Vellimana AK, Akbari SH, Shimony JS, et al. Resting-state functional magnetic resonance imaging for surgical planning in pediatric patients: a preliminary experience. J Neurosurg Pediatr. 2017; 20(6):583–90. https://doi.org/10.3171/2017.6.PEDS1711 PMID: 28960172

31. Venkatraghavan L, Bharadwaj S, Wourms V, Tan A, Jurkiewicz MT, Mikulis DJ, et al. Brain Resting-State Functional Connectivity Is Preserved Under Sevoflurane Anesthesia in Patients with Pervasive Developmental Disorders: A Pilot Study. Brain connectivity. 2017; 7(4):250–7. https://doi.org/10.1089/brain.2016.0448 PMID: 28443736

32. Yamamoto AK, Magerkurth J, Mancini L, White MJ, Miserocchi A, McEvoy AW, et al. Acquisition of sensorimotor fMRI under general anaesthesia: Assessment of feasibility, the BOLD response and clinical utility. Neuroimage Clin. 2019; 23:101923–. https://doi.org/10.1016/j.nicl.2019.101923 PMID: 31491826

33. Smith SM. Fast robust automated brain extraction. Human brain mapping. 2002; 17(3):143–55. https://doi.org/10.1002/hbm.10062 PMID: 12391568

34. Jenkinson M, Bannister P, Brady M, Smith S. Improved optimization for the robust and accurate linear registration and motion correction of brain images. NeuroImage. 2002; 17(2):825–41. https://doi.org/10.1016/s1053-8119(02)91132-8 PMID: 12377157

35. Jenkinson M, Smith S. A global optimisation method for robust affine registration of brain images. Medical image analysis. 2001; 5(2):143–56. https://doi.org/10.1016/s1361-8415(01)00036-6 PMID: 11516708

36. Bach JP, Lupke M, Dziallas P, Wefstaedt P, Uppenkamp S, Seifert H, et al. Functional magnetic resonance imaging of the ascending stages of the auditory system in dogs. BMC veterinary research. 2013; 9:210. https://doi.org/10.1186/1746-6148-9-210 PMID: 24131784

37. Dilks DD, Cook P, Weiller SK, Berns HP, Spivak M, Berns GS. Awake fMRI reveals a specialized region in dog temporal cortex for face processing. PeerJ. 2015; 3(2167–8359 (Print)):e1115.

38. Willis CK, Quinn RP, McDonell WM, Gati J, Partlow G, Vilis T. Functional MRI activity in the thalamus and occipital cortex of anesthetized dogs induced by monocular and binocular stimulation. Canadian journal of veterinary research = Revue canadienne de recherche veterinaire. 2001; 65(3):188–95. PMID: 11480525

39. Willis CKR, Quinn RP, McDonell WM, Gati J, Parent J, Nicolle D. Functional MRI as a tool to assess vision in dogs: the optimal anesthetic. Veterinary ophthalmology. 2001; 4(4):243–53. https://doi.org/10.1046/j.1463-5216.2001.00183.x PMID: 11906659

40. Nickerson LD, Smith SM, Öngür D, Beckmann CF. Using Dual Regression to Investigate Network Shape and Amplitude in Functional Connectivity Analyses. Frontiers in neuroscience. 2017; 11:115. https://doi.org/10.3389/fnins.2017.00115 PMID: 28348512

41. Beckmann CEM C.F., Filippini N., and Smith S.M. Group comparison of resting-state FMRI data using multi-subject ICA and dual regression2009; 47(Suppl 1):S148.

42. Beitz AJ F T. The Brain In: S W.B., editor. Miller's Anatomy of the dog 4th Edition Elsevier LDT, Oxford 2012.

43. Thompkins AM, Deshpande G, Waggoner P, Katz JS. Functional Magnetic Resonance Imaging of the Domestic Dog: Research, Methodology, and Conceptual Issues. Comparative cognition & behavior reviews. 2016; 11:63–82.

44. Venkatraghavan L, Bharadwaj S, Wourms V, Tan A, Jurkiewicz MT, Mikulis DJ, et al. Brain Resting-State Functional Connectivity Is Preserved Under Sevoflurane Anesthesia in Patients with Pervasive Developmental Disorders: A Pilot Study. Brain Connect. 2017; 7(4):250–7. https://doi.org/10.1089/brain.2016.0448 PMID: 28443736

45. Rioja E, Kerr CL, McDonell WN, Dobson H, Konyer NB, Poma R, et al. Effects of hypercapnia, hypocapnia, and hyperoxemia on blood oxygenation level-dependent signal intensity determined by use of susceptibility-weighted magnetic resonance imaging in isoflurane-anesthetized dogs. American journal of veterinary research. 2010; 71(1):24–32. https://doi.org/10.2460/ajvr.71.1.24 PMID: 20043777

46. Wang R, Foniok T, Wamsteeker JI, Qiao M, Tomanek B, Vivanco RA, et al. Transient blood pressure changes affect the functional magnetic resonance imaging detection of cerebral activation. NeuroImage. 2006; 31(1):1–11. https://doi.org/10.1016/j.neuroimage.2005.12.004 PMID: 16460967

47. Chuang KH, Nasrallah FA. Functional networks and network perturbations in rodents. NeuroImage. 2017; 163:419–36. https://doi.org/10.1016/j.neuroimage.2017.09.038 PMID: 28942060

48. Mantini D, Gerits A, Nelissen K, Durand JB, Joly O, Simone L, et al. Default mode of brain function in monkeys. The Journal of neuroscience: the official journal of the Society for Neuroscience. 2011; 31 (36):12954–62.

49. Brett M, Johnsrude IS, Owen AM. The problem of functional localization in the human brain. Nature reviews Neuroscience. 2002; 3(3):243–9. https://doi.org/10.1038/nrn756 PMID: 11994756

50. Nitzsche B, Boltze J, Ludewig E, Flegel T, Schmidt MJ, Seeger J, et al. A stereotaxic breed-averaged, symmetric T2w canine brain atlas including detailed morphological and volumetrical data sets. NeuroImage. 2018.

51. Lee MH, Smyser CD, Shimony JS. Resting-state fMRI: a review of methods and clinical applications. AJNR American journal of neuroradiology. 2013; 34(10):1866–72. https://doi.org/10.3174/ajnr.A3263 PMID: 22936095

52. Mohan A, Roberto AJ, Mohan A, Lorenzo A, Jones K, Carney MJ, et al. The Significance of the Default Mode Network (DMN) in Neurological and Neuropsychiatric Disorders: A Review. The Yale journal of biology and medicine. 2016; 89(1):49–57. PMID: 27505016

53. Robinson JL, Baxi M, Katz JS, Waggoner P, Beyers R, Morrison E, et al. Characterization of Structural Connectivity of the Default Mode Network in Dogs using Diffusion Tensor Imaging. Scientific reports. 2016; 6:36851. https://doi.org/10.1038/srep36851 PMID: 27886204

54. Greicius MD, Supekar K, Menon V, Dougherty RF. Resting-state functional connectivity reflects structural connectivity in the default mode network. Cereb Cortex. 2009; 19(1):72–8. https://doi.org/10.1093/cercor/bhn059 PMID: 18403396

55. Beckmann CF, DeLuca M, Devlin JT, Smith SM. Investigations into resting-state connectivity using independent component analysis. Philosophical transactions of the Royal Society of London Series B, Biological sciences. 2005; 360(1457):1001–13. https://doi.org/10.1098/rstb.2005.1634 PMID: 16087444

56. Prichard A, Cook PF, Spivak M, Chhibber R, Berns GS. Awake fMRI Reveals Brain Regions for Novel Word Detection in Dogs. Frontiers in neuroscience. 2018; 12:737. https://doi.org/10.3389/fnins.2018.00737 PMID: 30374286

57. Brown TA, Joanisse MF, Gati JS, Hughes SM, Nixon PL, Menon RS, et al. Characterization of the blood-oxygen level-dependent (BOLD) response in cat auditory cortex using high-field fMRI. NeuroImage. 2013; 64:458–65. https://doi.org/10.1016/j.neuroimage.2012.09.034 PMID: 23000258

58. Cheung MM, Lau C, Zhou IY, Chan KC, Cheng JS, Zhang JW, et al. BOLD fMRI investigation of the rat auditory pathway and tonotopic organization. NeuroImage. 2012; 60(2):1205–11. https://doi.org/10.1016/j.neuroimage.2012.01.087 PMID: 22297205

59. Nickel RS, A; Seiferle, E. Nervensytsem, Sinnesorgane, Endokrine Drüsen. 4th ed: Parey; 2004. 550 p.

60. Laird AR, Fox PM, Eickhoff SB, Turner JA, Ray KL, McKay DR, et al. Behavioral interpretations of intrinsic connectivity networks. J Cogn Neurosci. 2011; 23(12):4022–37. https://doi.org/10.1162/jocn_a_00077 PMID: 21671731

61. Rosazza C, Minati L. Resting-state brain networks: literature review and clinical applications. Neurological sciences: official journal of the Italian Neurological Society and of the Italian Society of Clinical Neurophysiology. 2011; 32(5):773–85.

62. Murta T, Leite M, Carmichael DW, Figueiredo P, Lemieux L. Electrophysiological correlates of the BOLD signal for EEG-informed fMRI. Human brain mapping. 2015; 36(1):391–414. https://doi.org/10.1002/hbm.22623 PMID: 25277370

63. Jann K, Dierks T, Boesch C, Kottlow M, Strik W, Koenig T. BOLD correlates of EEG alpha phase-locking and the fMRI default mode network. NeuroImage. 2009; 45(3):903–16. https://doi.org/10.1016/j.neuroimage.2009.01.001 PMID: 19280706

scientific reports

Check for updates

OPEN

Increased resting state connectivity in the anterior default mode network of idiopathic epileptic dogs

Katrin M. Beckmann[1]✉, Adriano Wang-Leandro[2], Henning Richter[2,3], Rima N. Bektas[4], Frank Steffen[1], Matthias Dennler[2], Ines Carrera[5] & Sven Haller[6,7]

Epilepsy is one of the most common chronic, neurological diseases in humans and dogs and considered to be a network disease. In human epilepsy altered functional connectivity in different large-scale networks have been identified with functional resting state magnetic resonance imaging. Since large-scale resting state networks have been consistently identified in anesthetised dogs' application of this technique became promising in canine epilepsy research. The aim of the present study was to investigate differences in large-scale resting state networks in epileptic dogs compared to healthy controls. Our hypothesis was, that large-scale networks differ between epileptic dogs and healthy control dogs. A group of 17 dogs (Border Collies and Greater Swiss Mountain Dogs) with idiopathic epilepsy was compared to 20 healthy control dogs under a standardized sevoflurane anaesthesia protocol. Group level independent component analysis with dimensionality of 20 components, dual regression and two-sample *t* test were performed and revealed significantly increased functional connectivity in the anterior default mode network of idiopathic epileptic dogs compared to healthy control dogs ($p = 0.00060$). This group level differences between epileptic dogs and healthy control dogs identified using a rather simple data driven approach could serve as a starting point for more advanced resting state network analysis in epileptic dogs.

Abbreviations

BOLD	Blood oxygenation level dependent
DMN	Default mode network
EPI	Gradient-echo planar imaging
$EtCO_2$	End-tidal partial pressure of carbon dioxide
FOV	Field of view
HR	Heart rate
ICA	Independent component analysis
IE	Idiopathic epilepsy
MAP	Mean arterial blood pressure
RR	Respiratory rate
rs-fMRI	Resting state functional magnetic resonance imaging
RSN	Resting state network
SpO_2	Percutaneous arterial oxygen saturation

Epilepsy represents one of the most common chronic neurological diseases in dogs and humans, affecting approximately 0.64% of the human[1] and 0.6–0.75% of the canine population[2,3]. Epilepsy is considered a disease

[1]Section of Neurology, Department of Small Animals, Vetsuisse Faculty Zurich, University of Zurich, Zurich, Switzerland. [2]Clinic for Diagnostic Imaging, Department of Diagnostics and Clinical Services, Vetsuisse-Faculty Zurich, University of Zurich, Zurich, Switzerland. [3]Clinic for Neuroradiology, University Hospital Bonn, Bonn, Germany. [4]Section of Anaesthesiology, Department of Diagnostics and Clinical Services, Vetsuisse Faculty, University of Zurich, Zurich, Switzerland. [5]Willows Veterinary Centre and Referral Service, Highlands Road, Shirley, UK. [6]Department of Surgical Sciences, Radiology, Uppsala University, Uppsala, Sweden. [7]Faculty of Medicine, University of Geneva, Geneva, Switzerland. ✉email: kbeckmann@vetclinics.uzh.ch

of the brain network[4]. Resting state functional magnetic resonance imaging (rs-fMRI) is a non-invasive tool to evaluate network structure in neurological diseases such as epilepsy. It can be performed in non-task related conditions and during anaesthesia[5]. Over the last decade, rs-fMRI has become increasingly important as a research tool for understanding brain networking during epileptic syndromes[6–8]. Resting state networks (RSN) share similar features in humans and animals[9] but information regarding rs-fMRI in epilepsy in non-human species are spare and limited to rodent models so far[7]. Although the dog is an established large animal model for human epilepsy[10,11], studies describing rs-fMRI of the canine brain in dogs affected by naturally-occurring epilepsy are currently lacking.

In human epileptic syndromes, rs-fMRI has shown altered functional connectivity in different large-scale networks including attentional[12], perceptual[13] and default mode[5,14,15]. These alterations of large-scale networks potentially explain seizure generation and spread and therefore give insight into the pathophysiology of epilepsy[7]. The most widely studied network in patients affected by epilepsy is the default mode network (DMN)[7]. The alteration detected depend on the underlying epileptic syndrome and therefore could potentially be used as a diagnostic and prognostic biomarker[16]. Epilepsy is commonly accompanied by neurobehavioral and/or psychiatric comorbidities such as depression, anxiety and cognitive impairments[17,18]. Emerging evidence suggests that network alterations detected by rs-fMRI do not only correlate with generation of ictal activity, but may also contribute to neurobehavioral comorbidities[19].

Naturally occurring canine idiopathic epilepsy has been proposed as a translational model for human epilepsy because the two species share similarities such as prevalence, clinical manifestation, electroencephalographic manifestation, and pharmacological response[10,11,20–23]. However, characterization of brain regions involved in canine epilepsy is lacking[11,21,23,24]. For example, the extent to which the temporal lobe is involved remains controversial[25]. In dogs, pedigree studies have demonstrated an hereditary basis for idiopathic epilepsy in several breeds including Border Collies[26,27] and greater Swiss mountain dogs[28]. Furthermore, neurobehavioral comorbidities reported in human epilepsy, such as anxiety disorder[29], attention-deficit/hyperactivity disorder[30,31] and cognitive impairment[32,33], have been recently recognized in canine epilepsy and have been reported to negatively impact the quality of life of the effected dogs[34,35]. Therefore, privately-owned epileptic dogs make it possible to bridge the gap between experimental animal models and a realistic clinical setting.

Magnetic resonance imaging of the brain is performed routinely as part of the clinical work-up of the canine idiopathic epileptic patient[36]. Currently, clinical imaging is mainly limited to the morphological structure of the brain; however, increased availability of high-field scanners in veterinary medicine have raised the demand for advanced imaging techniques[37]. Moreover, feasibility and consistency of rs-fMRI in awake and anesthetized dogs have been demonstrated recently, which opens the door for translational research[38–40]. It is particularly interesting that detected canine networks include those with altered resting state connectivity in human epilepsy. While in human epilepsy pattern of altered connectivity is depended on the underlying epileptic syndrome, lack of standardization of epileptic syndromes and lack of characterization of brain regions involved in canine epilepsy does not allow precise assumptions regarding possible localization of altered connectivity in canine epilepsy beforehand[11,21,23,24]. In human epilepsy commonly areas of decreased connectivity possibly alongside with areas of increased connectivity can be identified[41]. Therefore, we also expected areas of decreased connectivity possibly alongside with areas of increased connectivity in our study without being able to predict specific areas.

The aim of our study was to investigate differences in large-scale RSN in epileptic dogs compared to healthy controls. Our hypothesis was, that large-scale networks differ between epileptic dogs and healthy control dogs.

Material and methods

Subjects. Border Collies and greater Swiss Mountain dogs diagnosed with idiopathic epilepsy according to the veterinary epilepsy task force criteria[42] and breed-matched healthy control dogs of were prospectively enrolled in this study during a period of 3.2 years (2017–2020). Additionally, 10 research beagles were included in the healthy control group. These beagle dogs have been part of a preliminary study investigating the feasibility of RSN detection under general anaesthesia[39].

The present study is in accordance with the Swiss Animal Welfare Act (TSchG, 2005) and the Swiss Animal Welfare Ordinance (TSchV, 2008) and was approved by the Swiss Federal Veterinary Office Zurich (animal license numbers ZH272/16 and ZH046/20) ethics committee. The authors complied with the ARRIVE guidelines.

All dogs underwent clinical and neurological examinations by a board-certified veterinary neurologist. Preanesthetic laboratory as recommend by the international veterinary epilepsy task force for investigations of idiopathic epilepsy was performed including a complete blood cell count and serum biochemistry panel, electrolytes as well as fasted ammonia, bile acids, and urinalysis[42]. MRI of the brain including structural imaging and fMRI was performed in all dogs. Afterwards, cerebrospinal fluid was collected from the cisterna cerebellomedullaris in idiopathic epileptic dogs; nucleated cell count, differential cell count and total protein concentration were evaluated.

Dogs that fulfilled the TIERII criteria for canine idiopathic epilepsy (suspected genetic epilepsy) based on the criteria of the veterinary epilepsy task force[42] and manifested generalized tonic–clonic seizures built the group of the idiopathic epileptic dogs.

The group of healthy control dogs included relatives of the epileptic dogs (Border collies and greater Swiss mountain dogs) and a group of healthy beagle dogs from the above-mentioned preliminary study. All these dogs without history of seizures had to have a normal clinical and neurological examination. Further inclusion criteria represented a normal hematologic and blood-chemical work-up and a normal structural MRI examination of the brain (structural MRI reported as normal by a board-certified (ECVDI) radiologist).

Animal preparation and rs-fMRI protocol were performed as previously described[39]:

Shortly, Butorphanol served as premedication. (0.1–0.2 mg/kg). Depending on the temperament of the dog Butorphanol was administered intramuscularly prior to catheter placement or intravenously after catheter placement. Oro-tracheal intubation was performed, after induction of anaesthesia with Propofol 1% (MCT Fresenius Kabi, Oberdorf, Switzerland) IV, given to effect. Anaesthesia was maintained with sevoflurane vaporized in oxygen and medical air. Vaporizer settings were adjusted to the minimum possible dosage to prevent motion of the dogs. End-tidal concentration of sevoflurane, heart rate (HR), respiratory rate (RR), non-invasive mean blood pressure, percutaneous arterial oxygen saturation (SpO_2) and end-tidal partial pressure of carbon dioxide ($EtCO_2$) were monitored using a medical monitor (DatexOhmeda) and recorded every 5 min. Normocapnia ($EtCO_2$ between 35 and 38 mmHg) was maintained and FiO_2 was kept between 45–61%. Blood pressures were maintained stable within physiological values under general anaesthesia (Mean arterial blood pressure (MAP) > 60 mmHg) using RiAc infusion.

MAP under 60 mmHg was treated first with fluid/RiAc challenges of 3 ml/kg IV administered over 5–10 min. After 3 fluid challenges of RiAc, a dobutamine (Dobutrex, Teva Pharma AG, Basel, Switzerland) constant rate infusion (1-5 µg/kg/min) was started to maintain MAP over 60 mmHg.

Image acquisition. All data were acquired as previously described[39] with a 3 Tesla scanner (Philips Ingenia, Philips AG, Zurich, Switzerland) using a 16-channel receive-transmit head coil (dStream HeadSpine coil solution, Philips AG). From the anatomical evaluation, a 3D T1-weighted (T1W; TR 13 ms; TE 6 ms; FOV 130 mm; slice thickness 0.6 mm; Flip angle 8°) sequence was depicted for the registration with anatomical images. Following the anatomical scans, around one hour after induction of anaesthesia, rs-fMRI scans were acquired in all dogs.

A gradient-echo planar imaging (EPI) sequence was performed using the following protocol: TR 2.0 s; TE 30 ms; FOV 236 mm; slice thickness 3.0 mm; acquisition time 12.07 min. Phase encoding direction was anterior–posterior.

MR data processing. Processing of the rs-fMRI data was carried out using FEAT (FMRI Expert Analysis Tool) Version 6.04, part of FSL (FMRIB's Software Library, http://www.fmrib.ox.ac.uk/fsl). The following pre-statistics processing was applied: motion correction using MCFLIRT[43], non-brain removal using BET[44], spatial smoothing using a Gaussian kernel of FWHM 5 mm; grand-mean intensity normalization of the entire 4D dataset by a single multiplicative factor and high-pass temporal filtering (Gaussian-weighted least-squares straight line fitting, with sigma = 50.0 s). Registration to high resolution structural and standard space images was carried out using FLIRT[43,45]. As standard space image, a recently published, open-source stereotactic atlas of the canine brain was used[46]. Registration from high resolution structural to standard space was then further refined using FNIRT nonlinear registration[47,48] Degree of motion of each dog as well as the quality of registration were assessed afterwards.

Independent component analysis. Due to different number of healthy control dogs and epileptic dogs from each breed, independent component analysis (ICA) was first performed only in the healthy control group and the RSN were compared across breeds to assess possible effects of breed on RSNs. A second independent component analysis was performed in all healthy control and epileptic dogs together to identify differences between healthy controls and epileptic dogs.

Analysis was carried out using Probabilistic Independent Component Analysis[49] as implemented in MELODIC (Multivariate Exploratory Linear Decomposition into Independent Components) Version 3.15, part of FSL (FMRIB's Software Library, http://www.fmrib.ox.ac.uk/fsl). The following data pre-processing was applied to the input data: masking of non-brain voxels; voxel-wise de-meaning of the data and normalisation of the voxel-wise variance. Pre-processed data were whitened and projected into a 20-dimensional subspace using Principal Component Analysis. Twenty components were chosen based on the results of our previous study[39]. The whitened observations were decomposed into sets of vectors which describe signal variation across the temporal domain (time-courses), the session/subject domain and across the spatial domain (maps) by optimising for non-Gaussian spatial source distributions using a fixed-point iteration technique[50]. Estimated component maps were divided by the standard deviation of the residual noise and the threshold set by fitting a mixture model to the histogram of intensity values[51].

Criteria for selection of RSNs in the different components were the following: (1) consistency of relatively large continuous regions of increased BOLD signal, (2) predominant bilaterality and/or (3) reference to anatomical landmarks or previously described RSNs in existing literature of dogs[40,52–56]. The detected RSNs were overlaid with the mean functional image of all dogs and with the selected RSNs and were visually assessed to rule out distortion and signal loss from susceptibility artefacts[38]. Furthermore signal to noise ratio maps were generated to evaluate the influence of differences in signal to noise ratios between both groups (Supplementary Materials M1).

Statistical analysis. Descriptive statistics and non-parametric variance analysis by means of Mann–Whitney test were performed to compare population characteristics and physiological parameters during anaesthesia between both groups with a significance threshold of $p < 0.05$.

For fMRI data, mean deviation time series of six affine parameters (three translations and three rotations) were plotted to evaluate whether there was significant head movement during the functional scan. Furthermore, one and two sample *t* test after dual regression analysis of the data were performed. Specifically, a set of spatial maps from the group-average analysis was used to generate subject-specific versions of the spatial maps, and associated time series, using dual regression[57]. First, for each subject, the group-average set of spatial maps was regressed (as spatial regressors in a multiple regression) into the subject's 4D space–time dataset. This resulted

	Epileptic dogs	Healthy controls
Breed		
Beagle	0	10
Border Collie	11	4
Greater Swiss Mountain Dog	6	6
Sex		
Male	10	9
Male castrated	1	3
Female	2	8
Female spayed	4	0
Ratio male:female	11:6	3:2
Bodyweight		
kg [median, range]	32.6, 14.0–70.0	25.7, 9.6–52.0
Age		
Years [median, range]	3.7, 0.8–8.5	5.0, 1.2–8.5

Table 1. Population characteristics.

in a set of subject-specific time series, one per group-level spatial map. Afterwards, those time series were regressed (as temporal regressors, again in a multiple regression) into the same 4D dataset, resulting in a set of subject-specific spatial maps, one per group-level spatial map. A one sample *t* test was performed using FSL's randomize permutation-testing tool[58]. Clusters of increased or decreased BOLD signal within the RSNs were confirmed using a significance level of $p < 0.05$. Furthermore, two sample *t* test was performed for between group comparison of the individual components in both directions. For the between group comparison p-values were corrected via Bonferroni for the number of independent components defined and for running the test in both directions: for significant changes between the groups $p < 0.003125$ had to be reached for epileptic versus healthy control dogs. A second two sample *t* test was performed for the signal to noise ratio maps between both groups in both directions (Supplementary Material M1 and Supplementary Fig. S4).

Results

Study population. Twenty Border Collies, seventeen Greater Swiss Mountain Dogs and ten research Beagles matched the inclusion criteria and were initially included in the study.

Three Border Collies and two Greater Swiss Mountain Dogs were excluded due to acquisition problems of raw data. Two Border Collies and three Greater Swiss Mountain Dogs were excluded because of insufficient quality of the registration of the functional images to the high-resolution images. The summary registration fMRI to standard space of all 37 included dogs can be found in the Supplementary Materials (Fig. S1).

For the ICA 15 Border Collies, 12 Greater Swiss Mountain Dogs and 10 Beagle dogs were included. Of those 37 dogs included in the ICA, 17 dogs suffered from idiopathic epilepsy (11 Border Collies and 6 Greater Swiss Mountain Dogs) and 20 dogs served as healthy controls (4 Border Collies, 6 Greater Swiss Mountain Dogs and 10 Beagles). All greater swiss mountain dogs and all but one Border collie of the healthy control dogs had either one littermate or one direct offspring with epilepsy. The remaining border collie had an undefined familiar history of epilepsy. Thirteen dogs were females (9 sexually intact, 4 spayed) and 24 were males (20 sexually intact, 4 castrated). Age ranged from 0.8–8.5 years (mean age 4.7 years). The body weight was between 9.6 and 70 kg (mean weight 28.9 kg). The population characteristics of both groups is summarized in Table 1. Both subpopulations showed no significant difference related to age, weight, RR, HR, $SEVO_{begin}$ BOLD and $SEVO_{end}$ BOLD ($p > 0.05$, $p_{min} = 0.053$, $p_{max} = 0.220$). Time interval from the last reported seizure to MRI ranged from 2 days to 1 month. Details about seizure semiology are summarized in Table 2.

Anaesthesia. Anaesthesia was uneventful in all dogs. End-tidal Sevofluran level during rs-fMRI ranged from 1.8 to 3.8% (mean: 2.4%) in all dogs. Compared to the healthy control group, mean end-tidal sevoflurane was slightly higher in the epileptic dogs. It ranged from 1.8 to 2.9% (mean: 2.6%) in the healthy control dogs and from 1.9 to 3.8% (mean: 2.3%) in the epileptic dogs. Heart rate varied during rs-fMRI between 48 to 130/min (mean: 81/min). The mean heart rate in epileptic dogs was 78 beats/min (range from 48 to 105 beats/min), slightly lower than in healthy controls (mean: 88 beats/min, range from 58 to 130 beats/min).

Motion correction. The motion was minimal in all patients with a mean relative displacement of 0.08 mm (0.03–0.32 mm) and a mean absolute displacement 0.08 mm (0.04–0.21 mm).

Results independent component- and dual-regression-analysis. In the control population, seven RSNs were identified and labelled according to Uddin et al.[59]. Initially, the identified RSN were labelled according to their anatomical localisation, and in a second step a cognitive label was given if possible[59]. One network was identified as medial frontoparietal network (Fig. 1A: RSN 1 anterior DMN), one was identified as a limbic-occipital network (Fig. 1A: RSN2 posterior DMN), three networks were identified in the occipital cortex

	[n]
Medical treatment at the timepoint of MRI	
Phenobarbital	9
Potassium bromide	4
Levetiracetam	3
Imepitoin	1
Type of therapy	
Mono	2
Double	5
Triple	2
Special diet or dietary supplement before MRI	
Medium chain triglycerides	2
Cannabidiol	2
Time between first seizure to MRI	
< 1 month	2
> 1–3 months	6
> 3–12 months	6
> 12 months	3
Time between last reported seizure to MRI	
2–7 days	6
8–31 days	11
Seizures	
Status epilepticus	1
Cluster seizures	6
Seizure semiology	
Tonic–clonic	16
Tonic	1
Focal onset secondary generalisation	9
Unknown onset	8
Additional focal seizures	1
Autonomic signs	
Salivation	9
Urination	11
Defecation	5
Postictal aggression	4
Interictal behavioural changes	
Anxiety	3

Table 2. Semiology of epileptic events in the affected population.

(Fig. 1B: RSN3: primary visual, RSN 4 and 5 higher order visual) and two networks were identified in areas corresponding to the pericentral networks (Fig. 1C: RSN 6 and RSN 7: auditory).

After dual regression analysis, no significant differences were detected in RSNs when comparing the different breeds, therefore excluding the effect of breed on RSNs and indicating that the observed networks can be compared across breeds.

When comparing ICA between the population of epileptic dogs with controls (Fig. 2), a total of eight RSNs were identified and labelled as described above. Of those eight networks, one was identified as medial frontoparietal network (Fig. 2A: RSN 1 anterior DMN), one was identified as limbic-occipital network (Fig. 2A: RSN 2 posterior DMN), three were identified in the occipital cortex (Fig. 2B: RSN3: primary visual, RSN 4 and RSN 5: higher order visual) and three were identified in areas corresponding to the pericentral networks (Fig. 2C: RSN 5 and RSN 6: auditory and RSN 7 somatosensory network).

Statistical difference of large-scale networks between the epileptic dogs and the healthy controls was found at the rostral component of the DMN and the primary visual network, which showed increased connectivity in the epileptic group relative to healthy controls. In the two-sample *t* test the rostral component of the DMN showed a p-value of 0.00060 (Fig. 3) and the primary visual network a p-value of 0.0018 (taking in account the Bonferroni correction, p had to < 0.003125 for statistical significance).

In the remaining six RSN, no statistical difference between epileptic and controls were found (Table 3).

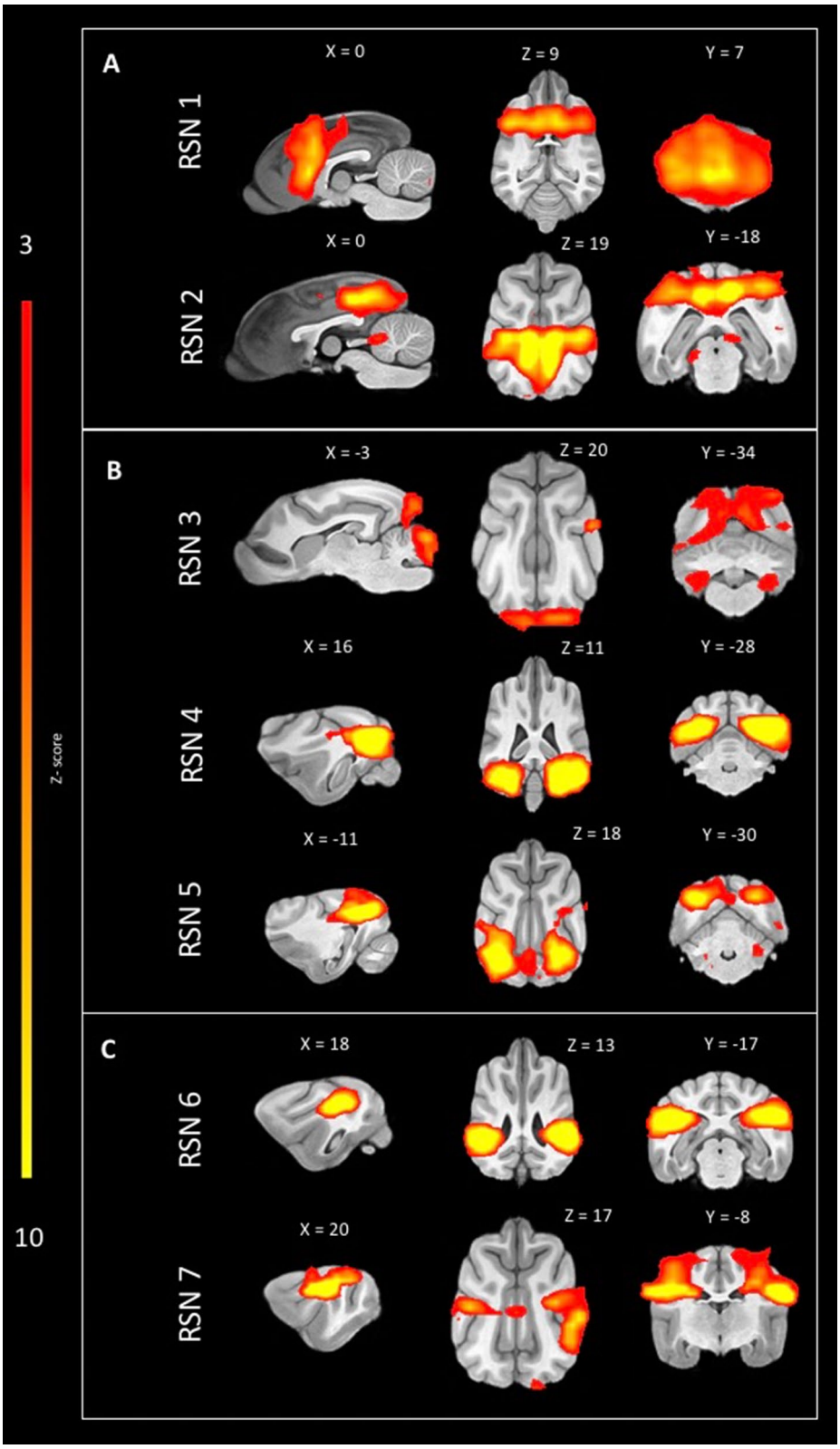

Figure 1. Sagittal, dorsal and transversal images of RSN obtained by means of group ICA of the healthy control dogs only and overlaid on a T1W open-source stereotactic atlas[46]. The results are reported as local false discovery rate controlled ($p < 0.05$) thresholded z-maps, with red-yellow color encoding using a $3 < Z$-score threshold. This figure was created using FSLeyes (version 2.1 https://fsl.fmrib.ox.ac.uk/fsl/fslwiki/FSLeyes) and Microsoft Powerpoint (version 16.16.19, http://www.microsoft.com).

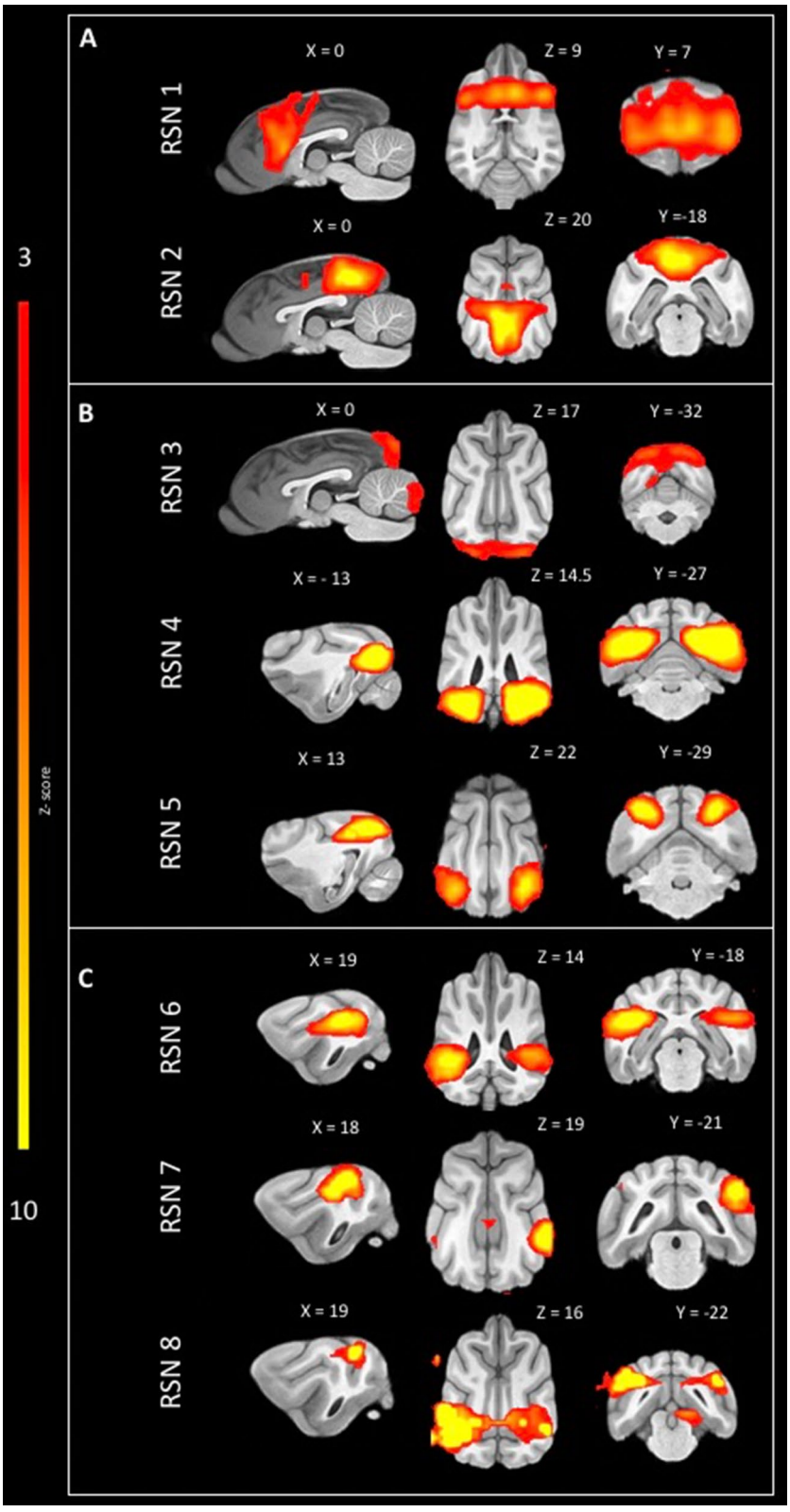

Figure 2. Sagittal, dorsal and transversal images of RSN obtained by means of group ICA of healthy control and epileptic dogs overlaid on a T1W open-source stereotactic atlas[46]. The results are reported as local false discovery rate controlled ($p < 0.05$) thresholded z-maps, with red-yellow color encoding using a $3 < Z$-score threshold. This figure was created using FSLeyes (version 2.1 https://fsl.fmrib.ox.ac.uk/fsl/fslwiki/FSLeyes) and Microsoft Powerpoint (version 16.16.19, http://www.microsoft.com).

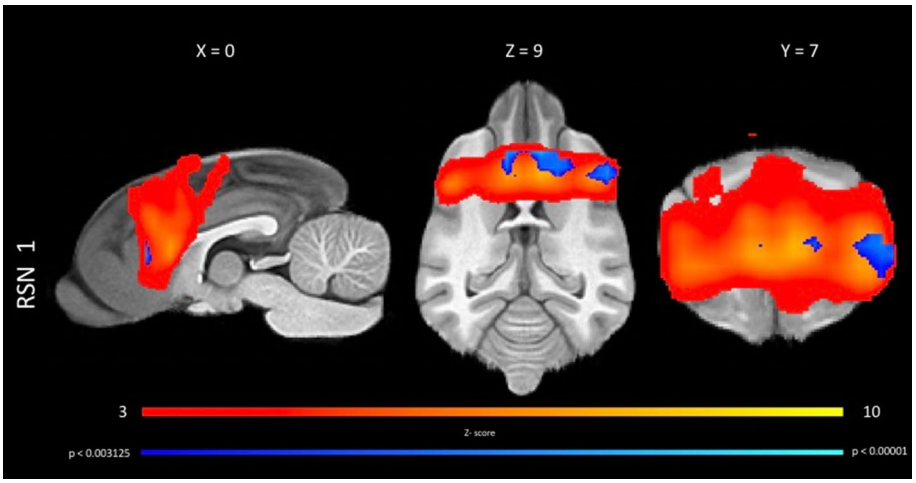

Figure 3. Results of the two-sample *t* tests for increased connectivity in the anterior DMN between the idiopathic epileptic dogs and control dogs in a sagittal, dorsal and transversal plane. The voxel with significantly increased connectivity ($p < 0.003125$) within the regions of the anterior DMN in epileptic dogs compared to healthy control dogs are shown in blue. The results are overlaid on the local false discovery rate controlled ($p < 0.05$) thresholded z-maps of the anterior DMN, with red-yellow color encoding using a $3 < Z$-score threshold and on a T1W open-source stereotactic atlas[46]. This figure was created using FSLeyes (version 2.1 https://fsl.fmrib.ox.ac.uk/fsl/fslwiki/FSLeyes) and Microsoft Powerpoint (version 16.16.19, http://www.microsoft.com).

Network	Label	Healthy controls—epileptic dogs	Epileptic dogs—healthy controls
Anterior DMN	1	0.019	0.00060*
Posterior DMN	2	0.1174	0.1092
Primary visual	3	0.47	0.0018*
Higher order visual	4	0.6532	0.4502
Higher order visual	5	0.2310	0.2482
Auditory	6	0.9980	0.1784
Auditory	7	0.086	0.6694
Somatosensory	8	0.4260	0.0354

Table 3. Dual regression analysis of independent components for comparison between healthy and epileptic dogs. *Significance set at $p < 0.003125$ after Bonferroni correction.

Discussion

Significant differences in large-scale networks in epileptic dogs compared to healthy control dogs were found in this study. The most significant difference was identified in the anterior component of the putative DMN using group independent component analysis, a purely data driven approach, and a conservative statistical approach using a Bonferroni correction for significance level. These findings notably support the hypothesis of altered large-scale networks in dogs with natural occurring idiopathic epilepsy.

In human epilepsy alteration detected in rs-fMRI depend on the underlying epileptic syndrome and therefore pattern of rs-fMRI changes have been suggested as potential diagnostic and prognostic biomarker[16]. Canine IE is not a single disease but rather an umbrella term for different epileptic syndromes[60]. These canine epileptic syndromes currently lack stringent standardization[60] and a therefore a clear homology to a specific human epileptic syndrome is still to be elucidated. In order to standardize the population in absence of well-defined epileptic syndromes, two breeds were chosen, Border Collies and Greater Swiss Mountain Dogs, with assumed genetic background and similar epileptic syndrome in regard to seizure onset, seizure semiology and response to treatment. Only dogs were included that showed the breed specific seizure pattern[26–28]. In both breeds focal onset with secondary generalization is the most common seizure type. In addition, medically refractory epilepsy is common in both breeds[26–28]. The detected increased DMN connectivity in epileptic Border Collies and Greater Swiss Mountain dogs suffering from generalized tonic–clonic seizures suggests a potential target area for further studies, but the degree of functional reorganization in dogs affected by natural occurring idiopathic epilepsy is still unknown and whether or not distinct pattern of altered connectivity, corresponding to specific pattern in human epileptic syndromes, can be found for example in different breed specific epileptic syndrome has to be proven in the future.

Group level ICA as purely data driven whole brain approach was chosen to investigate the RSN in our canine population, as this approach is beneficial in absence of strong assumptions beforehand[61]. Subject specific special maps obtained by dual regression were entered into group level analysis[58]. The individual maps from both groups were analyzed using a GLM-based group level statistical approach. The result of this group level analysis was a map in which the value of each voxel represents the test statistic or p-value obtained (Fig. 3). The highlighted voxel in the result maps (Fig. 3) essentially participated more in the anterior DMN processes of idiopathic epileptic dogs than to those of healthy control dogs. These results reflect differences in both activity and spatial spread of the processes between the groups[57]. In summary, our approach allows us to identify with a high degree of certainty the network as being different in the two groups but does not allow us to draw very firm conclusions about connectivity and shape changes and about the pathophysiological nature of these differences detected.

The DMN is the most extensively studied network in the healthy and diseased brain[62] and was the first RSN identified in dogs[40]. Compared to humans the DMN in dogs has been reported as dissociated in an anterior and posterior component. This dissociation is also supported by reduced structural connectivity between anterior and posterior cingulate cortex in dogs compared to humans[63]. In the present study, these previously described dissociation could be reproduced[39,40,63]. Nevertheless the DMN in dogs is not as well studied as in humans and proof of the function of what has been identified as DMN in dogs must still be provided[38,39].

Interestingly, in one of these putative DMN components (anterior DMN) significant differences between idiopathic epileptic dogs and healthy control dogs were found.

Group differences in the DMN in epileptic dogs are of special interest for translational research, as extensive evidence of altered connectivity of the DMN exists in humans affected by epilepsy[15,64]. With few exceptions, the DMN connectivity changes in human epilepsy are reported to be decreased[5,65]. However, increased connectivity within the anterior DMN has been identified in frontal lobe epilepsy alongside with decreased connectivity in humans[65]. Increased functional connectivity was suspected to be caused by compensatory mechanisms in this study. In general, loss of functional integrity accounts for decreased functional connectivity in rs-fMRI[9], while increased functional connectivity is more difficult to explain. Gorges et al.[9] hypothesized that increased functional connectivity reflects first/early stage of neurodegenerative diseases and epilepsy, when neuronal reserve is exhausted while normal behavior is still maintained and afterwards it transfers to a state of reduced connectivity when neuronal damage continues. A further explanation could be the loss of inhibitory influence[66]. For these reasons, a possible explanation for the increased functional connectivity seen in the anterior DMN of the epileptic dog population may be due to compensatory mechanisms.

Paralleling the results reported in human epilepsy studies, changes in functional connectivity and network topology are variable in rodent epilepsy models as well[67]. The high connectivity within the DMN in epileptic dogs appears to be similar to results of a kainite-acid rodent model for temporal lobe epilepsy[68]. In this kainic acid epilepsy model increased connectivity within the DMN, specifically the anterior cingulate cortex, without concurrently decreased connectivity in other RSN was found in rs-fMRI under isoflurane anaesthesia[68]. While behavioral, electroencephalographical and neuropathological features of kainate-induced model resemble those of temporal lobe epilepsy in humans, dispersity between rs-fMRI in the rodent model and human temporal lobe epilepsy is a known phenomenon[68]. Increased functional connectivity within the DMN in the rodent kainate-model were thought to be caused by functional reorganization following the induced status epilepticus and an expansion of the multi-synaptic projections within the areas that manifested seizure activity. The reason for this dispersity between human temporal lobe epilepsy and the rodent kainate-model was thought to be caused by bilateral, instead of unilateral, seizure onset in rodents compared to humans, as well as factors including cerebral function reserve, etiology and duration of epilepsy.

Comorbidities are increasingly recognized in canine epilepsy[29,30,33,34]. Changes in RSN concurrent with anxiety and other behavioral comorbidities have been investigated in humans[19]. In people affected by anxiety decreased and increased activation of the anterior DMN[69] in the region of the anterior cingulate cortex[70–72] have been found, consistent with impaired function of the DMN during regulation of emotions[73]. Although dog behavior suggestive for anxiety and post ictal anxiety-related aggression were reported by some owners of the epileptic dog population, whether or not the resting state changes detected in the anterior cingulate cortex in the present study also contribute to the behavior changes reported by some owner remains open. However, the fact that dogs have been successfully used as a model of selected human mental and behavioral disorders[74] and rs-fMRI may also contribute to understand the role in behavioral disorder in canine versus human epilepsy in the future.

All our dogs were scanned in general anaesthesia using an anaesthesia protocol designed to minimize effect on the RSN[39] and to match the needs for anaesthesia in clinical veterinary patients. More numerous critical parameters were recorded than in other studies during the scan[75]. No significant differences of anaesthesia related parameters were detected between the healthy controls and the idiopathic epileptic patients, indicating no anaesthesia related difference in the RSN between the two groups. Nevertheless, anaesthetic agents, unequally affect RSN and higher-order networks linked to cognition are more severely affected than lower-order, such as basic sensorimotor networks[76]. It is therefore possible, that detection of group differences in higher order networks could have been missed, as they were masked by the effect of general anaesthesia. The DMN can be reliably identified under general anaesthesia. Anterior and posterior hubs of the DMN showed decreased connectivity with continuation of anaesthesia in humans[77]. Effects of different anaesthesia protocols on the DMN of dogs has not been investigated so far. While dissociated anterior and posterior DMN components were detected in awake dogs[40] and in dogs under Ketamine/Xylazine[40] as well as under Sevoflurane anaesthesia[39], this dissociation could not be detected in another study in awake dogs[38]. Because of the standardized anaesthetic protocol applied to both groups, it is less likely that anaesthesia related cofounders cause the changes in the DMN.

Correlation between reduced connectivity and duration of epilepsy has been shown in humans[13]. Eight dogs included in our study had epilepsy for less than 3 month and only 3 dogs suffered from epilepsy for more than 1 year. Dogs affected by seizures have better chance of receiving a clinical-neurological and MRI examination

as part of their initial evaluation. It is more difficult to convince owners of follow-up examinations. It remains unclear if, by performing long-term follow up rs-fMRI in the epileptic dogs, disease progression leads to an increased number of networks showing differences in comparison to controls and if reduced instead of increased connectivity can be found with longer diseases duration.

In rodent models increased connectivity appears to be triggered by status epilepticus via functional reorganization and an expansion of the multi-synaptic projections[68]. However, only one of the included dogs had experienced status epilepticus before the MRI scan. Therefore, it is unlikely that the increased connectivity within the epileptic dog group is triggered by status epilepticus.

There are several limitations to the study. First of all, the number of dogs was limited due to ethical reasons of animal welfare for the healthy controls and due to restricted availability of clinical patients. No statistical differences between groups could be identified regarding to age, weight and anaesthesia related parameters, but it was not possible to match for age, sex and environmental background with the number of animals included. The same holds true for distribution between breeds: more border collies were included in the epileptic dogs group compared to the healthy controls, but the lack of significant differences in any of the detected RSN between the breeds in healthy controls confirms that RSN are comparable between breeds.

Second, the onset of the seizures was not documented in more than half of the dogs, and the seizure category remains unknown. In a clinical setup, this is a challenging event to document, since the majority of dog owners witness first the generalized ictal episode or post-ictal phase first.

Third, electroencephalography was not available immediately before or during the scan to rule out interictal spike activity. However, non-invasive scalp electroencephalography has several issues in dogs compared to humans related to skull thickness, muscle artefacts and restricted number of electrodes limiting its use in clinical studies[24].

Fourth, while pre- and postprocessing of rs-fMRI has been further developed over the last few years, rs-fMRI in animals, especially dogs is still in its infancy[78]. Software for registration is optimized for human use and how, for example, the artefacts in the area of the frontal sinus can be minimized by optimizing the scanning parameters is still open. Therefore, we have to treat the results with some caution, especially since the artefact of the frontal sinus, which is much more pronounced in dogs than in humans (Fig. S2), is directly adjacent to the anterior DMN. It is possible that parts of the network are obscured by signal extinction in the area of the artefact. This caution must also include the interpretation of the lateralization of the area of increased connectivity visible in the anterior DMN (Fig. 3). The apparent lateralization might be influenced by differences in signal to noise ratio between groups in this area (further information can be found in the Supplementary M1 and the Supplementary Fig. S4).

Last, all idiopathic epileptic dogs would have been investigated while drug-naïve to test the effects of epilepsy alone without the bias of medication, ideally. However, for ethical reasons it was not possible to withhold medications in a clinical scenario. More than 50% of the idiopathic epileptic dogs (9/17) were treated with various drug combinations compared to none in the healthy control group. Unfortunately, assessing their individual effect statistically in this small group of patients was not possible.

The present study further confirms the feasibility to perform rs-fMRI in dogs in a clinical setting and indicates differences between healthy controls and epileptic dogs, and consequently enhancing the potential of canine epilepsy as a translational model for human epileptic syndromes. To allow comparison of data across multiple MRI scans from different animals of a given species, it is essential to align the acquired images into a common anatomical space. We used a recently published canine neuroimaging atlas[46] that allows reporting of fMRI results with standard coordinates and in relation to anatomical structures.

Conclusion

Increased functional connectivity in large-scale brain networks, the anterior DMN and the primary visual network, can be found in Border Collies and Greater Swiss Mountain Dogs affected by natural occurring canine idiopathic epilepsy compared to healthy control dogs. This group level differences between epileptic dogs and healthy control dogs identified with using a rather simple data driven approach could serve as a starting point for more advanced resting state network analysis in epileptic dogs.

Data availability

The raw imaging data generated during the current study are available on https://openneuro.org/datasets/ds003830. The datasets generated and analyzed during the current study are available from the corresponding author on reasonable request.

Received: 22 April 2021; Accepted: 30 November 2021
Published online: 13 December 2021

References

1. (© World Health Organization 2019, 2019).
2. Kearsley-Fleet, L., O'Neill, D. G., Volk, H. A., Church, D. B. & Brodbelt, D. C. Prevalence and risk factors for canine epilepsy of unknown origin in the UK. *Vet. Rec.* **172**, 338. https://doi.org/10.1136/vr.101133 (2013).
3. Heske, L., Nødtvedt, A., Jäderlund, K. H., Berendt, M. & Egenvall, A. A cohort study of epilepsy among 665,000 insured dogs: Incidence, mortality and survival after diagnosis. *Vet. J.* **202**, 471–476. https://doi.org/10.1016/j.tvjl.2014.09.023 (2014).
4. Berg, A. T. *et al.* Revised terminology and concepts for organization of seizures and epilepsies: Report of the ILAE Commission on Classification and Terminology, 2005–2009. *Epilepsia* **51**, 676–685. https://doi.org/10.1111/j.1528-1167.2010.02522.x (2010).
5. Gonen, O. M., Kwan, P., O'Brien, T. J., Lui, E. & Desmond, P. M. Resting-state functional MRI of the default mode network in epilepsy. *Epilepsy Behav.* **111**, 107308. https://doi.org/10.1016/j.yebeh.2020.107308 (2020).

6. Tracy, J. I. & Doucet, G. E. Resting-state functional connectivity in epilepsy: Growing relevance for clinical decision making. *Curr. Opin. Neurol.* **28**, 158–165. https://doi.org/10.1097/wco.0000000000000178 (2015).
7. Centeno, M. & Carmichael, D. W. Network connectivity in epilepsy: Resting state fMRI and EEG-fMRI contributions. *Front. Neurol.* **5**, 93. https://doi.org/10.3389/fneur.2014.00093 (2014).
8. Wurina, Zang, Y. F. & Zhao, S. G. Resting-state fMRI studies in epilepsy. *Neurosci. Bull.* **28**, 449–455. https://doi.org/10.1007/s12264-012-1255-1 (2012).
9. Gorges, M. *et al.* Functional connectivity mapping in the animal model: Principles and applications of resting-state fMRI. *Front. Neurol.* **8**, 200–200. https://doi.org/10.3389/fneur.2017.00200 (2017).
10. Hanael, E. *et al.* Blood–brain barrier dysfunction in canine epileptic seizures detected by dynamic contrast-enhanced magnetic resonance imaging. *Epilepsia* **60**, 1005–1016. https://doi.org/10.1111/epi.14739 (2019).
11. Patterson, E. E. Canine epilepsy: An underutilized model. *ILAR J.* **55**, 182–186. https://doi.org/10.1093/ilar/ilu021 (2014).
12. Zhang, Z. *et al.* Impaired attention network in temporal lobe epilepsy: A resting FMRI study. *Neurosci. Lett.* **458**, 97–101. https://doi.org/10.1016/j.neulet.2009.04.040 (2009).
13. Zhang, Z. *et al.* Impaired perceptual networks in temporal lobe epilepsy revealed by resting fMRI. *J. Neurol.* **256**, 1705–1713. https://doi.org/10.1007/s00415-009-5187-2 (2009).
14. Liao, W. *et al.* Default mode network abnormalities in mesial temporal lobe epilepsy: A study combining fMRI and DTI. *Hum. Brain Mapp.* **32**, 883–895. https://doi.org/10.1002/hbm.21076 (2011).
15. McGill, M. L. *et al.* Default mode network abnormalities in idiopathic generalized epilepsy. *Epilepsy Behav.* **23**, 353–359. https://doi.org/10.1016/j.yebeh.2012.01.013 (2012).
16. Pressl, C. *et al.* Resting state functional connectivity patterns associated with pharmacological treatment resistance in temporal lobe epilepsy. *Epilepsy Res.* **149**, 37–43. https://doi.org/10.1016/j.eplepsyres.2018.11.002 (2019).
17. Tellez-Zenteno, J. F., Patten, S. B., Jetté, N., Williams, J. & Wiebe, S. Psychiatric comorbidity in epilepsy: A population-based analysis. *Epilepsia* **48**, 2336–2344. https://doi.org/10.1111/j.1528-1167.2007.01222.x (2007).
18. Forthoffer, N., Brissart, H., Tyvaert, L. & Maillard, L. Long-term cognitive outcomes in patient with epilepsy. *Rev. Neurol. (Paris)* **176**, 448–455. https://doi.org/10.1016/j.neurol.2020.04.012 (2020).
19. Colmers, P. L. W. & Maguire, J. Network dysfunction in comorbid psychiatric illnesses and epilepsy. *Epilepsy Curr.* **20**, 205–210. https://doi.org/10.1177/1535759720934787 (2020).
20. Chandler, K. Canine epilepsy: What can we learn from human seizure disorders?. *Vet. J.* **172**, 207–217. https://doi.org/10.1016/j.tvjl.2005.07.001 (2006).
21. Potschka, H., Fischer, A., von Rüden, E. L., Hülsmeyer, V. & Baumgärtner, W. Canine epilepsy as a translational model?. *Epilepsia* **54**, 571–579. https://doi.org/10.1111/epi.12138 (2013).
22. Howbert, J. J. *et al.* Forecasting seizures in dogs with naturally occurring epilepsy. *PLoS One* **9**, e81920. https://doi.org/10.1371/journal.pone.0081920 (2014).
23. Gregg, N. M. *et al.* Circadian and multiday seizure periodicities, and seizure clusters in canine epilepsy. *Brain Commun.* **2**, fcaa008. https://doi.org/10.1093/braincomms/fcaa008 (2020).
24. Uriarte, A. & Maestro Saiz, I. Canine versus human epilepsy: Are we up to date?. *J. Small Anim. Pract.* **57**, 115–121. https://doi.org/10.1111/jsap.12437 (2016).
25. Matiasek, K. *et al.* International veterinary epilepsy task force recommendations for systematic sampling and processing of brains from epileptic dogs and cats. *BMC Vet. Res.* **11**, 216. https://doi.org/10.1186/s12917-015-0467-9 (2015).
26. Hülsmeyer, V., Zimmermann, R., Brauer, C., Sauter-Louis, C. & Fischer, A. Epilepsy in Border Collies: Clinical manifestation, outcome, and mode of inheritance. *J. Vet. Intern. Med.* **24**, 171–178. https://doi.org/10.1111/j.1939-1676.2009.0438.x (2010).
27. Hülsmeyer, V. I. *et al.* International Veterinary Epilepsy Task Force's current understanding of idiopathic epilepsy of genetic or suspected genetic origin in purebred dogs. *BMC Vet. Res.* **11**, 175. https://doi.org/10.1186/s12917-015-0463-0 (2015).
28. Sauer-Delhées, S., Steffen, F., Reichler, I. & Beckmann, K. Clinical characteristics of idiopathic epilepsy in Greater Swiss Mountain dogs in Switzerland. *Schweiz. Arch. Tierheilkd.* **162**, 697–706. https://doi.org/10.17236/sat00279 (2020).
29. Shihab, N., Bowen, J. & Volk, H. A. Behavioral changes in dogs associated with the development of idiopathic epilepsy. *Epilepsy Behav.* **21**, 160–167. https://doi.org/10.1016/j.yebeh.2011.03.018 (2011).
30. Jokinen, T. S. *et al.* Behavioral abnormalities in Lagotto Romagnolo dogs with a history of benign familial juvenile epilepsy: A long-term follow-up study. *J. Vet. Intern. Med.* **29**, 1081–1087. https://doi.org/10.1111/jvim.12611 (2015).
31. Packer, R. M. *et al.* Effects of a ketogenic diet on ADHD-like behavior in dogs with idiopathic epilepsy. *Epilepsy Behav.* **55**, 62–68. https://doi.org/10.1016/j.yebeh.2015.11.014 (2016).
32. Winter, J., Packer, R. M. A. & Volk, H. A. Preliminary assessment of cognitive impairments in canine idiopathic epilepsy. *Vet. Rec.* **182**, 633. https://doi.org/10.1136/vr.104603 (2018).
33. Packer, R. M. A. *et al.* Cognitive dysfunction in naturally occurring canine idiopathic epilepsy. *PLoS One* **13**, e0192182. https://doi.org/10.1371/journal.pone.0192182 (2018).
34. Packer, R. M. & Volk, H. A. Epilepsy beyond seizures: A review of the impact of epilepsy and its comorbidities on health-related quality of life in dogs. *Vet. Rec.* **177**, 306–315. https://doi.org/10.1136/vr.103360 (2015).
35. Watson, F. *et al.* A review of treatment options for behavioural manifestations of clinical anxiety as a comorbidity in dogs with idiopathic epilepsy. *Vet. J.* **238**, 1–9. https://doi.org/10.1016/j.tvjl.2018.06.001 (2018).
36. Rusbridge, C. *et al.* International Veterinary Epilepsy Task Force recommendations for a veterinary epilepsy-specific MRI protocol. *BMC Vet. Res.* **11**, 194. https://doi.org/10.1186/s12917-015-0466-x (2015).
37. Hasegawa, D. Diagnostic techniques to detect the epileptogenic zone: Pathophysiological and presurgical analysis of epilepsy in dogs and cats. *Vet. J.* https://doi.org/10.1016/j.tvjl.2016.03.005 (2016).
38. Szabó, D. *et al.* Resting-state fMRI data of awake dogs (*Canis familiaris*) via group-level independent component analysis reveal multiple, spatially distributed resting-state networks. *Sci. Rep.* **9**, 15270. https://doi.org/10.1038/s41598-019-51752-2 (2019).
39. Beckmann, K. M. *et al.* Resting state networks of the canine brain under sevoflurane anaesthesia. *PLoS One* **15**, e0231955. https://doi.org/10.1371/journal.pone.0231955 (2020).
40. Kyathanahally, S. P. *et al.* Anterior-posterior dissociation of the default mode network in dogs. *Brain Struct. Funct.* **220**, 1063–1076. https://doi.org/10.1007/s00429-013-0700-x (2015).
41. Xiao, F., An, D. & Zhou, D. Functional MRI-based connectivity analysis: A promising tool for the investigation of the pathophysiology and comorbidity of epilepsy. *Seizure* **44**, 37–41. https://doi.org/10.1016/j.seizure.2016.10.003 (2017).
42. De Risio, L. *et al.* International veterinary epilepsy task force consensus proposal: Diagnostic approach to epilepsy in dogs. *BMC Vet. Res.* **11**, 148. https://doi.org/10.1186/s12917-015-0462-1 (2015).
43. Jenkinson, M., Bannister, P., Brady, M. & Smith, S. Improved optimization for the robust and accurate linear registration and motion correction of brain images. *Neuroimage* **17**, 825–841. https://doi.org/10.1016/s1053-8119(02)91132-8 (2002).
44. Smith, S. M. Fast robust automated brain extraction. *Hum. Brain Mapp.* **17**, 143–155. https://doi.org/10.1002/hbm.10062 (2002).
45. Jenkinson, M. & Smith, S. A global optimisation method for robust affine registration of brain images. *Med. Image Anal.* **5**, 143–156. https://doi.org/10.1016/s1361-8415(01)00036-6 (2001).
46. Johnson, P. J. *et al.* Stereotactic cortical atlas of the domestic canine brain. *Sci. Rep.* **10**, 4781. https://doi.org/10.1038/s41598-020-61665-0 (2020).
47. Andersson, J. L. R., Jenkinson, M. & Smith, S. *Non-Linear Optimisation* (FMRIB technical report TR07JA1, 2007).

48. Andersson, J. L. R., Jenkinson, M. & Smith, S. *Non-Linear Registration, aka Spatial Normalisation* (FMRIB technical report TR07JA2, 2007).
49. Beckmann, C. F. & Smith, S. M. Probabilistic independent component analysis for functional magnetic resonance imaging. *IEEE Trans. Med. Imaging* **23**, 137–152. https://doi.org/10.1109/tmi.2003.822821 (2004).
50. Hyvärinen, A. Fast and robust fixed-point algorithms for independent component analysis. *IEEE Trans. Neural Netw.* **10**, 626–634. https://doi.org/10.1109/72.761722 (1999).
51. Beckmann, C. F. & Smith, S. M. Tensorial extensions of independent component analysis for multisubject FMRI analysis. *Neuroimage* **25**, 294–311. https://doi.org/10.1016/j.neuroimage.2004.10.043 (2005).
52. Andics, A., Gacsi, M., Farago, T., Kis, A. & Miklosi, A. Voice-sensitive regions in the dog and human brain are revealed by comparative fMRI. *Curr. Biol. CB* **24**, 574–578. https://doi.org/10.1016/j.cub.2014.01.058 (2014).
53. Aguirre, G. K. *et al.* Canine and human visual cortex intact and responsive despite early retinal blindness from RPE65 mutation. *PLoS Med.* **4**, 1117–1128. https://doi.org/10.1371/journal.pmed.0040230 (2007).
54. Bach, J. P. *et al.* Functional magnetic resonance imaging of the ascending stages of the auditory system in dogs. *BMC Vet. Res.* **9**, 210. https://doi.org/10.1186/1746-6148-9-210 (2013).
55. Dilks, D. D. *et al.* Awake fMRI reveals a specialized region in dog temporal cortex for face processing. *PeerJ* **3**, e1115. https://doi.org/10.7717/peerj.1115 (2015).
56. Willis, C. K. R. *et al.* Functional MRI as a tool to assess vision in dogs: The optimal anesthetic. *Vet. Ophthalmol.* **4**, 243–253. https://doi.org/10.1046/j.1463-5216.2001.00183.x (2001).
57. Nickerson, L. D., Smith, S. M., Öngür, D. & Beckmann, C. F. Using dual regression to investigate network shape and amplitude in functional connectivity analyses. *Front. Neurosci.* **11**, 115. https://doi.org/10.3389/fnins.2017.00115 (2017).
58. Beckmann, C. F., Mackay, C. E., Filippini, N. & Smith, S. M. Group comparison of resting-state FMRI data using multi-subject ICA and dual regression. *Neuroimage* **47**(Suppl 1), S148 (2009).
59. Uddin, L. Q., Yeo, B. T. T. & Spreng, R. N. Towards a universal taxonomy of macro-scale functional human brain networks. *Brain Topogr.* **32**, 926–942. https://doi.org/10.1007/s10548-019-00744-6 (2019).
60. Berendt, M. *et al.* International veterinary epilepsy task force consensus report on epilepsy definition, classification and terminology in companion animals. *BMC Vet. Res.* **11**, 182. https://doi.org/10.1186/s12917-015-0461-2 (2015).
61. Beckmann, C. F., DeLuca, M., Devlin, J. T. & Smith, S. M. Investigations into resting-state connectivity using independent component analysis. Philos. Trans. R. *Soc. Lond. Ser. B Biol. Sci.* **360**, 1001–1013. https://doi.org/10.1098/rstb.2005.1634 (2005).
62. Buckner, R. L., Andrews-Hanna, J. R. & Schacter, D. L. The brain's default network: Anatomy, function, and relevance to disease. *Ann. N. Y. Acad. Sci.* **1124**, 1–38. https://doi.org/10.1196/annals.1440.011 (2008).
63. Robinson, J. L. *et al.* Characterization of structural connectivity of the default mode network in dogs using diffusion tensor imaging. *Sci. Rep.* **6**, 36851. https://doi.org/10.1038/srep36851 (2016).
64. Yang, S. *et al.* Temporal variability profiling of the default mode across epilepsy subtypes. *Epilepsia* https://doi.org/10.1111/epi.16759 (2020).
65. Cao, X. *et al.* Altered intrinsic connectivity networks in frontal lobe epilepsy: A resting-state fMRI study. *Comput. Math. Methods Med.* **2014**, 864979. https://doi.org/10.1155/2014/864979 (2014).
66. Douaud, G., Filippini, N., Knight, S., Talbot, K. & Turner, M. R. Integration of structural and functional magnetic resonance imaging in amyotrophic lateral sclerosis. *Brain* **134**, 3470–3479. https://doi.org/10.1093/brain/awr279 (2011).
67. Christiaen, E. *et al.* Alterations in the functional brain network in a rat model of epileptogenesis: A longitudinal resting state fMRI study. *Neuroimage* **202**, 116144. https://doi.org/10.1016/j.neuroimage.2019.116144 (2019).
68. Gill, R. S., Mirsattari, S. M. & Leung, L. S. Resting state functional network disruptions in a kainic acid model of temporal lobe epilepsy. *Neuroimage* **13**, 70–81. https://doi.org/10.1016/j.nicl.2016.11.002 (2017).
69. Sylvester, C. M. *et al.* Functional network dysfunction in anxiety and anxiety disorders. *Trends Neurosci.* **35**, 527–535. https://doi.org/10.1016/j.tins.2012.04.012 (2012).
70. McClure, E. B. *et al.* Abnormal attention modulation of fear circuit function in pediatric generalized anxiety disorder. *Arch. Gen. Psychiatry* **64**, 97–106. https://doi.org/10.1001/archpsyc.64.1.97 (2007).
71. Boshuisen, M. L., Ter Horst, G. J., Paans, A. M. J., Reinders, A. A. T. S. & den Boer, J. A. rCBF differences between panic disorder patients and control subjects during anticipatory anxiety and rest. *Biol. Psychiatry* **52**, 126–135. https://doi.org/10.1016/S0006-3223(02)01355-0 (2002).
72. Blair, K. *et al.* Response to emotional expressions in generalized social phobia and generalized anxiety disorder: Evidence for separate disorders. *Am. J. Psychiatry* **165**, 1193–1202. https://doi.org/10.1176/appi.ajp.2008.07071060 (2008).
73. Campbell-Sills, L. *et al.* Functioning of neural systems supporting emotion regulation in anxiety-prone individuals. *Neuroimage* **54**, 689–696. https://doi.org/10.1016/j.neuroimage.2010.07.041 (2011).
74. Danek, M., Danek, J. & Araszkiewicz, A. Large animals as potential models of human mental and behavioral disorders. *Psychiatr. Pol.* **51**, 1009–1027. https://doi.org/10.12740/PP/74304 (2017).
75. Steiner, A. R., Rousseau-Blass, F., Schroeter, A., Hartnack, S. & Bettschart-Wolfensberger, R. Systematic review: Anaesthetic protocols and management as confounders in rodent blood oxygen level dependent functional magnetic resonance imaging (BOLD fMRI)—Part A: Effects of changes in physiological parameters. *Front. Neurosci.* **14**, 577119. https://doi.org/10.3389/fnins.2020.577119 (2020).
76. Paasonen, J., Stenroos, P., Salo, R. A., Kiviniemi, V. & Gröhn, O. Functional connectivity under six anesthesia protocols and the awake condition in rat brain. *Neuroimage* **172**, 9–20. https://doi.org/10.1016/j.neuroimage.2018.01.014 (2018).
77. Metwali, H., Ibrahim, T. & Raemaekers, M. Changes in intranetwork functional connectivity of resting state networks between sessions under anesthesia in neurosurgical patients. *World Neurosurg.* https://doi.org/10.1016/j.wneu.2020.10.102 (2020).
78. Mandino, F. *et al.* Animal functional magnetic resonance imaging: Trends and path toward standardization. *Front. Neuroinform.* https://doi.org/10.3389/fninf.2019.00078 (2020).

Acknowledgements

We are grateful to Jens Lehmann for his technical assistance in running the postprocessing and to Manuela Wieser for her assistance in the conduction of the study. This research was partially financially supported by the "Albert-Heim-Stiftung" and the "Stiftung für Kleintiere der Vetsuisse-Fakultät Universität Zürich".

Author contributions

K.B., H.R., I.C., M.D. and S.H. designed the experiment; K.B., F.S., M.D. and R.B. conducted the experiment; K.B., A.W. and H.R. analyzed the data; K.B. wrote the main manuskript text and prepared the figures. All authors reviewed the manuscript.

Competing interests

The authors declare no competing interests.

Additional information

Supplementary Information The online version contains supplementary material available at https://doi.org/10.1038/s41598-021-03349-x.

Correspondence and requests for materials should be addressed to K.M.B.

Reprints and permissions information is available at www.nature.com/reprints.

Publisher's note Springer Nature remains neutral with regard to jurisdictional claims in published maps and institutional affiliations.

frontiers | Frontiers in Veterinary Science

ORIGINAL RESEARCH
published: 07 July 2022
doi: 10.3389/fvets.2022.885044

Single-Voxel Proton Magnetic Resonance Spectroscopy of the Thalamus in Idiopathic Epileptic Dogs and in Healthy Control Dogs

Nico Mauri[1,2], *Henning Richter*[1], *Frank Steffen*[3], *Niklaus Zölch*[4†] *and Katrin M. Beckmann*[3*†]

[1] Clinic for Diagnostic Imaging, Department of Diagnostics and Clinical Services, Vetsuisse Faculty, University of Zurich, Zurich, Switzerland, [2] Vetimage Diagnostik GmbH, Oberentfelden, Switzerland, [3] Section of Neurology and Neurosurgery, Small Animal Clinic, Vetsuisse Faculty, University of Zurich, Zurich, Switzerland, [4] Department of Forensic Medicine and Imaging, Institute of Forensic Medicine, University of Zurich, Zurich, Switzerland

OPEN ACCESS

Edited by:
Holger Andreas Volk,
University of Veterinary Medicine Hannover, Germany

Reviewed by:
Sebastian Meller,
University of Veterinary Medicine Hanover Foundation, Germany
Curtis Wells Dewey,
Elemental Pet Vets, PLLC, United States

***Correspondence:**
Katrin M. Beckmann
katrin.beckmann@vetclinics.uzh.ch

[†] These authors have contributed equally to this work and share last authorship

Specialty section:
This article was submitted to Veterinary Neurology and Neurosurgery, a section of the journal Frontiers in Veterinary Science

Received: 27 February 2022
Accepted: 14 June 2022
Published: 07 July 2022

Citation:
Mauri N, Richter H, Steffen F, Zölch N and Beckmann KM (2022) Single-Voxel Proton Magnetic Resonance Spectroscopy of the Thalamus in Idiopathic Epileptic Dogs and in Healthy Control Dogs. Front. Vet. Sci. 9:885044. doi: 10.3389/fvets.2022.885044

The role of magnetic resonance spectroscopy (MRS) in the investigation of brain metabolites in epileptic syndromes in dogs has not been explored systematically to date. The aim of this study was to investigate metabolites in the thalamus in dogs affected by idiopathic epilepsy (IE) with and without antiepileptic drug treatment (AEDT) and to compare them to unaffected controls. Our hypothesis is that similar to humans with generalized epilepsy and loss of consciousness, N-acetyl aspartate (NAA) would be reduced, and glutamate–glutamine (Glx) would be increased in treated and untreated IE in comparison with the control group. In this prospective case–control study, Border Collie (BC) and Greater Swiss Mountain dog (GSMD) were divided into three groups: (1) healthy controls, IE with generalized tonic–clonic seizures with (2) and without (3) AEDT. A total of 41 BC and GSMD were included using 3 Tesla single-voxel proton MRS of the thalamus (PRESS localization, shortest TE, TR = 2000 ms, NSA = 240). After exclusion of 11 dogs, 30 dogs (18 IE and 12 healthy controls) remained available for analysis. Metabolite concentrations were estimated with LCModel using creatine as reference and compared using Kruskal–Wallis and Wilcoxon rank-sum tests. The Kruskal–Wallis test revealed significant differences in the NAA-to-creatine ($p = 0.04$) and Glx-to-creatine ($p = 0.03$) ratios between the three groups. The Wilcoxon rank-sum test further showed significant reduction in the NAA/creatine ratio in idiopathic epileptic dogs under AEDT compared to epileptic dogs without AEDT ($p = 0.03$) and compared to healthy controls ($p = 0.03$). In opposite to humans, Glx/creatine ratio was significantly reduced in dogs with IE under AEDT compared to epileptic dogs without AEDT ($p = 0.03$) and controls ($p = 0.02$). IE without AEDT and healthy controls did not show significant difference, neither in NAA/creatine ($p = 0.60$), nor in Glx-to-creatine ($p = 0.55$) ratio. In conclusion, MRS showed changes in dogs with IE and generalized seizures under AEDT, but not in those without AEDT. Based upon these results, MRS can be considered a useful advanced imaging technique for the evaluation of dogs with IE in the clinical and research settings.

Keywords: MRS—^{1}H nuclear magnetic resonance spectra, N-acetyl aspartate (NAA), glutamine (Gln), glutamate (Glu), glutamate-glutamine (Glx), canine, generalized seizures

INTRODUCTION

Advanced neuroimaging has been recently introduced in the diagnostic work-up and research of canine epilepsy (1, 2). One of these advanced neuroimaging techniques is magnetic resonance spectroscopy (MRS). In human epilepsy, MRS is, among other techniques, widely used to rule out metabolic diseases in structural negative epilepsy (3), for presurgical evaluation (3), and to study the biochemical composition during drug treatments (4, 5). MRS studies investigating canine epilepsy are sparse. Few case reports and studies showed the utility of MRS in genetic (6) and in structural epilepsy (7, 8). However, only one study examined MRS in idiopathic epileptic dogs (9).

MRS allows non-invasive estimation of metabolite concentrations within a selected volume of interest (VOI) by exploiting slight changes in the magnetic field sensed by nuclei, usually ^{1}H protons, in different metabolites. This so-called chemical shift results in specific peaks for different metabolites in a frequency spectrum (10). Metabolites that can be identified with MRS at 3 Tesla (3T) and are of specific interest in epilepsy include excitatory and inhibitory neurotransmitters, such as glutamate and gamma-amino-butyrate (GABA), but also markers for neuronal integrity, such as N-acetyl aspartate (NAA) (11).

Glutamate is the main excitatory neurotransmitter in the brain. Due to the overlap of glutamate and glutamine spectra and the difficulties in separating these two spectra at field strength lower than 3T, glutamate is commonly reported together with glutamine as glutamate–glutamine complex (Glx) (12). Excessive glutamate release is observed in chronic epilepsy and associated with recurrent seizures (13). In human epilepsy, significant changes in Glx have been identified in different brain regions depending on the underlying epileptic syndrome (11). While for temporal lobe epilepsy with hippocampal necrosis, reduced Glx was found in the ipsilateral hippocampus (14), and increased levels of Glx were detected in the medial prefrontal cortex in juvenile myoclonus epilepsy (15).

GABA is the major inhibitory neurotransmitter of the central nervous system. Furthermore, many antiepileptic drugs target the GABA system and cause increased GABA concentration in the brain (4). However, MRS evaluation of GABA is challenging. GABA concentration compared to other brain metabolites is much lower, and the peaks of GABA in MRS overlap with those of other metabolites (16). Because advanced techniques, such as spectral editing seem unavoidable to obtain reliable results at 3T, information regarding GABA levels in epilepsy is still scarce (11, 17).

NAA is one of the molecules with the highest concentration in the brain (18). Its function in the brain is still controversial and under investigation (18). NAA is mostly reported together with the neurotransmitter N-acetylaspartylglutamate (NAAG) as total NAA (tNAA) because these signals cannot be reliably separated under common conditions (19). NAA is an intraneuronal metabolite synthetized in the mitochondria. Although NAA is not only present in neurons but also in oligodendrocytes/myelin, NAA in MRS is considered the key neuronal marker for brain neuronal health, viability, and number of neurons (18). In human epilepsy, focal reductions in NAA were found in different forms of temporal lobe epilepsy (20). Furthermore, recovery of the NAA levels after successful epilepsy surgery was reported (21).

The presented clinical applications in human medicine demonstrate that alterations in brain metabolites can be detected with MRS. However, one should notice that the brain regions where these alterations can be detected, as well as the magnitude of the alterations strongly depends on the specific underlying epileptic syndrome are not uniform.

In single-voxel MRS, a VOI has to be selected. This represents a major challenge in veterinary medicine. First, because epileptic syndromes are not as well characterized in dogs as in humans (22). Second, as the main target area within the brain in canine epilepsy remains undefined and may be variable in subpopulations of dogs diagnosed with idiopathic epilepsy (IE).

To overcome the issue of the heterogenicity in canine epileptic syndromes, we decided to select breeds with rather well-characterized epileptic syndrome and familiar history of epilepsy, suggesting a common genetic background for the diseases in this breed (23). From those dog breeds presented to our hospital more commonly with IE, Border Collie (BC) and Greater Swiss Mountain Dog (GSMD) met these criteria (24, 25).

Target volume definition is more difficult to solve. One could argue that multivoxel MRS assessing the whole brain could be an alternative. However, standard multivoxel MRS at 3T suffers from long acquisition times, low spatial resolutions, and variable quality (26, 27). With regard to these problems, we decided to use single-voxel MRS, thus, facing the challenge of selecting a specific target VOI. In a recent study, Olszewska at al. selected the temporal lobe as target area in canine IE (9). However, the involvement of the temporal lobe in canine epilepsy is still controversial (9). In humans, a recent MRS study demonstrated alteration of brain metabolites in the thalamus in people affected by the loss of consciousness during seizures (28). Also, BC and GSMD are affected by generalized tonic–clonic seizures which are associated with the loss of consciousness (22). The thalamus is one of the most important center associated with the loss of consciousness in epilepsy in people (29). This together with the thalamic MRS changes detected in humans with the loss of consciousness during epileptic seizures makes the thalamus an appropriate target area for MRS evaluation also in dogs with seizures accompanied by the loss of consciousness.

The purpose of our study was therefore to assess and compare thalamic MRS spectra in healthy control dogs and in IE dogs affected by generalized seizures with a focus on NAA and Glx. Another aim of this study was to assess possible differences between IE dogs with and without antiepileptic drug treatment (IE with AEDT and IE without AEDT, respectively). Our hypothesis was that IE-affected dogs, similar to humans

Abbreviations: BC, Border Collie; Choline, Cho; CRLBs, Cramér Rao lower bounds; GABA, Gamma-aminobutyric acid; Glx, glutamate–glutamine complex; GSMD, Greater Swiss Mountain Dog; Hz, Hertz; IE, idiopathic epilepsy or idiopathic epileptic; LCModel, linear combination model; MRI, magnetic resonance imaging; MRS, magnetic resonance spectroscopy; NAA, N-acetyl aspartate; NAAG, N-acetylaspartylglutamate; NSA, number of signal averages; PRESS, point-resolved spectroscopy; SNR, signal-to-noise ratio; T, Tesla; VOI, volume of interest.

with seizures and loss of consciousness, show elevated Glx and reduced NAA concentration in the thalamus compared to control dogs and that significant differences in NAA and Glx could be detected between treated and untreated dogs with IE.

MATERIALS AND METHODS

Study Population

This prospective study was performed between 2017 and 2021 at the Veterinary hospital of the University of Zurich after approval by the cantonal authorities according to Swiss law under animal license no. ZH272/16 and ZH046/20.

We recruited GSMD and BC dogs with presumptive diagnosis of IE (cases) and clinically healthy relatives, GSMD and BC (controls) of the prospectively enrolled cases. Dogs affected by IE had to fulfill the TIER II criteria for IE of the veterinary epilepsy task force (suspected genetic epilepsy) (30) and had to show generalized tonic–clonic seizures.

All dogs underwent complete clinical and neurological examination performed by a board-certified veterinary neurologist, blood screening for metabolic epilepsy, magnetic resonance imaging (MRI) of the brain, and MRS of the thalamus. Dogs with IE had additionally cerebrospinal fluid (CSF) analyses performed.

The IE dogs were divided into two groups: one group of IE dog was drug-naïve (IE without AEDT), and the other one already received AEDT (IE with AEDT).

Exclusion criteria were MRS of nondiagnostic quality, voxel placement outside of the thalamus, abnormal clinical or neurological examination, abnormal CSF analyses, or identification of an underlying cause for the epilepsy.

Procedures

All dogs underwent MRI and MRS under general anesthesia with a standardized anesthesia protocol previously described (31). A part of the dogs included in this study has also been included in the aforementioned study.

MRI and MRS were performed with a 3T MRI (Philips Ingenia scanner, Philips AG, Zurich, Switzerland) with a 15-channel receive–transmit head coil (Stream Head-Spine coil solution, Philips AG, Zurich, Switzerland) in all patients.

Conventional morphological MR images included T2-weighted (W) turbo spin-echo sequences in transverse, dorsal, and sagittal planes, a fluid-attenuated inversion recovery (FLAIR), a T2* or a susceptibility-weighted sequence, and diffusion-weighted images in transverse, as well as a 3D T1-W sequence before and after intravenous injection of contrast media [gadodiamide (Omniscan) 0.3 mmol/kg, GE Healthcare AG, Glattbrugg, Switzerland, or gadoteric acid (Dotarem) 0.3 mmol/kg, Guerbet AG, Zürich, Switzerland].

Single-voxel MRS of the thalamus was performed with a previously described optimized protocol (32). In brief, transverse, dorsal, and sagittal T2-W images were used to graphically place the single voxel in the thalamus, preferably in the right thalamus. Voxel size was 1.8 cm^3 (10 x 12 x 15 mm), and care was taken to avoid CSF, as well as peripheral soft and bony tissues adjacent to the thalamus to prevent lipid contamination. Before MRS acquisition with point-resolved spectroscopy (PRESS) localization and water suppression using the excitation technique, field homogeneity was optimized with a second-order automatic pencil-beam shim. In addition, a water-unsuppressed spectrum was obtained as concentration reference to estimate metabolite concentrations. Spectra were obtained using the following parameters: shortest possible echo time (TE): 29 to 31 ms; repetition time (TR): 2,000 ms; number of signal averages (NSA): 240; bandwidth: 2,000 Hz. Spectra outside the thalamus and spectra with the presence of artifacts (e.g., presence of strong lipid contamination) were excluded based on visual inspection.

MRI image evaluation and visual MRS analyses were performed on each dog by a board-certified veterinary radiologist or a resident in diagnostic imaging under direct supervision of a board-certified veterinary radiologist.

Data Processing

Metabolite concentrations were estimated, as described before (32) with an automated data processing spectral fitting algorithm (linear combination model, LCModel, version 6.3, S Provencher, Oakville, ON, Canada) using a simulated basis set (details can be found in **Supplementary Table S1**).

To translate the fitted MRS signals into estimates of the metabolite concentrations, an external or internal reference is needed (33). The most common internal reference used in human medicine is tissue water signal (33). Tissue water signal has the advantage of being about 10,000 times higher than the signal of the metabolites. In addition, water signal does not have to be resolved from overlapping metabolites. Nevertheless, to use reliably tissue water signal, segmentation of voxel into gray, white matter, and CSF is recommended, especially to correct for the CSF contamination in the measured voxel (33). Because tissue segmentation was not available in our study, we initially opted for total creatine (tCr, sum of creatine and phosphocreatine) as an internal reference. However, as creatine is a marker for energy metabolism, creatine ratios have the disadvantage that this metabolite can also be affected by some diseases and by the process of aging (33). Successively, we also used the water signal as reference in order to check the results obtained with the creatine ratios.

Metabolite-to-water ratios expressed in institutional units were derived within LCModel using the unsuppressed water signal with a global correction for the relaxation attenuation of the water signal (ATTH20 = 0.7) and estimation of the water concentration in the measured voxel of WCONC = 43300. Metabolite signals were not corrected for relaxation attenuation.

To assess the quality of the spectra, signal-to-noise ratio (SNR), linewidth in form of full width at half maximum (FWHM), and relative Cramér Rao lower bounds (%CRLBs) as estimation of the lower bounds of fitting error (34) were collected from the LCModel output. In addition, the FWHM of the unsuppressed water scan was measured.

Comparison of metabolite ratios and MRS spectra in the thalamus was performed between dogs affected by IE with and without AEDT and healthy control dogs.

TABLE 1 | Population characteristics.

	Healthy controls	IE without AEDT	IE with AEDT
Breed			
BC	2	2	6
GSMD	10	7	3
Sex			
Male	8	6	4
Male castrated	-	-	1
Female	4	3	-
Female spayed	-	-	4
Bodyweight			
kg (median, range)	47.5, 20–55	48, 14–70	21, 15–60
Age			
Years (median, range)	5.4, 1.3–8.1	4.7, 1–7, 4	5.3, 3.3–7

IE, idiopathic epilepsy; AEDT, antiepileptic drug treatment; BC, Border Collie; GSMD, Great Swiss Mountain Dog.

TABLE 2 | Semiology of epileptic events in the affected population.

	IE without AEDT	IE with AEDT
Seizures		
Status epilepticus	-	1
Cluster seizures	-	5
Seizure semiology		
Tonic-clonic	9	9
Tonic	-	-
Focal onset secondary generalization	3	3
Unknown onset	6	6
Additional focal seizures	-	-
Autonomic signs	4	5
Time between first seizure to MRI		
<1 month	-	-
>1–3 month	3	1
>3–12 month	4	3
>12 months	-	2
>24 months	2	3
Time between last reported seizure to MRI		
2–7 days	2	2
8–31 days	5	5
>1 month	2	2
Medical treatment at the timepoint of MRI		
Phenobarbital	-	9
Potassium bromide	-	2
Levetiracetam	-	3
Imepitoin	-	3
Gabapentin	-	1
Special diet or dietary supplement before MRI		
Medium chain triglycerides	1	1
Cannabidiol	1	1

IE, idiopathic epilepsy; AEDT, antiepileptic drug treatment.

Statistical Analysis

Statistical analysis was performed using R (version 4.1.2 in RStudio) (35). All groups (IE without AEDT, IE with AEDT, and healthy control dogs) were compared using a non-parametric Kruskal–Wallis test on all metabolite ratios to total creatine and on all metabolite ratios to water, respectively. Pairwise comparison between groups was performed using the Wilcoxon rank-sum test. Overall, $p < 0.05$ was considered to be statistically significant.

RESULTS

Study Population

Forty-one dogs fulfilled the inclusion criteria. Nine of these 41 dogs were excluded due to mispositioning of the VOI, one dog was excluded due to incorrectly set echo time during the MRS examination, and one dog was excluded due to visual identification of a broad and abnormal peak in the lipid region. Of the remaining 30 dogs, breeds were represented as follows: 20 GSMD (66.7%) and 10 BC (33.3 %). Population characteristics and seizure semiology are listed in **Tables 1**, **2**, respectively. In the majority of the cases, the VOI for the MRS was placed in the right part of the thalamus (25; 83%) and in the remaining dogs in the left part (5; 17%).

Spectral Quality

All spectra obtained were of good quality, with no spectra being rejected (**Figure 1**). The SNR in the study was between 19 and 8, and the FWHM of the fit (LCModel Output) was 2.9–5.9 Hz (**Figure 2**). No significant differences between the groups were found for these quality parameters. However, the FWHM of the water peak (between 5.6 and 7.8 Hz) was slightly higher (0.5 Hz) in the treated group.

MRS Results

The metabolite-to-total creatine ratios of all measured metabolites and the %CRLB are listed in the **Supplementary Table S2**.

The Kruskal–Wallis test revealed significant differences in the NAA-to-creatine ($p = 0.04$) and Glx-to-creatine ($p = 0.03$) ratios between the three groups. Significant differences were also found in the tNAA-to-water ratios ($p = 0.04$) (**Figure 3**).

Pairwise comparisons showed significant decrease in NAA-to-creatine ratios in IE dogs under AEDT compared to IE dogs without AEDT ($p = 0.03$) and compared to healthy control dogs ($p = 0.03$). However, tNAA-to-creatine ratio was not significantly reduced between the IE dogs with AEDT compared to IE without AEDT ($p = 0.06$) nor compared to healthy control dogs ($p = 0.17$).

Glx-to-creatine ratio was significantly reduced in IE dogs under AEDT compared to IE dogs without AEDT ($p = 0.03$) and compared to healthy dogs ($p = 0.02$).

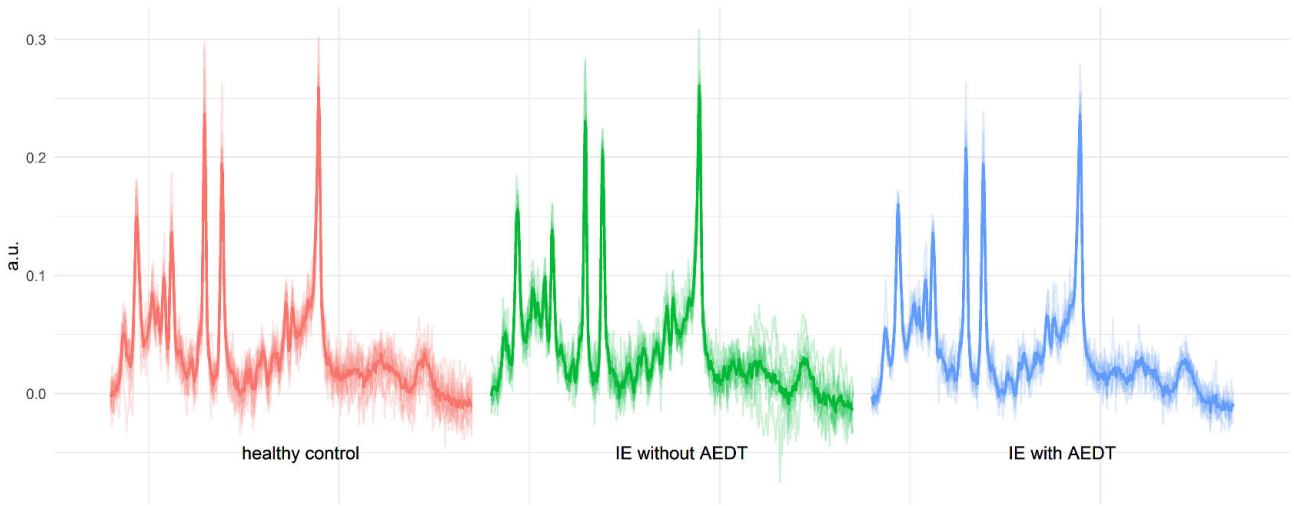

FIGURE 1 | All measured spectra of the three investigated groups. In the background, the individual spectra of all dogs are plotted as outputted from LCModel (.coord files). The thicker line shows the calculated mean spectrum in each group. The spectra show a consistent quality, and the observed differences in N-acetyl aspartate (NAA) and glutamate–glutamine (Glx) in idiopathic epilepsy (IE) with antiepileptic drug treatment (AEDT) are already indicated in this visual overview.

Pairwise comparison of IE without AEDT and healthy controls did not show significant difference, neither in NAA-to-creatine ($p = 0.60$), nor for tNAA-to-creatine ($p = 0.81$) or for Glx-to-creatine ($p = 0.55$) ratio.

NAA and tNAA-to-water ratios were significantly reduced in IE dogs with AEDT compared to IE dogs without AEDT ($p = 0.04$; $p = 0.01$, respectively) but not compared to healthy dogs. Glx to water was not significantly reduced between the compared latter groups of IE dogs ($p = 0.08$).

DISCUSSION

In human epilepsy, MRS has been introduced into the work-up since more than two decades. In contrast, MRS application in canine epilepsy is still in its early days. We investigated thalamic metabolite concentrations with MRS in healthy control dogs and IE dogs with and without AEDT. It was hypothesized that dogs affected by IE showed elevated Glx and reduced NAA concentration in the thalamus compared to control dogs, similar to humans with seizures and loss of consciousness (28). In this study, dogs with IE under AEDT, but not those without AEDT, had significantly lower NAA-to-creatine ratios compared to healthy controls, as well as compared to IE dogs without AEDT. With also reduced tNAA in IE with AEDT, this would convey a relatively clear picture. However, although the tNAA-to-creatine ratio is also generally lower in dogs with IE on AEDT, the differences are not significant. NAA and NAAG are spectroscopically very similar (19), as can also be seen in **Figure 2**. Thus, a distinction at 3T is difficult and strongly dependent on the spectral quality. With linewidths of <8 Hz obtained herein, which is considered excellent for measurements in humans (36), a reliable assignment seems at least plausible. In this case, the absence of differences in tNAA could be explained by changes in NAAG. However, given the observed differences in water linewidth, we must at least consider that the observed difference in NAA could reflect the difference in linewidth and thus a biased fitting. The measured ratios to water confirm the differences for NAA between IE dogs under AEDT compared to IE dogs without AEDT, but there are no significant differences in NAA or tNAA water ratios to the healthy dogs, which do not simplify the interpretation of the results.

Reduction in NAA in MRS is considered a sign for neuronal loss (18), and several factors can contribute to decreased NAA levels in human epilepsy. Some of these factors may also explain the lower NAA-to-creatine ratio found in IE dogs under AEDT compared to those without AEDT.

The number of seizures is an important reason for reduced NAA levels. In humans with generalized tonic–clonic seizures, reduction in NAA was more severe in patients who experienced more than ten generalized tonic–clonic seizures during their lifetime, than in patients with less seizure episodes (37–39). In our study, the total number of seizures per dog was not available, but overall longer duration of epilepsy and more common occurrence of cluster seizures and status epilepticus in dogs with AEDT compared to those without AEDT, suggests a higher number of seizures in this group. Therefore, the NAA reduction in IE dogs with AEDT might reflect the findings in humans, where patients with more seizure episodes showed severer NAA diminution (37–39).

Another reason for reduced NAA levels is poor seizure control. In humans, lower NAA levels were found in the mesial temporal lobe in patients failing to respond to the first AEDT compared to those with seizure freedom after first AEDT (40). Of the nine dogs in our study with AEDT, six had more than one antiepileptic drug. The high number of cases with multidrug treatment suggests a high level of resistance to the first antiepileptic drug in this group. One possible explanation in humans for lower NAA in non-responders is more severe

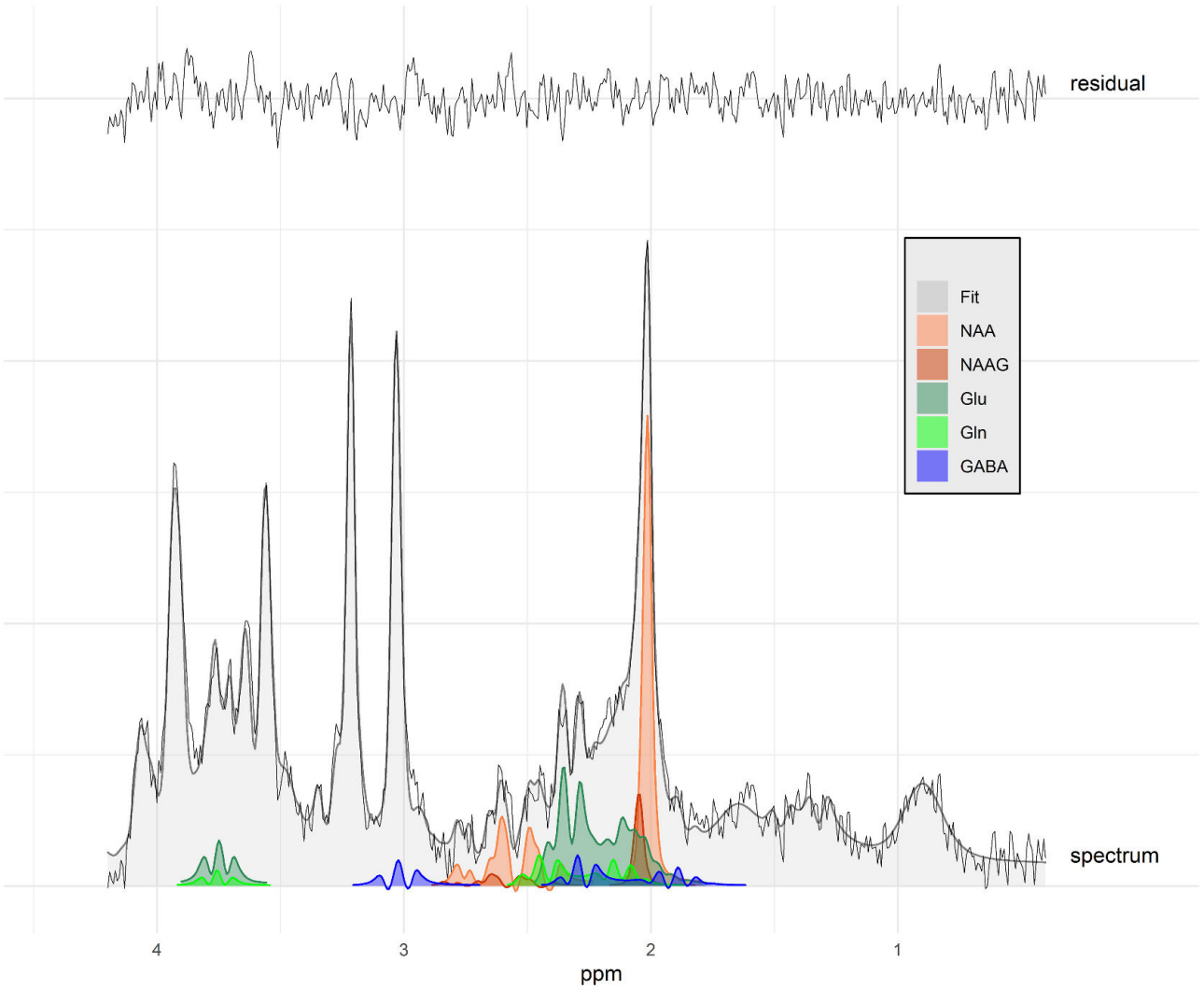

FIGURE 2 | Spectrum with signal-to-noise ratio of 16 (study mean: 12.9) and water peak full width at half maximum of 6.8 Hz (study mean: 6.79 Hz) of an idiopathic epileptic dog with antiepileptic drug treatment. The black line shows the acquired data, the gray area the overall fit, and the colors the individual fit components displayed for selected metabolites. Fit residuals are shown at the top. NAA, N-acetyl aspartate; NAAG, N-acetylaspartylglutamate; Glu, glutamate; Gln, glutamine; GABA, gamma-amino-butyrate.

neuronal damage in this group compared to responders (41). We may speculate that this is also the case in IE dogs with multidrug AEDT in our study. Longitudinal MRS studies during the course of epilepsy with comparison of MRS results between first drug responders and non-responders could help to answer this question.

The third factor resulting in decreased NAA levels is the disease duration and aging. Decreased NAA in humans has been reported with aging in medical resident temporal lobe epilepsy and with increased duration of epilepsy in secondary generalized tonic–clonic seizures bilaterally in the thalamus (28, 42). In our population, dogs under AEDT had slightly higher median age and longer disease duration compared to IE dogs without AEDT. This may also have contributed to the NAA changes, similarly as in human medicine.

Little is known about NAA ratios in dogs suffering from IE. The only study investigating MRS in canine IE was performed with magnetic field strength of 1.5T, MRS VOI placement in the temporal lobe, and included only drug-naïve dogs, without reporting seizure frequency or severity (9). Similar to our findings in IE dogs without AEDT, in the study of Olszewska et al., no significant differences were identified in either NAA/Cr, NAA/choline (Cho), or Cho/Cr between drug-naïve IE dogs and control dogs (9). Interestingly, Olszewska and colleagues found a temporal correlation between NAA/Cho and Cho/NAA ratios and time elapsed between MRS scan and the last reported seizure episode. Higher NAA/Cho ratios were present in dogs with very recent seizure activity, in contrast to lower ratios in dogs with less recent seizure episodes (9). In our study, we included only dogs with a gap of at least 2 days between last reported seizure event

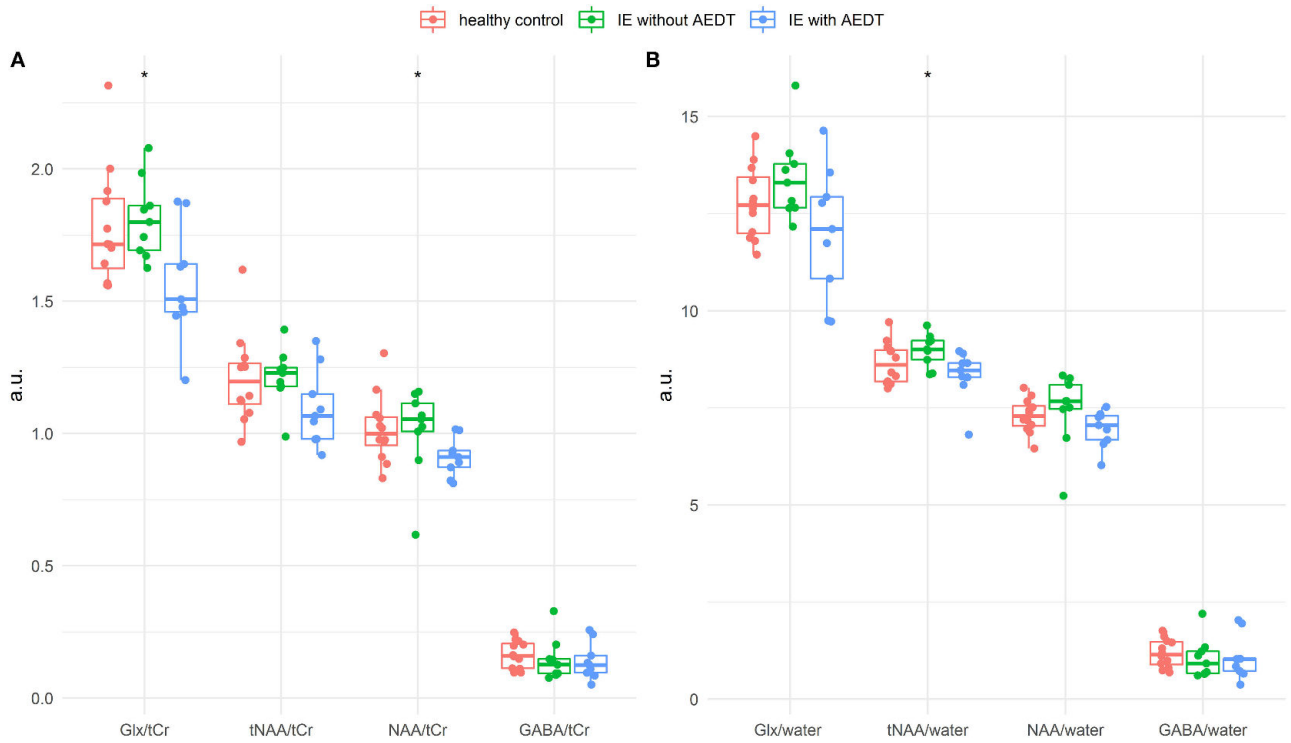

FIGURE 3 | Box plot of thalamic metabolite concentrations relative to creatine **(A)** and water **(B)** in healthy control dogs (red), dogs affected by idiopathic epilepsy with antiepileptic drug treatment (IE with AEDT in blue), and non-treated epileptic dogs (IE without AEDT in green). The Kruskal–Wallis test revealed statistically significant difference in the metabolites NAA/creatine and Glx/creatine, as well as tNAA/water (asterisk). Glx, glutamate–glutamine complex; tCr, total creatine; tNAA, total NAA; NAA, N-acetyl aspartate; GABA, gamma-amino-butyrate.

and MRI/MRS scan. In addition, interval between last reported seizure and MRI/MRS was similar in IE dogs with and without AEDT. Thus, it seems unlikely that the lower NAA ratios detected in our study were influenced by the time interval between the last seizure episode and the time of scanning. It is beyond the scope of this study to draw definitive conclusions about the cause of reduced NAA. Pathological studies systematically proving evidence for neuronal loss in canine epilepsy are lacking (43, 44), but early onset of mental decline/cognitive dysfunction supports impaired neuronal integrity in dogs suffering from IE (45).

In contrast to our hypothesis, we did not find an increase, but rather a decrease in thalamic Glx-to-creatine ratios in dogs with IE under AEDT compared to healthy controls and cases without AEDT.

Even relatively small differences in linewidth have been shown to bias estimates of Glx (46). The linewidth of the water peak was 0.5 Hz higher in IE dogs under AEDT, than in the other groups, and we cannot exclude an influence of the different linewidths on the Glx results. The Glx ratios to water show a similar picture as in the case for NAA. While the difference between IE dogs with and without AEDT stays visible, the difference in the healthy control disappears. This indicates possible differences in the reference signals total creatine or water between the healthy and the IE dogs, which weaken or amplify the differences.

Glx is the sum of glutamine and glutamate, which are present in both neuronal and glial cells. Concentrations of glutamate and glutamine are coupled *via* glutamate–glutamine cycling. Slow rates of glutamate–glutamine cycling, reduced glutamine levels, and a relative increase in glutamate levels have been found in resected epileptogenic hippocampi (47). Glx-to-creatine ratios in human epilepsy depend on the epileptic syndrome investigated and the area of interest within the brain and are not without controversy. While for example increased Glx-to-creatine ratios have been reported in the thalamus in juvenile myoclonic epilepsy, decreased levels have been reported in the frontal cortex (48). Another study investigating the prefrontal cortex in juvenile myoclonus epilepsy found also increased Glx-to-creatine ratios in the thalamus but decreased ratios in the medial prefrontal cortex, an area anatomically very close to the frontal cortex (15). A decrease in Glx is also considered an early biomarker of neuronal degeneration (49), and reduced frontal cortex Glx ratios have been linked to deficient frontal lobe functions in juvenile myoclonus epilepsy (48). No consistent effects of different types of AEDT on Glx levels in humans have been reported (4). It is assumed that antiepileptic drugs do not alter the glutamate concentration directly, but instead decrease the sensitivity of the glutamate receptor. A negative modulation of the voltage-gated channels might then lead to decreased glutamate concentrations (4). So far, no studies have been conducted on the effect of

antiepileptic drugs on Glx concentrations in dogs, making it impossible to distinguish the effect of the drug from the effect of the disease on the Glx results in or study. Remarkably, potential contribution of AEDT associated lower glutamate levels to suboptimal cognitive functioning in patients with epilepsy has been stated (5). Cognitive decline has also been reported in canine IE, with dogs showing cluster seizures and higher seizure frequency having more severe cognitive decline (45). In our study, IE dogs with AEDT had more often history of cluster seizures than those without AEDT. Therefore, having a higher risk for cognitive declines. However, because cognitive function has not been systematically investigated in our study, we cannot draw definitive conclusion on this aspect, and it remains unclear whether lower Glx levels also reflect lower cognitive function in our study population. Glx is difficult to detect with long echo time MRS at 1.5 T, and therefore, the only study investigating canine IE so far has not reported Glx levels (9). Glutamate levels have been measured in the CSF of IE dogs, and CSF levels of this metabolite have been reported as increased in drug-naïve dogs with IE, as well as in dogs under AEDT (50). On the first sight, these results may look contradictory to our data. However, as highlighted before, with the MRS technique applied in this study, one is not able to measure glutamate separately from glutamine. Therefore, the decrease in Glx could rather reflect a reduction in glutamine than one glutamate. Moreover, MRS detects the intra- and extracellular Glx pool. As the intracellular concentration of glutamate greatly exceeds the extracellular glutamate concentration, small increases in the extracellular glutamate concentration can be easily overlaid by intracellular changes (51). In human medicine, impairment of the glutamate–glutamine cycle has been identified in epilepsy, but as we only measured the sum of both metabolites we cannot make conclusions on this aspect. In future, these limitations may be overcome using magnetic field strength higher than 3T or utilizing advanced MRS techniques, which allows an improved separate evaluation of glutamate and glutamine (11).

Beside NAA and Glx, the third major brain metabolite in epilepsy which can be detected by MRS is GABA. GABA is not only the major inhibitory neurotransmitter in the brain, but it is also directly connected to Glx *via* the glutamate–glutamine cycle (11). Moreover, dogs under AEDT received medications with a GABAergic mechanism of action. GABAergic antiepileptic drugs have been shown to increase the GABA concentration in MRS in humans, and GABA concentration has been positively associated with seizure control in humans (4). In our study, GABA was detected in our MRS spectra and we could not identify any significant difference between healthy controls and IE dogs with and without AEDT, respectively. However, a mean %CRLB of GABA of more than 50% clearly demonstrates the difficulty of measuring GABA with the setup used and precludes definitive conclusions. This limitation is partially due to the much lower GABA concentration in comparison with other brain metabolites and the GABA is obscured by signals from more abundant metabolites. Measurements at higher magnetic field strengths and dedicated sequences could help to overcome this technical issue (52).

In this study, we selected our VOI based on human studies in patients suffering from idiopathic generalized epilepsy, which showed significantly different metabolite concentrations primarily in the thalamus (38, 39, 53). In addition, in humans, the thalamus is one of the most important center associated with the loss of consciousness in epilepsy. This also makes the thalamus region interesting for canine IE, which is associated with the loss of consciousness (29). Furthermore, the planning of the VOI in the thalamus is straightforward and contaminations from other tissue types can be mostly avoided despite the small size of the dog brain (**Figure 4**). In epileptic dogs, the thalamus has not been an area of major interest so far. One perfusion study indicated differences in perfusion in the brain of IE dogs compared to healthy control dogs, among others, also in the thalamus (54). Additional support for thalamic involvement has recently been reported by Unger et al. that found bilateral rotary saturation effects in the thalamus using phase-cycled stimulus-induced rotary saturation sequence in an Old English Bulldog with generalized tonic–clonic seizures (55). Even peri-ictal MRI changes have been found in parts of the thalamus in dogs (56). Network analysis of peri-ictal lesions has shown high correlation with cingulate lesions. Combining MRS of the thalamus with MRS in the cingulate gyrus could therefore be one approach for further studies. Although the role of the thalamus in canine IE has still to be elucidated, our study is in line with previous studies and supports the involvement of this brain region in the pathogenesis of canine IE. However, the involvement of the thalamus does not allow conclusions about a possible epilepsy focus. To locate seizure-onset zones, combining MRS with electroencephalography or advanced imaging techniques, such as phase-cycled stimulus-induced rotary saturation could improve diagnostic sensitivity (2, 55).

The limitations of the study include a small sample size and inhomogeneity of the study population. In spite of finite access to cases and healthy controls, this limitation is in balance with expected number of accessible cases per year and in line with animal welfare aspects that reduce the number of experimental animals used. The study population was heterogenous in aspect of (1) IE dogs with and without AEDT, (2) different breeds of dogs, and (3) dogs not matched for age and sex. It would have been necessary to include drug-naïve dogs only, to eliminate a potential bias due to medical treatment on the MRS results. On the contrary, this would have been a preselection criterion influencing the population to newly diagnosed epileptic dogs or dogs with a milder course of the disease, which does not require AEDT. Another limitation is the fact that we evaluated the thalamus only on one side what excludes a side-by-side comparison and does not allow conclusions about possible lateralization. The choice to use the right thalamus was completely arbitrary and not supported by clinical signs. Nevertheless, we cannot exclude that measuring in the minority of the cases the left thalamus instead of the right could have influenced our results. Until now, a potential influence of the dog breed on MRS results has not been investigated. Different breeds have different skull conformations, and this also affects the shape and size of the area of interest in the brain. These anatomical differences could lead to different tissue sampling

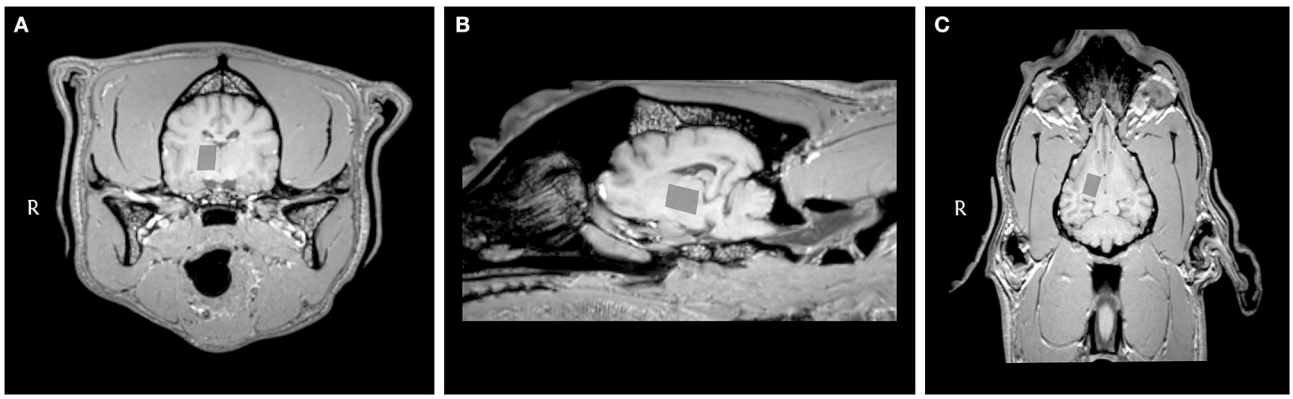

FIGURE 4 | Transverse **(A)**, sagittal **(B)**, and dorsal **(C)** T1-weighted MRI images of the brain of a dog with idiopathic epilepsy showing the location of the voxel of interest in the right part of the thalamus.

with a standardized VOI (e.g., different ratios of gray and white matter and even contamination of the VOI with CSF). Thus, we cannot fully exclude a potential bias based on this effect (33). As the study population was not matched for age and sex, we cannot rule out a potential effect on our measurements. Pairwise comparison between the treatment groups was not corrected for multiple comparison. Considering the set of statistical inferences, this seems to be balanced with the fact that comparing three groups is the lowest level of multiple comparisons possible. All these points probably contributed to the scatter of the results, and additional examinations on a larger and more homogeneous study population may help to get more precise answers.

In our study, MRS was used in research setting to assess advanced MRI techniques. However, it has been demonstrated that MRS, also in veterinary medicine, can be useful in a clinical approach (6–8, 57). Therefore, MRS should be considered as routine supplementary tool in selected patients together with conventional MRI to permit an improvement in diagnostic sensitivity. In human epilepsy research, it was suggested that future MRS studies should include MRS techniques that allow differentiation between glutamate and glutamine and to also measure GABA (11). Possibly, the availability of MRI scanners with higher field strength and the availability of new sequences will also allow this in canine epilepsy research. Furthermore, longitudinal studies with a larger and homogenous study population could improve and unfold the potential of MRS in the investigation of IE in veterinary medicine. This might help to develop biomarkers for drug response in (canine) IE and could strengthen the dog as model for the human epilepsy.

In 2015, the veterinary epilepsy task force has introduced MRI guidelines for canine IE, but these guidelines do not specify the use of MRS (1). Such consensus recommendation exists for MRS methods in humans and rodents (58, 59). By addressing MRS in canine epilepsy and applying human recommendations for reporting of methods (**Supplementary Table S1**) and results, we also aimed to improve standardization in MRS in veterinary medicine and we hope that in the next update of the veterinary epilepsy task force, imaging guidelines for MRS in IE will be included (60).

CONCLUSION

Using MRS, we have detected reduced NAA-to-creatine ratios in IE dogs with AEDT compared to healthy controls and IE dogs without AEDT, as well as reduced Glx-to-creatine ratios in IE dogs under AEDT compared to IE dogs without AEDT. MRS can be considered as an additional imaging technique to characterize disease severity and an additional tool for canine epilepsy research, but technical limitations have to be kept in mind when interpreting the results. Further studies are needed to improve and unfold the potential of MRS in the investigation of IE in veterinary medicine and possibly create a canine model for the study of epilepsy with MRS.

DATA AVAILABILITY STATEMENT

The original contributions presented in the study are included in the article/**Supplementary Material**, further inquiries can be directed to the corresponding author/s.

ETHICS STATEMENT

The animal study was reviewed and approved by the Cantonal Authorities according to Swiss Law under Animal License Nos. ZH272/16 and ZH046/20. Written informed consent was obtained from the owners for the participation of their animals in this study.

CONTRIBUTION TO THE FIELD

Magnetic resonance spectroscopy (MRS) is an advanced neuroimaging technique, which allows non-invasive estimation of metabolite concentrations within a selected volume of interest. Although MRS is extensively investigated in human epilepsy and rodent epilepsy models, MRS information in canine epilepsy is

scarce. The aim of our study was to assess and compare thalamic MRS in healthy control dogs and in idiopathic epileptic dogs affected by generalized seizures, as well as to assess possible differences between idiopathic epileptic dogs with and without antiepileptic drug treatment. Significant differences, similar but not in complete accordance with MRS studies in human medicine, were detected between the investigated canine groups. In this article, we discuss these novel results and the possible reasons for the discrepancies between human and veterinary medicine. With our study, we encourage the use of MRS in canine epilepsy research and propose to add a standardized MRS protocol in the magnetic resonance imaging guidelines for canine idiopathic epilepsy, similar to the consensus recommendation approved for MRS application in humans and rodents. Further studies are needed to improve and unfold the potential of MRS in the investigation of idiopathic epilepsy in veterinary medicine, which may be used as canine model for the study of epilepsy with MRS.

AUTHOR CONTRIBUTIONS

KB, HR, and NZ designed the study. KB and FS collected clinical data. NM collected the MRS data and drafted the initial manuscript. NZ selected the MRS protocol and performed the LCModel and the statistical analysis. All authors edited the manuscript and approved the final manuscript.

FUNDING

This research was partially financially supported by the Albert-Heim-Stiftung and the Stiftung für Kleintiere der Vetsuisse-Fakultät Universität Zürich.

ACKNOWLEDGMENTS

Preliminary data of these studies were presented at the 33rd online Symposium ECVN 2021 by the first author (61). The authors are grateful to all dog owners who allowed examination and publication of valuable information regarding their dogs. We thank all collaborators of the Clinic for Diagnostic Imaging, Department of Diagnostics and Clinical Services, Vetsuisse Faculty, University of Zurich, for the technical support.

SUPPLEMENTARY MATERIAL

The Supplementary Material for this article can be found online at: https://www.frontiersin.org/articles/10.3389/fvets.2022.885044/full#supplementary-material

REFERENCES

1. Rusbridge C, Long S, Jovanovik J, Milne M, Berendt M, Bhatti SF, et al. International veterinary epilepsy task force recommendations for a veterinary epilepsy-specific MRI protocol. *BMC Vet Res.* (2015) 11:194. doi: 10.1186/s12917-015-0466-x
2. Hasegawa D. Diagnostic techniques to detect the epileptogenic zone: Pathophysiological and presurgical analysis of epilepsy in dogs and cats. *Vet J.* (2016). doi: 10.1016/j.tvjl.2016.03.005
3. Caruso PA, Johnson J, Thibert R, Rapalino O, Rincon S, Ratai E-M. The use of magnetic resonance spectroscopy in the evaluation of epilepsy. *Neuroimaging Clin N Am.* (2013) 23:407–24. doi: 10.1016/j.nic.2012.12.012
4. van Veenendaal TM DM IJ, Aldenkamp AP, Hofman PA, Vlooswijk MC, Rouhl RP, et al. Metabolic and functional MR biomarkers of antiepileptic drug effectiveness: a review. *Neurosci Biobehav Rev.* (2015) 59:92–9. doi: 10.1016/j.neubiorev.2015.10.004
5. van Veenendaal TM, DM IJ, Aldenkamp AP, Lazeron RHC, Puts NAJ, Edden RAE, et al. Glutamate concentrations vary with antiepileptic drug use and mental slowing. *Epilepsy Behav.* (2016) 64:200–5. doi: 10.1016/j.yebeh.2016.08.027
6. Alisauskaite N, Beckmann K, Dennler M, Zölch N. Brain proton magnetic resonance spectroscopy findings in a Beagle dog with genetically confirmed Lafora disease. *J Vet Intern Med.* (2020) 34:1594–8. doi: 10.1111/jvim.15799
7. Carrera I, Richter H, Beckmann K, Meier D, Dennler M, Kircher PR. Evaluation of intracranial neoplasia and noninfectious meningoencephalitis in dogs by use of short echo time, single voxel proton magnetic resonance spectroscopy at 3.0 Tesla. *Am J Vet Res.* (2016) 77:452–62. doi: 10.2460/ajvr.77.5.452
8. Sievert C, Richter H, Beckmann K, Kircher PR, Carrera I, COMPARISON BETWEEN PROTON MAGNETIC RESONANCE SPECTROSCOPY FINDINGS IN DOGS WITH TICK-BORNE ENCEPHALITIS AND CLINICALLY NORMAL DOGS. *Vet Radiol Ultrasound.* (2016) 58:53–61. doi: 10.1111/vru.12427
9. Olszewska A, Schmidt MJ, Failing K, Nicpoń J, Podgórski P, Wrzosek MA. Interictal single-voxel proton magnetic resonance spectroscopy of the temporal lobe in dogs with idiopathic epilepsy. *Front Vet Sci.* (2020) 7:644. doi: 10.3389/fvets.2020.00644
10. Soares DP, Law M. Magnetic resonance spectroscopy of the brain: review of metabolites and clinical applications. *Clin Radiol.* (2009) 64:12–21. doi: 10.1016/j.crad.2008.07.002
11. Sarlo GL, Holton KF. Brain concentrations of glutamate and GABA in human epilepsy: a review. *Seizure.* (2021) 91:213–27. doi: 10.1016/j.seizure.2021.06.028
12. Ramadan S, Lin A, Stanwell P. Glutamate and glutamine: a review of in vivo MRS in the human brain. *NMR Biomed.* (2013) 26:1630–46. doi: 10.1002/nbm.3045
13. Barker-Haliski M, White HS. Glutamatergic mechanisms associated with seizures and epilepsy. *Cold Spring Harb Perspect Med.* (2015) 5:a022863. doi: 10.1101/cshperspect.a022863
14. Woermann FG, McLean MA, Bartlett PA, Parker GJ, Barker GJ, Duncan JS. Short echo time single-voxel 1H magnetic resonance spectroscopy in magnetic resonance imaging-negative temporal lobe epilepsy: different biochemical profile compared with hippocampal sclerosis. *Ann Neurol.* (1999) 45:369–76. doi: 10.1002/1531-8249(199903)45:3<369::aid-ana13>3.0.co;2-q
15. de Araújo Filho GM, Lin K, Lin J, Peruchi MM, Caboclo LO, Guaranha MS, et al. Are personality traits of juvenile myoclonic epilepsy related to frontal lobe dysfunctions? A proton MRS study. *Epilepsia.* (2009) 50:1201–9. doi: 10.1111/j.1528-1167.2009.02021.x
16. Mullins PG, McGonigle DJ, O'Gorman RL, Puts NA, Vidyasagar R, Evans CJ, et al. Current practice in the use of MEGA-PRESS spectroscopy for the detection of GABA. *Neuroimage.* (2014) 86:43–52. doi: 10.1016/j.neuroimage.2012.12.004
17. Choi IY, Andronesi OC, Barker P, Bogner W, Edden RAE, Kaiser LG, et al. Spectral editing in (1) H magnetic resonance spectroscopy: Experts' consensus recommendations. *NMR Biomed.* (2021) 34:e4411. doi: 10.1002/nbm.4411
18. Rae CD, A. guide to the metabolic pathways and function of metabolites observed in human brain 1H magnetic resonance spectra. *Neurochem Res.* (2014) 39:1–36. doi: 10.1007/s11064-013-1199-5
19. Govindaraju V, Young K, Maudsley AA. Proton NMR chemical shifts and coupling constants for brain metabolites. *NMR Biomed.* (2000) 13:129–53. doi: 10.1002/1099-1492(200005)13:3<129::aid-nbm619>3.0.co;2-v

20. Cendes F, Knowlton RC, Novotny E, Min LL, Antel S, Sawrie S, et al. Magnetic resonance spectroscopy in epilepsy: clinical issues. *Epilepsia.* (2002) 43:32–9. doi: 10.1046/j.1528-1157.2002.043s1032.x
21. Cendes F, Andermann F, Dubeau F, Matthews PM, Arnold DL. Normalization of neuronal metabolic dysfunction after surgery for temporal lobe epilepsy. Evidence from proton MR spectroscopic imaging. *Neurology.* (1997) 49:1525–33. doi: 10.1212/WNL.49.6.1525
22. Berendt M, Farquhar RG, Mandigers PJ, Pakozdy A, Bhatti SF, De Risio L, et al. International veterinary epilepsy task force consensus report on epilepsy definition, classification and terminology in companion animals. *BMC Vet Res.* (2015) 11:182. doi: 10.1186/s12917-015-0461-2
23. Hulsmeyer VI, Fischer A, Mandigers PJ, DeRisio L, Berendt M, Rusbridge C, et al. International veterinary epilepsy task force's current understanding of idiopathic epilepsy of genetic or suspected genetic origin in purebred dogs. *BMC Vet Res.* (2015) 11:175. doi: 10.1186/s12917-015-0463-0
24. Hulsmeyer V, Zimmermann R, Brauer C, Sauter-Louis C, Fischer A. Epilepsy in Border Collies: clinical manifestation, outcome, and mode of inheritance. *J Vet Intern Med.* (2010) 24:171–8. doi: 10.1111/j.1939-1676.2009.0438.x
25. Sauer-Delhées S, Steffen F, Reichler I, Beckmann K. [Clinical characteristics of idiopathic epilepsy in greater swiss mountain dogs in Switzerland]. *Schweiz Arch Tierheilkd.* (2020) 162:697–706. doi: 10.17236/sat00279
26. Bertholdo D, Watcharakorn A, Castillo M. Brain proton magnetic resonance spectroscopy: introduction and overview. *Neuroimaging Clin N Am.* (2013) 23:359–80. doi: 10.1016/j.nic.2012.10.002
27. Maudsley AA, Andronesi OC, Barker PB, Bizzi A, Bogner W, Henning A, et al. Advanced magnetic resonance spectroscopic neuroimaging: experts' consensus recommendations. *NMR Biomed.* (2021) 34:e4309. doi: 10.1002/nbm.4309
28. Tan Z, Long X, Tian F, Huang L, Xie F, Li S. Alterations in brain metabolites in patients with epilepsy with impaired consciousness: a case-control study of interictal multivoxel (1)H-MRS findings. *AJNR Am J Neuroradiol.* (2019) 40:245–52. doi: 10.3174/ajnr.A5944
29. Blumenfeld H. Impaired consciousness in epilepsy. *Lancet Neurol.* (2012) 11:814–26. doi: 10.1016/S1474-4422(12)70188-6
30. De Risio L, Bhatti S, Muñana K, Penderis J, Stein V, Tipold A, et al. International veterinary epilepsy task force consensus proposal: diagnostic approach to epilepsy in dogs. *BMC Vet Res.* (2015) 11:148. doi: 10.1186/s12917-015-0462-1
31. Beckmann KM, Wang-Leandro A, Richter H, Bektas RN, Steffen F, Dennler M, et al. Increased resting state connectivity in the anterior default mode network of idiopathic epileptic dogs. *Sci Rep.* (2021) 11:23854. doi: 10.1038/s41598-021-03349-x
32. Carrera I, Richter H, Meier D, Kircher PR, Dennler M. Regional metabolite concentrations in the brain of healthy dogs measured by use of short echo time, single voxel proton magnetic resonance spectroscopy at 3.0 Tesla. *Am J Vet Res.* (2015) 76:129–41. doi: 10.2460/ajvr.76.2.129
33. Near J, Harris AD, Juchem C, Kreis R, Marjańska M, Öz G, et al. Preprocessing, analysis and quantification in single-voxel magnetic resonance spectroscopy: experts' consensus recommendations. *NMR Biomed.* (2021) 34:e4257. doi: 10.1002/nbm.4257
34. Kreis R. The trouble with quality filtering based on relative Cramér-Rao lower bounds. *Magn Reson Med.* (2016) 75:15–8. doi: 10.1002/mrm.25568
35. Team RC. *A Language and Environment for Statistical Computing*. Vienna: R Foundation for Statistical Computing (2019).
36. Öz G, Deelchand DK, Wijnen JP, Mlynárik V, Xin L, Mekle R, et al. Advanced single voxel 1H magnetic resonance spectroscopy techniques in humans: Experts' consensus recommendations. *NMR Biomed.* (2021) 34:e4236. doi: 10.1002/nbm.4236
37. Bernasconi A, Bernasconi N, Natsume J, Antel SB, Andermann F, Arnold DL. Magnetic resonance spectroscopy and imaging of the thalamus in idiopathic generalized epilepsy. *Brain.* (2003) 126:2447–54. doi: 10.1093/brain/awg249
38. Helms G, Ciumas C, Kyaga S, Savic I. Increased thalamus levels of glutamate and glutamine (Glx) in patients with idiopathic generalised epilepsy. *J Neurol Neurosurg Psychiatry.* (2006) 77:489–94. doi: 10.1136/jnnp.2005.074682
39. Savic I, Osterman Y, Helms G. MRS shows syndrome differentiated metabolite changes in human-generalized epilepsies. *Neuroimage.* (2004) 21:163–72. doi: 10.1016/j.neuroimage.2003.08.034
40. Campos BA, Yasuda CL, Castellano G, Bilevicius E, Li LM, Cendes F. Proton MRS may predict AED response in patients with TLE. *Epilepsia.* (2010) 51:783–8. doi: 10.1111/j.1528-1167.2009.02379.x
41. Caciagli L, Xiao F, Wandschneider B, Koepp MJ. Imaging biomarkers of anti-epileptic drug action: insights from magnetic resonance imaging. *Curr Pharm Des.* (2017) 23:5727–39. doi: 10.2174/1381612823666170809113636
42. Riederer F, Bittsanský M, Lehner-Baumgartner E, Baumgartner C, Mlynárik V, Gruber S, et al. Decrease of NAA with aging outside the seizure focus in mesial temporal lobe epilepsy–a proton-MRS study at 3 Tesla. *Brain Res.* (2007) 1179:131–9. doi: 10.1016/j.brainres.2007.06.063
43. Matiasek K, Pumarola IBM, Rosati M, Fernandez-Flores F, Fischer A, Wagner E, et al. International veterinary epilepsy task force recommendations for systematic sampling and processing of brains from epileptic dogs and cats. *BMC Vet Res.* (2015) 11:216. doi: 10.1186/s12917-015-0467-9
44. Buckmaster PS, Smith MO, Buckmaster CL, LeCouteur RA, Dudek FE. Absence of temporal lobe epilepsy pathology in dogs with medically intractable epilepsy. *J Vet Intern Med.* (2002) 16:95–9. doi: 10.1111/j.1939-1676.2002.tb01612.x
45. Packer RMA, McGreevy PD, Salvin HE, Valenzuela MJ, Chaplin CM, Volk HA. Cognitive dysfunction in naturally occurring canine idiopathic epilepsy. *PLoS One.* (2018) 13:e0192182. doi: 10.1371/journal.pone.0192182
46. Zhang Y, Shen J. Effects of noise and linewidth on *in vivo* analysis of glutamate at 3 T. *J Magn Reson.* (2020) 314:106732. doi: 10.1016/j.jmr.2020.106732
47. Petroff OA, Errante LD, Rothman DL, Kim JH, Spencer DD. Glutamate-glutamine cycling in the epileptic human hippocampus. *Epilepsia.* (2002) 43:703–10. doi: 10.1046/j.1528-1157.2002.38901.x
48. Lin K, Carrete H Jr., Lin J, Peruchi MM, de Araújo Filho GM, Guaranha MS, et al. Magnetic resonance spectroscopy reveals an epileptic network in juvenile myoclonic epilepsy. *Epilepsia.* (2009) 50:1191–200. doi: 10.1111/j.1528-1167.2008.01948.x
49. Zeydan B, Kantarci K. Decreased glutamine and glutamate: an early biomarker of neurodegeneration. *Int Psychogeriatr.* (2021) 33:1–2. doi: 10.1017/S1041610219001807
50. Creevy KE, Gagnepain JF, Platt SR, Edwards GL, Kent M. Comparison of concentrations of γ-aminobutyric acid and glutamate in cerebrospinal fluid of dogs with idiopathic epilepsy with and without seizure-related magnetic resonance imaging hyperintense areas in the limbic system. *Am J Vet Res.* (2013) 74:1118–25. doi: 10.2460/ajvr.74.8.1118
51. Lipton SA, Rosenberg PA. Excitatory amino acids as a final common pathway for neurologic disorders. *N Engl J Med.* (1994) 330:613–22. doi: 10.1056/NEJM199403033300907
52. Lim SI, Xin L. γ-aminobutyric acid measurement in the human brain at 7 T: short echo-time or Mescher-Garwood editing. *NMR Biomed.* (2022) 37:e4706. doi: 10.1002/nbm.4706
53. Haki C, Gümüştaş OG, Bora I, Gümüştaş AU, Parlak M. Proton magnetic resonance spectroscopy study of bilateral thalamus in juvenile myoclonic epilepsy. *Seizure.* (2007) 16:287–95. doi: 10.1016/j.seizure.2007.02.017
54. Hartmann A, von Klopmann C, Lautenschlager IE, Scholz VB, Schmidt MJ. Quantitative analysis of brain perfusion parameters in dogs with idiopathic epilepsy by use of magnetic resonance imaging. *Am J Vet Res.* (2018) 79:433–42. doi: 10.2460/ajvr.79.4.433
55. Unger DM, Wiest R, Kiefer C, Raillard M, Dutil GF, Stein VM, et al. Neuronal current imaging: An experimental method to investigate electrical currents in dogs with idiopathic epilepsy. *J Vet Int Med.* (2021) 35:2828–36. doi: 10.1111/jvim.16270
56. Nagendran A, McConnell JF, De Risio L, José-López R, Quintana RG, Robinson K, et al. Peri-ictal magnetic resonance imaging characteristics in dogs with suspected idiopathic epilepsy. *J Vet Intern Med.* (2021) 35:1008–17. doi: 10.1111/jvim.16058
57. Ito D, Ishikawa C, Jeffery ND, Ono K, Tsuboi M, Uchida K, et al. Two-year follow-up magnetic resonance imaging and spectroscopy findings and cerebrospinal fluid analysis of a dog with sandhoff's disease. *J Vet Intern Med.* (2018) 32:797–804. doi: 10.1111/jvim.15041
58. Choi IY, Kreis R. Advanced methodology for in vivo magnetic resonance spectroscopy. *NMR Biomed.* (2021) 34:e4504. doi: 10.1002/nbm.4504
59. Kreis R, Boer V, Choi IY, Cudalbu C, de Graaf RA, Gasparovic C, et al. Terminology and concepts for the characterization of in vivo MR

spectroscopy methods and MR spectra: background and experts' consensus recommendations. *NMR Biomed.* (2020) 34:e4347. doi: 10.1002/nbm.4347
60. Lin A, Andronesi O, Bogner W, Choi IY, Coello E, Cudalbu C, et al. Minimum Reporting Standards for in vivo Magnetic Resonance Spectroscopy (MRSinMRS): experts' consensus recommendations. *NMR Biomed.* (2021) 34:e4484. doi: 10.1002/nbm.4484
61. Mauri N, Richter H, Zölch N, Beckmann KM. Proceedings 33rd On-line Symposium ESVN-ECVN. *J Vet Intern Med.* (2022) 36:300–52. doi: 10.1111/jvim.16332

Conflict of Interest: NM was employed by Vetimage Diagnostik GmbH.

The remaining authors declare that the research was conducted in the absence of any commercial or financial relationships that could be construed as a potential conflict of interest.

Publisher's Note: All claims expressed in this article are solely those of the authors and do not necessarily represent those of their affiliated organizations, or those of the publisher, the editors and the reviewers. Any product that may be evaluated in this article, or claim that may be made by its manufacturer, is not guaranteed or endorsed by the publisher.

frontiers | Frontiers in Veterinary Science

TYPE Original Research
PUBLISHED 06 January 2023
DOI 10.3389/fvets.2022.1093267

OPEN ACCESS

EDITED BY
Holger Andreas Volk,
University of Veterinary Medicine Hannover, Germany

REVIEWED BY
Andrea Fischer,
Ludwig Maximilian University of Munich, Germany
Sofie F. M. Bhatti,
Ghent University, Belgium

*CORRESPONDENCE
Manuela Wieser
✉ manuela.wieser@uzh.ch

†These authors have contributed equally to this work and share last authorship

SPECIALTY SECTION
This article was submitted to Veterinary Neurology and Neurosurgery, a section of the journal Frontiers in Veterinary Science

RECEIVED 08 November 2022
ACCEPTED 12 December 2022
PUBLISHED 06 January 2023

CITATION
Wieser M, Beckmann KM, Kutter APN, Mauri N, Richter H, Zölch N and Bektas RN (2023) Ketamine administration in idiopathic epileptic and healthy control dogs: Can we detect differences in brain metabolite response with spectroscopy? *Front. Vet. Sci.* 9:1093267. doi: 10.3389/fvets.2022.1093267

Ketamine administration in idiopathic epileptic and healthy control dogs: Can we detect differences in brain metabolite response with spectroscopy?

Manuela Wieser[1]*, Katrin Melanie Beckmann[2], Annette P. N. Kutter[1], Nico Mauri[3,4], Henning Richter[3], Niklaus Zölch[5†] and Rima Nadine Bektas[1†]

[1]Section of Anesthesiology, Department of Clinical Diagnostics and Services, University of Zurich, Zurich, Switzerland, [2]Section of Neurology, Clinic of Small Animals, University of Zurich, Zurich, Switzerland, [3]Department of Clinical Diagnostics and Services, Clinic for Diagnostic Imaging, University of Zurich, Zurich, Switzerland, [4]Vetimage Diagnostik AG, Oberentfelden, Switzerland, [5]Department of Forensic Medicine and Imaging, Institute of Forensic Medicine, University of Zurich, Zurich, Switzerland

Introduction: In recent years ketamine has increasingly become the focus of multimodal emergency management for epileptic seizures. However, little is known about the effect of ketamine on brain metabolites in epileptic patients. Magnetic resonance spectroscopy (MRS) is a non-invasive technique to estimate brain metabolites *in vivo*. Our aim was to measure the effect of ketamine on thalamic metabolites in idiopathic epileptic (IE) dogs using 3 Tesla MRS. We hypothesized that ketamine would increase the glutamine—glutamate (GLX)/creatine ratio in epileptic dogs with and without antiseizure drug treatment, but not in control dogs. Furthermore, we hypothesized that no different responses after ketamine administration in other measured brain metabolite ratios between the different groups would be detected.

Methods: In this controlled prospective experimental trial IE dogs with or without antiseizure drug treatment and healthy client-owned relatives of the breeds Border Collie and Greater Swiss Mountain Dog, were included. After sedation with butorphanol, induction with propofol and maintenance with sevoflurane in oxygen and air, a single voxel MRS at the level of the thalamus was performed before and 2 min after intravenous administration of 1 mg/kg ketamine. An automated data processing spectral fitting linear combination model algorithm was used to estimate all commonly measured metabolite ratios. A mixed ANOVA with the independent variables ketamine administration and group allocation was performed for all measured metabolites. A $p < 0.05$ was considered statistically significant.

Results: Twelve healthy control dogs, 10 untreated IE and 12 treated IE dogs were included. No significant effects for GLX/creatine were found. However, increased glucose/creatine ratios were found ($p < 0.001$) with no effect of group allocation. Furthermore, increases in the GABA/creatine ratio were found in IEU dogs.

Discussion: MRS was able to detect changes in metabolite/creatine ratios after intravenous administration of 1 mg/kg ketamine in dogs and no evidence was found that excitatory effects are induced in the thalamus.

Although it is beyond the scope of this study to investigate the antiseizure potential of ketamine in dogs, results of this research suggest that the effect of ketamine on the brain metabolites could be dependent on the concentrations of brain metabolites before administration.

KEYWORDS

spectroscopy, glutamate, GABA, glucose, MRS, GLX, thalamus, seizures

1. Introduction

The use of ketamine in canine epilepsy has undergone a paradigm shift in recent years. Historically, it has been suggested to avoid ketamine in epileptic humans and dogs due to its proconvulsive properties (1–5), but in recent years, ketamine has been increasingly promoted as a game changer for status epilepticus in human (6–9) as well as in veterinary medicine (10–12).

Ketamine exerts its action over non-competitive N-methyl-d-aspartate (NMDA) receptor antagonism (13–15). In the brain, these receptors are located in the cerebral cortex, thalamus and hippocampus (16–19). NMDA receptors are glutamate receptors and are expressed as autoreceptors or as heteroreceptors. In autoreceptors there is a binding with a specific ligand, whereas in heteroreceptors neurotransmitters from other neurons can bind. NMDA heteroreceptors might modulate not only glutamate release but also the release of γ-aminobutyric acid (GABA) (20), noradrenaline (21, 22) or dopamine (23). During status epilepticus an up-regulation of NMDA receptors in the brain takes place (24). Blockage of these NMDA receptors through ketamine can inhibit conduction of excitation and could therefore resolve status epilepticus (25).

The exact etiology of the proconvulsant effect of ketamine remains unclear (26). The avoidance of ketamine in dogs suffering from epilepsy has been based on limited evidence (2, 3). It has been postulated by Ferrer-Allado et al. (2) that doses of ketamine between 2 and 4 mg/kg intravenous (IV) caused electrical seizure activity. This electroconvulsive phenomenon coincided with the peak concentration of ketamine in the arterial blood. This finding, together with case reports of dogs experiencing seizure after ketamine administration, most likely contributed to the fact that people were reluctant to use ketamine in epileptic animals (4, 5).

Not only during the epileptic seizure activity but also in between epileptic seizures, in the interictal period, the epileptic brain shows functional and metabolic abnormalities (27–30) and these changes might differ between treated and non-treated epileptic dogs (31). Evidence for such a difference comes from recent studies. In idiopathic epileptic (IE) dogs significantly lower GABA levels were found in urine specimens in untreated compared to treated dogs (32). Besides these indirect metabolite measurements in the urine, lower glutamine—glutamate (GLX)/creatine ratios have been detected in the brain of IE dogs under antiseizure drug treatment compared to those without antiseizure drug treatment and to healthy control dogs (31, 32).

In human medicine ketamine has been shown to have different effects on brain metabolites in healthy people than in those suffering from functional brain diseases such as depression or compulsive behavioral disorders (33, 34). Those different effects were detected by using proton magnetic resonance spectroscopy (^{1}H-MRS). It is suspected that not only a pre-existing abnormal neurotransmitter level of GABA or glutamate can cause different changes in the response of brain metabolites after ketamine administration, but that also different doses of ketamine can affect neurotransmitter levels (35).

Single voxel ^{1}H-MRS enables non-invasive *in vivo* measurement of metabolites ratios or concentrations in a selected volume of interest within the brain and allows detection of changes in metabolites after drug administration (36). ^{1}H-MRS allows, among others, the measurement of glutamate, glutamine and GABA (37). At 3 Tesla (T) glutamate and glutamine are commonly reported together as GLX due to the overlap of glutamate and glutamine spectra and the difficulties in separating these two spectra at this field strength (38). Furthermore, also GABA measurements by 3 T MRS have to be interpreted with caution, due to the low concentration of GABA in the brain and the spectral overlap with other metabolites (39, 40).

In humans and experimental animals MRS has been used to investigate the effect of multiple drugs in health and disease (41–43). In the canine population, MRS has been used to evaluate metabolic changes in IE dogs (31, 44) and to investigate the effect of anesthetic drugs on brain metabolites in healthy epilepsy unaffected animals (45, 46). However, studies investigating the effect of drugs in IE are currently lacking.

The aim of this study was to compare metabolites in the thalamus before and after IV administration of 1 mg/kg ketamine in IE dogs with and without antiseizure drug treatment and in their not affected relatives using single voxel MRS.

We hypothesized that a bolus of ketamine would increase GLX/creatine ratio in the thalamus in epileptic dogs with and without antiseizure drug treatment, but not in control dogs.

Furthermore, we hypothesized that the change of the other commonly measured metabolite ratios would not be different between groups after 1 mg/kg ketamine administration.

2. Materials and methods

The study was performed as a prospective experimental trial. This project was approved by the local ethical committee according to the Swiss laws of animal protection and welfare and was licensed under the numbers ZH272/16 and ZH046/20. The project consisted of the currently reported study and concurrent brain imaging studies (30, 31). Informed owner consent was obtained from the owners of the dogs.

2.1. Animals

Client-owned dogs of both sexes from the breeds Greater Swiss Mountain Dogs and Border Collies, diagnosed with IE with or without antiseizure drug treatment and their not affected first degree relatives were enrolled into the study. Idiopathic epilepsy was diagnosed based on the International Veterinary Epilepsy Task Force TIER II confidence level (47). They were divided into newly diagnosed dogs without antiseizure drug treatment (IEU) and into dogs already under antiseizure drug treatment (IET). Idiopathic epileptic dogs were only included if they were scanned at least 2 days apart from the last recognized epileptic seizure to limit the possible influence of ictal changes on the spectroscopy (44). As a control group (control) not affected relatives (first degree relative to an epileptic dog but not clinically affected by IE) were included. All healthy relatives were followed up by telephone interviews at the time of writing the manuscript and are still free of seizures (minimum follow up period 2.5 years).

2.2. Study design

All dogs were fasted 8–12 h before anesthesia, with water being always accessible. In all dogs, medical history was collected, including information about administration of antiseizure drugs. All patients underwent a clinical and neurological examination performed by a board-certified neurologist. Furthermore, if no recent blood work was available, blood chemistry and hematology were obtained.

^{1}H-MRS was performed under general anesthesia. All dogs received 0.2 mg/kg butorphanol (Alvegesic 1% forte ad us. vet., Virbac, Switzerland) either intramuscularly (IM) or IV if a venous catheter (VasoVet, B. Braun Melsungen AG, Germany) had already been placed. The decision of placing a venous catheter into a cephalic vein before or after sedation with butorphanol depended on the behavior of the individual dog. In the Greater Swiss Mountain Dogs 1 mg/kg esomeprazole (Esomep 40 mg, Gruenenthal Pharma AG, Switzerland) was administered IV before induction. All dogs were preoxygenated for 5 min, before induction of general anesthesia with propofol (Propofol 1% MCT Fresenius, Fresenius Kabi AG, Switzerland). The dogs' tracheae were intubated with a cuffed endotracheal tube (Super Safety Clear, Teleflex Medical, Switzerland) of suitable size.

Anesthesia was maintained with sevoflurane (Sevorane, AbbVie AG, Switzerland) to effect, in oxygen and air. The dogs were mechanically ventilated with pressure—controlled ventilation (8–12 cmH_2O) through a circle system and respiratory rate was adapted to maintain end—tidal CO_2 between 35 and 38 mmHg. Animals were placed in dorsal recumbency during the ^{1}H-MRS, and the following parameters were measured continuously and recorded every 5 min throughout the procedure with a magnetic resonance imaging (MRI) compatible multiparameter monitor (Datex Ohmeda GE N-MRI2-01, Finland): peripheral oxygen saturation, heart rate, non-invasive blood pressure, respiratory rate, end-tidal CO_2, and end-tidal sevoflurane concentration.

All dogs received an infusion of Ringer's acetate (Ringer Acetate, Fresenius Kabi AG, Switzerland) at rates of 5 ml/kg/h IV. To maintain normotension, which was defined as a mean arterial blood pressure above 60 mmHg five ml/kg of Ringer's acetate were given IV over 10 min as bolus if needed. If up to four fluid boli of Ringer's acetate (5 ml/kg) did not increase the mean arterial blood pressure above 60 mmHg, a dobutamine (Dobutrex 250 mg/50 ml, Teva Pharma AG, Switzerland) constant rate infusion was started at a rate of 0.5 µg/kg/min to increase the mean arterial blood pressure above 60 mmHg.

2.3. Spectroscopy data collection and preparation

MRI and MRS of the brain were performed with a 3 T MRI (Philips Ingenia, Philips AG, Switzerland) using a 15 channel receiver transmitter head coil (Stream Head-Spine coil solution, Philips AG, Zurich, Switzerland). Conventional morphological MRI was performed prior to the MRS acquisition. Single voxel MRS acquisition of the right or left thalamus with point resolved spectroscopy (PRESS) was subsequently performed as described in the study of Mauri et al. (31). Briefly summarized T2-W images in all 3 planes were used to place the single voxel in the thalamus, preferably in the right thalamus and carefully avoiding cerebrospinal fluid, as well as peripheral soft and bony tissues adjacent to the thalamus to prevent lipid contamination. Voxel

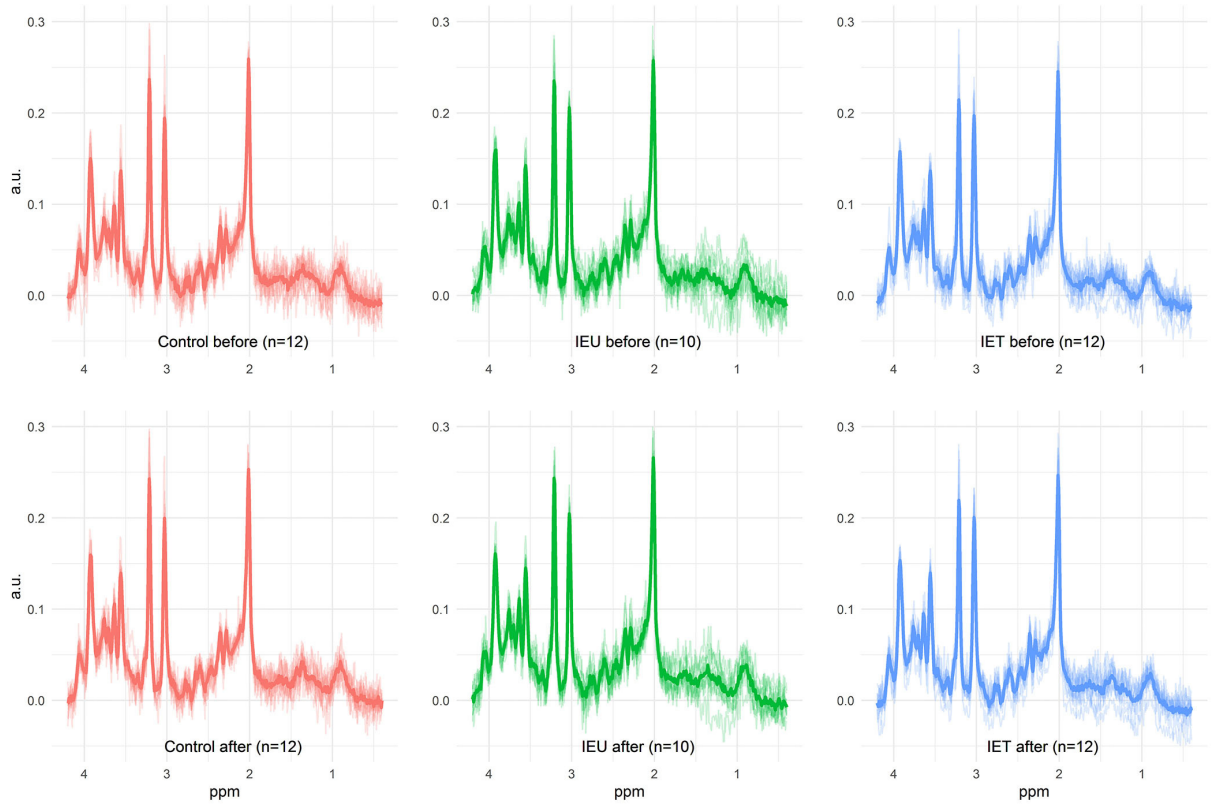

FIGURE 1
All measured spectra of the three investigated groups prae and post ketamine administration. In the background, the individual spectra of all dogs are plotted as output from LCModel. The thicker line shows the calculated mean spectrum in each group. This figure illustrates the achieved quality of all ^{1}H-MRS measurements beyond the quality measures such as SNR and FWHM. In particular, the absence of artifacts can be verified. Metabolite differences described in this study are not visually detectable.

size was 1.8 cm^3 (10 × 12 × 15 mm). Details of the MRS protocol and analysis are given in the Supplementary Table S1.

After the first MRS acquisition, 1 mg/kg ketamine was administered IV and 2 min later the MRS scan was repeated. Prior to further analysis the quality of the spectra of the dogs were evaluated. Only spectra of dogs with a morphological normal brain, with correct voxel placement in the thalamus, and with adequate spectral quality (visual inspection for artifacts) were included in our study (Figure 1). The spectral quality in the final data set was assessed based on the signal to noise ratio and the full width at half maximum (FWHM) as given by the software used to analyze the spectra (LCModel, S Provencher, Oakville, ON, Canada) and the full width at half maximum (FWHM) from the unsuppressed water peak.

LCModel was used to estimate metabolite ratios to total creatine and water. Due to a variety of factors contributing to the signal (including not only voxel size, T1 and T2 relaxation times and repetition and echo times, but many more), these measured signals were calibrated against a commonly used reference metabolite (creatine) (48). The ratio of metabolite to total creatine was chosen because tissue segmentation required for correcting the ratio to water was not available in this study (31). Nevertheless, the ratios to water were used to check the results from the ratios to creatine. From all metabolites present in the basis set, only metabolites fitted with a median (over all measurements) relative Cramér Rao lower bound (CRLB) lower than 50 % were included in the following analysis (49).

2.4. Statistical analysis and data handling

A mixed ANOVA with the independent factors ketamine administration within subjects and group allocation (control, IEU, IET) between subjects was performed for all measured metabolites, heart rate and mean arterial blood pressure after checking assumptions for normality, outliers and homogeneity of variances and covariances. If significant effects were found, appropriate *post-hoc* tests were run with a Bonferroni correction for multiple comparisons. If the assumptions were not met, we

10.3389/fvets.2022.1093267

performed a linear mixed effects model. A p-value <0.05 was considered statistically significant.

3. Results

Data from 34 dogs fulfilled our quality measures and all quality of spectra were good (Figure 1). These included 12 dogs in the Control group (2 Border Collies and 10 Greater Swiss Mountain Dogs), 10 dogs in the IEU group (2 Border Collies and 8 Greater Swiss Mountain Dogs) and 12 dogs in the IET group (8 Border Collies and 4 Greater Swiss Mountain Dogs). In Table 1 breed, sex, age and weight distribution are presented. The first MRS of 30 of these 34 dogs have been analyzed and published in an independent study (31).

At the timepoint of MRS, dogs in IET group were under one or more antiseizure drugs (mean, minimum and maximum dosages): phenobarbital [3.8 (1.2–4.3) mg/kg BID] in 10 dogs (83%), imepitoin [5.5 (4.3–10) mg/kg BID] in 3 dogs (25%), potassium bromide [16 (14–30) mg/kg BID] in 3 dogs (25%) and / or levetiracetam [15.5 (12–19) mg/kg BID] in 2 dogs (17%), all given orally.

A dobutamine CRI was administered in 10 dogs (7 dogs in the control group, 1 dog in the IEU group and 2 dogs in the IET group) during the ^{1}H-MRS scan.

The ^{1}H-MRS scan started 77 (55–100) min [median (range)] after propofol administration [4 (2–6) mg/kg]. End-tidal sevoflurane concentration during the scan was 2.3 % (1.8–3.8 %).

All dogs completed the study and recovered uneventfully, except for one dog in the IET group. This dog showed a seizure like phenomenon during the recovery phase and received midazolam 0.5 mg/kg IV as a treatment, which resolved the event.

The spectra of these 34 dogs had a signal to noise ratio of 12.5 (8–20) and a FWHM of 3.96 Hz (2.94–5.88 Hz) according to the LCModel output. The measured FWHM of the water peak was 6.3 Hz (5.4–7.8 Hz). No significant differences in these values were observed between the different groups. The achieved spectral quality is illustrated in Figure 1. Median relative CRLBs were below 50% for the following metabolites: total creatine (sum of creatine and phosphocreatine), the sum of glycerophosphocholine and phosphocholine, the sum of N-acetylaspartate and N-acetylaspartylglutamate, the sum of myo-inositol and glycine, GLX, ascorbate, aspartate, glutathione, and glucose. For GABA, the median relative CRLB was 50.5%. Due to the great interest, GABA was nevertheless analyzed further. The obtained CRLBs are summarized in Supplementary Table S2.

No significant effects of ketamine administration ($p = 0.356$), group allocation ($p = 0.073$) and interaction ($p = 0.4$) for GLX/Creatine were found. However, we found effects on glucose/creatine (Figure 2A), GABA/Creatine (Figure 2B) and ascorbate (Figure 2C).

TABLE 1 Sex, median and ranges (minimum and maximum) for age and weight for each group and each breed.

Breed	Control							IEU							IET						
	n (f/m)	Age (months)			Weight (kg)			n (f/m)	Age (months)			Weight (kg)			n (f/m)	Age (months)			Weight (kg)		
		Med	Min	Max	Med	Min	Max		Med	Min	Max	Med	Min	Max		Med	Min	Max	Med	Min	Max
BC	2 (1/1)	56	14	98	20.7	19.6	21.8	4 (2/2)	33.5	28	48	18	14	22.7	8 (3/5)	60	45	92	18	15	23
GSMD	10 (6/4)	43.5	21	82	48.5	36	54.8	9 (4/5)	39	11	88	48	32.8	70	4 (1/3)	57.5	9	65	55.5	53	60

Control, healthy siblings; IEU, untreated idiopathic epilepsy; IET, treated idiopathic epilepsy; BC, Border Collie; GSMD, Greater Swiss Mountain Dogs; max, maximum; med, median; min, minimum.

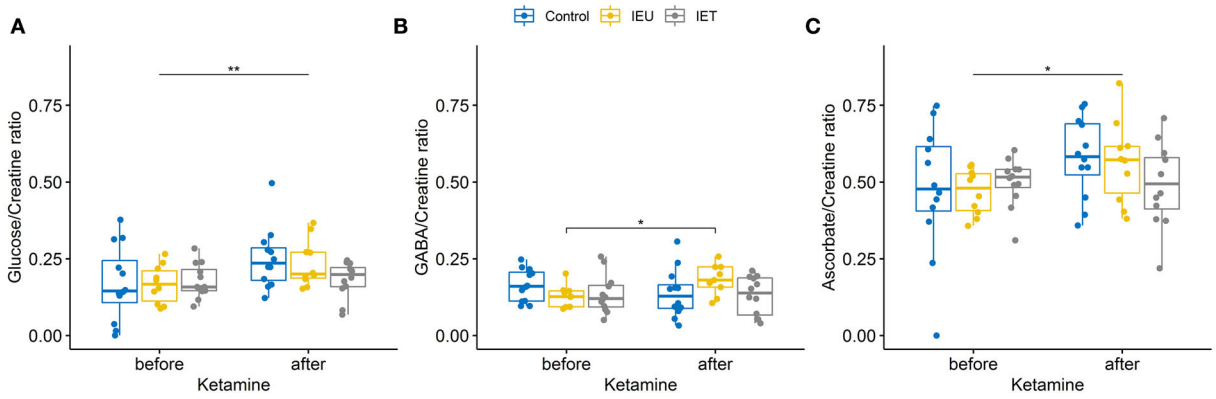

FIGURE 2
(A–C) Boxplot of thalamic metabolite concentrations [**(A)** glucose, **(B)** GABA, **(C)** ascorbate] prae and post ketamine relative to creatine in healthy control dogs (blue), dogs affected by idiopathic epilepsy without antiepileptic drug treatment (IEU in yellow) and treated epileptic dogs (IET in gray). **(A)** Ketamine increased glucose/creatine ratios significantly ($p < 0.001$) but no effect of group allocation was found. A trend for an interaction between group allocation and ketamine administration was observed [p = 0.065, **(A)**]. **(B)** For GABA/creatine ratios no significant effects of ketamine administration ($p = 0.544$) or group allocation ($p = 0.525$) were found, however there was a significant interaction between group allocation and ketamine administration [$p = 0.038$, **(B)**]. *post-hoc* tests revealed a significant increase after ketamine for group IEU ($p = 0.031$). **(C)** For ascorbate a significant effect of ketamine administration could be found using a linear mixed effect model ($p = 0.033$). *$p < 0.05$, **$p < 0.01$.

For all other measured metabolites ratios (sum of glycerophosphocholine and phosphocholine/creatine ratio, the sum of N-acetylaspartate and N-acetylaspartylglutamate/creatine ratio, the sum of myo-inositol and glycine/creatine ratio, aspartate/creatine and glutathione/creatine) no significant effects of ketamine administration, group allocation and interaction were found.

All metabolites' measures (ratio to total creatine) obtained before and after ketamine are summarized in Supplementary Table S3. The results observed in the ratios to creatine were confirmed by the ratios to water signal [glucose/water ($p < 0.0005$) increased significantly with a trend for an interaction between group allocation and ketamine ($p = 0.061$); significant interaction for GABA/water ($p = 0.035$); increase of ascorbate/water using a linear mixed effect model ($p = 0.036$)]. Heart rate, systolic, mean and diastolic blood pressures decreased significantly (all $p < 0.01$) after ketamine administration, while no group or interaction effects could be found.

4. Discussion

This study investigated the acute effects of the intravenous administration of 1 mg/kg ketamine on brain metabolites in the thalamus with MRS in dogs suffering from IE with or without antiseizure treatment and in healthy relatives in general anesthesia maintained with sevoflurane. Glucose/creatine ratio increased significantly after ketamine administration in all groups. In contrary to our hypothesis no increase of the excitatory metabolite GLX were found. Interestingly, for the inhibitory metabolite GABA an interaction between ketamine and group allocation was found with IEU showing a significant increase after ketamine administration in comparison to the IET and control group.

4.1. Effects on GLX/creatine ratio

Our study did not show any significant effects of ketamine or group allocation on GLX/creatine ratio in the thalamus. Glutamate as the major excitatory neurotransmitter is of special interest in epilepsy and an increased extracellular glutamate in the brain and / or a reduction in GABA concentrations are leading to excitotoxicity, epileptic seizures, and cell death (50).

Former MRS results for glutamate/creatine or GLX/creatine ratio after ketamine administration are limited and controversial, both for people and animals. Reported changes range from an increase to a decrease in glutamate or GLX levels. No changes were found in the GLX/creatine ratio in the thalamus of healthy awake volunteers 2 h after 0.8 mg/kg of ketamine IV administered over 50 min (51). Increased glutamate/creatine ratios were reported in the frontal cortex in healthy rats 30 min after a subanesthetic dose of 30 mg/kg of ketamine subcutaneously (52). Increased levels of glutamine were reported in the anterior cingulate cortex in humans after subanesthetic doses of 0.27 mg/kg ketamine IV followed by a constant rate infusion (CRI) for 2 hours (53). In contrast, decreasing GLX levels were measured in the medial prefrontal cortex of humans suffering from depression with increasing subanesthetic doses of ketamine (0.1–0.5 mg/kg IV) (35).

When looking at the canine literature, higher levels of GLX were reported in the striatum during general anesthesia with 15 mg/kg ketamine IV than during general anesthesia with 8 mg/kg pentobarbital IV (46). However, this study evaluated the absolute difference between these two types of anesthetic drugs in healthy dogs only. Thus, it is not clear if ketamine increased the GLX levels or if pentobarbital decreased them (46). Bektas et al. (manuscript in preparation) evaluated the acute effect of 2 mg/kg ketamine IV on GLX/creatine ratio in the in the hippocampus in healthy Beagle dogs under sevoflurane anesthesia and, in line with our results, did not find any significant changes in GLX/creatine ratios before and after ketamine administration. Comparisons to published studies are difficult due to differences in species and health status, dosage and administration modes of ketamine and variances in timing related to ketamine administration as well as differences in location of the MRS in the brain. There are some possible explanations why we could not detect significant changes in GLX/creatine ratio after ketamine administration.

Firstly, with the current MRS technics applied we were only able to measure GLX/creatine ratio, the sum of glutamine and glutamate. glutamine and glutamate are linked *via* the glutamine–glutamate cycle (54). Changes in the glutamine/glutamate ratios, with an increase in glutamine and a decrease in glutamate have been detected after NMDA—antagonist administration (55). Such changes in opposite directions after ketamine might stay undetected when only the sum of glutamate and glutamine can be measured. To differentiate between glutamate and glutamine a higher magnetic field strength or advanced MRS sequences would be needed.

Secondly, MRS is not able to differentiate between extra—and intracellular metabolites (56). Ketamine is expected to cause an increase of the extracellular glutamate levels (57). Furthermore, the total amount of glutamate is much higher intracellular than extracellular (58). Therefore, a possible extra—or intracellular shift of glutamate after ketamine administration cannot be detected with the current method. As the extracellular levels of glutamate determine the extent of excitation, separation of extra—and intracellular concentrations would be interesting, but currently no non—invasive technique is able to assess such shifts.

Thirdly, we investigated the effect of ketamine administration on the thalamic GLX/creatine ratios only. Since brain regions have different GLX/creatine ratios and different NMDA receptor distribution, it is possible that in other brain areas, changes in GLX/creatine ratios after ketamine administration could have been measured. More studies, with similar doses of ketamine and with voxel placement in different brain areas at higher magnetic field strengths could give us more insights into the effect of ketamine on glutamine and glutamate levels.

In a concurrent study investigating a similar group of dogs the MRS of the thalamus before ketamine showed decreased GLX/creatine ratios in the treated IE dogs compared to Controls and untreated IE dogs (31). The current study shows that, although changes in GLX/creatine ratio may be present in IET dogs, their reaction to a low dose of ketamine in general anesthesia seems comparable to their healthy and their untreated IE relatives.

4.2. Effects on glucose/creatine ratio

The detected increase in glucose/creatine ratio in MRS could have two possible explanations. Firstly, ketamine could have increased the supply of glucose to the brain by increasing the blood glucose level, by decreasing the regional metabolic rate of glucose or by increasing the brain perfusion (59). Secondly, ketamine could have decreased brain glucose consumption (60). The decreased consumption is possibly caused by a direct NMDA blockade (54, 61) or indirectly by an increased anesthetic depth (62). Decreases in heart rate and blood pressure after ketamine in our study indicate deeper plane of anesthesia. Ketamine and deeper plane of anesthesia lead to vasodilation (63) with a possible concurrent increase in blood supply to the brain.

In people, a bolus of 0.5 mg/kg of ketamine IV showed reduction or increases of the regional metabolic rate of glucose in different brain regions (64). In contrast, a target-controlled ketamine infusion (0.3 μg/ml) led to an overall increase of regional metabolic rate of glucose in the whole brain, with the highest increase in the thalamus (65). However, another study revealed no change after a target-controlled s-ketamine infusion (0.75 μg/ml) of regional metabolic rate of glucose at all (66). In rats, high intraperitoneal dosages of ketamine (170 mg/kg) decreased regional metabolic rate of glucose in the thalamus in one study (67), whereas in another study 10–30 mg/kg of ketamine IV lead to different results according to the brain area, with no effect measured in the thalamus (68).

In human IE patients, glucose consumption is reduced inter-ictally and elevated ictally compared to baseline (69, 70). We did not detect different glucose/creatine response after ketamine administration between IE dogs and healthy control dogs. However, a trend for an interaction between group allocation and ketamine administration was found (Figure 2A) and the effect of ketamine on glucose/creatine ratio was most prominent in the IEU dogs. Interestingly, the dog with the reported seizure like phenomenon during recovery had the lowest increase in glucose/creatine. Whether this low increase of glucose/creatine ratio had been caused by an already ongoing silent epileptic seizure activity during the MRS or if it is a coincidental finding cannot be further elucidated.

Not only the regional metabolic rate of glucose, but also the blood glucose concentration can be changed by ketamine

administration and can therefore be a reason for a change in brain glucose/creatine ratio. In rabbits, a low dose of 0.17 mg/kg of ketamine IV produced hyperglycemia and higher doses of 1–2 mg/kg IV produced hypoglycemia (71). In dogs, no elevation in blood glucose after a ketamine bolus of 1 or 2 mg/kg IV could be detected in one study (72). However, another study documented an elevation in blood glucose using 10 mg/kg of ketamine IV (73), so, a dose dependent elevation in blood glucose can be assumed. Unfortunately, blood glucose levels were not measured in the current study, which presents a limitation to discuss further what caused the elevated glucose/creatine ratios in the thalamus. Further studies are needed to explain the exact mechanism between ketamine and glucose/creatine ratio in the brain. Studying different dosages and different brain regions might give further insights into this finding.

4.3. Effects on GABA/creatine ratio

Measuring GABA using ^{1}H-MRS is challenging due to the low concentration of GABA in the brain and the spectral overlap with other metabolites. Thus, GABA levels should be interpreted with caution, unless measured at higher magnetic field strength (≥7 T MRS) or special sequences (74). Even though we found a significant increase of GABA/creatine ratio in group IEU, the median relative CRLB were high, so the current results should be interpreted with care. In future studies the measurement of GABA in dogs could be optimized, although the voxel size is limited due to the small size of our patients' brain. Using spectral editing sequences such as MEGA-PRESS with longer scan times and correction for B_0 instability would enable more reliable GABA levels (75).

Ketamine administration blocks the postsynaptic NMDA receptor, therefore more glutamate can bind to pre-synaptic inhibitory glutamate receptors (76). When these receptors are activated by glutamate binding, a retrograde messenger is released, which can result in an increase in GABA (20, 77) and could further explain the increase in GABA/creatine ratio after ketamine administration. An increase in the GABA/creatine ratio could indicate a neuroprotective effect of ketamine in the epileptic dogs, by shifting the balance toward more inhibitory metabolites in the brain (12, 50).

Furthermore, lower GABA concentrations have been found in the urine in untreated IE dogs compared to treated IE dogs and healthy controls (32). Interestingly, ketamine reverses the GABA deficit in human major depression patients (35) which may also apply to untreated epileptic dogs. In epileptic patients, GABA turnover can be reduced, with not yet fully understood reasons (69). A reduced glycolysis and therefore a decrease in glutamate turnover in inter-ictal IE patients has been reported as a possible reason. As glutamate can be transformed into GABA *via* the glutamic acid decarboxylase, a decrease in glutamate turnover can lead to a decrease in GABA (69). It is possible that dogs treated with GABAergic anti-epileptic drugs, have GABA concentrations in the brain, that are more similar to concentrations in healthy individuals, which could be shown in studies in human medicine (41, 78, 79) and which is supported by the recent study from Mauri et al. (31). Furthermore, increases in GABA levels were reported in the medial prefrontal cortex after 0.5 mg/kg over 40 min of ketamine IV in humans suffering from obsessive—compulsive disorder (33). Possibly ketamine reverses the GABA deficit reported in untreated canine IE patients (51, 80).

4.4. Effects on ascorbate/creatine

Not only an increase in glucose/creatine ratio, but also a significant increase in ascorbate/creatine ratio was detected after ketamine administration. Ascorbate is an important antioxidant in the brain that can be reliably detected using MRS at 3 T field strength (81, 82) and resonates at 3.73 ppm which is close to the GLX compounds resonation (81). To preserve antioxidant effects, ascorbate underlies strict homeostasis in the brain (82). Increases in extracellular glutamate concentrations have been associated with increases in ascorbate concentrations in the brain under experimental conditions (83, 84). While the effect of ketamine on brain ascorbate levels has not been investigated, premedication with ascorbate before ketamine anesthesia has shown to enhance the effect of ketamine anesthesia in rabbits (85). In animal epileptic seizure models, administration of a high dose of ascorbate has shown anti–seizure and neuroprotective effects, but it is unknown whether ascorbate regulation is impacted by natural occurring epilepsy (86). No differences between groups have been found in the current study.

It is difficult to transfer the current findings into clinical implications as no studies comparing metabolite estimates and clinical effects in dogs are available. In this study we could prove that the effect of a drug on brain metabolites can be measured non-invasively using ^{1}H-MRS in clinical patients. This opens the door for future studies exploring the effect of antiseizure medication in epileptic dogs. Possible indication might be the investigation of drug resistance in epilepsy and to elucidate how ketamine interrupts refractory status epilepticus in dogs.

4.5. Limitations

In the current study all animals were under general anesthesia and metabolite concentrations can be altered due to anesthetic choice of drugs (45, 87). It is therefore debatable if the findings after administration of ketamine under general anesthesia can be translated to the administration of ketamine in awake patients. To minimize the interaction of anesthetic drugs during the current study, we chose

short acting drugs for premedication (butorphanol) and induction (propofol). For maintenance of anesthesia, we chose sevoflurane, as a recent study found that sevoflurane had only minor effects without clinical relevance on GLX concentrations (45).

We decided to use 1 mg/kg ketamine IV as this dosage is often used as co-induction agent and also for analgesic purposes (88). As we used a lower dose than the commonly used doses for status epilepticus treatment in dogs and because our dogs were scanned inter-ictally we cannot draw direct conclusions about the effects of higher dosages of ketamine in ictal dogs (10).

Antiseizure drug treatment can result in chronic changes in brain metabolite concentrations (89). The effects might differ between different drugs, different epileptic syndromes, and different brain areas (79, 90). The dogs included in our study were not on a standardized treatment and a variety of drugs in different dosages were used, precluding a definitive conclusion about the effect on antiseizure drug treatment on the MRS results.

As a further limitation electroencephalography (EEG) of the IE dogs was not available. Clinically no epileptic seizures were reported at least 2 days before the MRS scan for all IE dogs, but the absence of epileptic seizures was not confirmed by EEG and underlying epileptic seizure activity could have been missed. Additionally, we cannot prove the absence of any ictal activity during MRS scans, because of the lack of EEG during the MRS scan.

The volume of interest was chosen in the thalamus, due to the region's involvement in IE in humans (91) and dogs (92) and the presence of NMDA-receptors in the thalamus. As IE is not only involving the thalamus and ketamine is acting also in other parts of the brain (hippocampus, cortex), the effects of ketamine in other parts of the brain could be different and should be investigated in future studies by examining different brain regions.

The sample size was relatively small with groups not balanced regarding breeds, age and sex. However, the sex distribution with more males than female in IEU and IET dogs reflects the natural distribution of the disease in dogs, with a higher risk of epilepsy in male dogs (93, 94). Further studies assessing differences among breeds are needed to exclude a possible bias.

Some dogs were treated with dobutamine to maintain non-invasive mean arterial blood pressure above 60 mmHg. However, no change of rate before and after the ketamine administration was performed, so a possible influence of dobutamine would not interfere with our study results.

Increase of GABAergic transmission can be also due to acute or chronic stress (95). Dogs are commonly stressed in veterinary environment (96), but we did not investigate stress levels of the individual dogs to account for stress as a possible cofounder.

5. Conclusion

^{1}H-MRS was able to detect changes in metabolite/creatine ratios after intravenous administration of 1 mg/kg ketamine IV in dogs. We found no evidence of excitatory effects induced in the thalamus. A slight difference in the response to ketamine was detected between IEU dogs and healthy control and IET dogs. Although it is beyond the scope of this study to investigate the antiseizure potential of ketamine in dogs, results of this research suggest that the effect of ketamine on the brain metabolites in dogs could be dependent on the concentrations of brain metabolites before administration.

Data availability statement

The original contributions presented in the study are included in the article/Supplementary material, further inquiries can be directed to the corresponding author.

Ethics statement

The animal study was reviewed and approved by the Cantonal Authorities according to Swiss Law Under Animal License Nos. ZH272/16 and ZH046/20. Written informed consent was obtained from the owners for the participation of their animals in this study.

Author contributions

RB and KB conceived the project. NZ made technical contributions to the ^{1}H MRS protocol and accomplished MRS data sampling and analyzing, supported by NM and MW. RB, AK, HR, and MW participated in interpretation of the study results. MW drafted the paper and was supported by KB, RB, and AK. The manuscript was revised by KB, AK, NZ, HR, NM, and RB. All authors read and approved the final manuscript.

Funding

This research was partially financially supported by the Albert-Heim-Stiftung and the Stiftung für Kleintiere der Vetsuisse-Fakultät Universität Zürich.

Conflict of interest

NM was employed by Vetimage Diagnostik AG.

The remaining authors declare that the research was conducted in the absence of any commercial or financial

relationships that could be construed as a potential conflict of interest.

Publisher's note

All claims expressed in this article are solely those of the authors and do not necessarily represent those of their affiliated organizations, or those of the publisher, the editors and the reviewers. Any product that may be evaluated in this article, or claim that may be made by its manufacturer, is not guaranteed or endorsed by the publisher.

Supplementary material

The Supplementary Material for this article can be found online at: https://www.frontiersin.org/articles/10.3389/fvets.2022.1093267/full#supplementary-material

References

1. Miyasaka M, Domino EF. Neural mechanisms of ketamine-induced anesthesia. *Int J Neuropharmacol.* (1968) 7:557–73. doi: 10.1016/0028-3908(68)90067-1

2. Ferrer-Allado T, Brechner VL, Dymond A, Cozen H, Crandall P. Ketamine-induced electroconvulsive phenomena in the human limbic and thalamic regions. *Anesthesiology.* (1973) 38:333–44. doi: 10.1097/00000542-197304000-00006

3. Myslobodsky MS, Golovchinsky V, Mintz M. Ketamine: Convulsant or anti-convulsant? *Pharmacol Biochem Behav.* (1981) 14:27–33. doi: 10.1016/0091-3057(81)90099-X

4. Adami C, Spadavecchia C, Casoni D. Seizure activity occurring in two dogs after S-ketamine-induction. *Schweizer Archiv für Tierheilkunde.* (2013) 155:569–72. doi: 10.1024/0036-7281/a000513

5. Lervik A, Haga HA, Becker M. Abnormal motor activity during anaesthesia in a dog: a case report. *Acta Vet Scand.* (2010) 52:64. doi: 10.1186/1751-0147-52-64

6. Fujikawa DG. Starting ketamine for neuroprotection earlier than its current use as an anesthetic/antiepileptic drug late in refractory status epilepticus. *Epilepsia.* (2019) 60:373–80. doi: 10.1111/epi.14676

7. Gaspard N, Foreman B, Judd LM, Brenton JN, Nathan BR, McCoy BM, et al. Intravenous ketamine for the treatment of refractory status epilepticus: a retrospective multicenter study. *Epilepsia.* (2013) 54:1498–503. doi: 10.1111/epi.12247

8. Rosati A, Ilvento L. L'Erario M, Masi S, Biggeri A, Fabbro G, et al. Efficacy of ketamine in refractory convulsive status epilepticus in children: a protocol for a sequential design, multicentre, randomised, controlled, open-label, non-profit trial (KETASER01). *BMJ Open.* (2016) 6:e011565. doi: 10.1136/bmjopen-2016-011565

9. Rosati A. L'Erario M, Ilvento L, Cecchi C, Pisano T, Mirabile L, et al. Efficacy and safety of ketamine in refractory status epilepticus in children. *Neurology.* (2012) 79:2355–8. doi: 10.1212/WNL.0b013e318278b685

10. Serrano S, Hughes D, Chandler K. Use of ketamine for the management of refractory status epilepticus in a dog. *J Vet Internal Med.* (2006) 20:194–7. doi: 10.1111/j.1939-1676.2006.tb02841.x

11. Gioeni D, Di Cesare F, D'Urso ES, Rabbogliatti V, Ravasio G. Ketamine-dexmedetomidine combination and controlled mild hypothermia for the treatment of long-lasting and super-refractory status epilepticus in 3 dogs suffering from idiopathic epilepsy. *J Vet Emerg Crit Care.* (2020) 30:455–60. doi: 10.1111/vec.12956

12. Charalambous M, Bhatti SFM, Volk HA, Platt S. Defining and overcoming the therapeutic obstacles in canine refractory status epilepticus. *Vet J.* (2022) 283–4:105828. doi: 10.1016/j.tvjl.2022.105828

13. Reich DL, Silvay G. Ketamine: an update on the first twenty-five years of clinical experience. *Can J Anaes.* (1989) 36:186–97. doi: 10.1007/BF03011442

14. Thomson AM, West DC, Lodge D. An N-methylaspartate receptor-mediated synapse in rat cerebral cortex: a site of action of ketamine? *Nature.* (1985) 313:479–81. doi: 10.1038/313479a0

15. Anis NA, Berry SC, Burton NR, Lodge D. The dissociative anaesthetics, ketamine and phencyclidine, selectively reduce excitation of central mammalian neurones by N-methyl-aspartate. *Br J Pharmacol.* (1983) 79:565–75. doi: 10.1111/j.1476-5381.1983.tb11031.x

16. Conti F. Localization of NMDA receptors in the cerebral cortex: a schematic overview. *Braz J Med Biol Res.* (1997) 30:555–60. doi: 10.1590/S0100-879X1997000500001

17. Siegel SJ, Brose N, Janssen WG, Gasic GP, Jahn R, Heinemann SF, et al. Regional, cellular, and ultrastructural distribution of N-methyl-D-aspartate receptor subunit 1 in monkey hippocampus. *Proc Natl Acad Sci U S A.* (1994) 91:564–8. doi: 10.1073/pnas.91.2.564

18. Scherzer CR, Landwehrmeyer GB, Kerner JA, Counihan TJ, Kosinski CM, Standaert DG, et al. Expression of N-Methyl-D-Aspartate receptor subunit mRNAs in the human brain: Hippocampus and cortex. *J Compar Neurol.* (1998) 390:75–90. doi: 10.1002/(SICI)1096-9861(19980105)390:1<75::AID-CNE7>3.0.CO;2-N

19. Standaert DG, Bernhard Landwehrmeyer G, Kerner JA, Penney JB, Young AB. Expression of NMDAR2D glutamate receptor subunit mRNA in neurochemically identified interneurons in the rat neostriatum, neocortex and hippocampus. *Mol Brain Res.* (1996) 42:89–102. doi: 10.1016/S0169-328X(96)00117-9

20. DeBiasi S, Minelli A, Melone M, Conti F. Presynaptic NMDA receptors in the neocortex are both auto-and heteroreceptors. *Neuroreport.* (1996) 7:2773–6. doi: 10.1097/00001756-199611040-00073

21. Pittaluga A, Raiteri M. Release-enhancing glycine-dependent presynaptic NMDA receptors exist on noradrenergic terminals of hippocampus. *Eur J Pharmacol.* (1990) 191:231–4. doi: 10.1016/0014-2999(90)94153-O

22. Pittaluga A. Presynaptic release-regulating NMDA receptors in isolated nerve terminals: a narrative review. *Br J Pharmacol.* (2020) 178:1001–17. doi: 10.1111/bph.15349

23. Krebs MO, Desce JM, Kemel ML, Gauchy C, Godeheu G, Cheramy A, et al. Glutamatergic control of dopamine release in the rat striatum: evidence for presynaptic N-methyl-D-aspartate receptors on dopaminergic nerve terminals. *J Neurochem.* (1991) 56:81–5. doi: 10.1111/j.1471-4159.1991.tb02565.x

24. Naylor DE, Liu H, Niquet J, Wasterlain CG. Rapid surface accumulation of NMDA receptors increases glutamatergic excitation during status epilepticus. *Neurobiol Dis.* (2013) 54:225–38. doi: 10.1016/j.nbd.2012.12.015

25. Fang Y, Wang X. Ketamine for the treatment of refractory status epilepticus. *Seizure.* (2015) 30:14–20. doi: 10.1016/j.seizure.2015.05.010

26. Modica PA, Tempelhoff R, White PF. Pro- and anticonvulsant effects of anesthetics (Part II). *Anesth Analg.* (1990) 70:433–44. doi: 10.1213/00000539-199004000-00016

27. Hartmann A, Sager S, Failing K, Sparenberg M, Schmidt MJ. Diffusion-weighted imaging of the brains of dogs with idiopathic epilepsy. *BMC Vet Res.* (2017) 13:338. doi: 10.1186/s12917-017-1268-0

28. Hartmann A, von Klopmann C, Lautenschläger IE, Scholz VB, Schmidt MJ. Quantitative analysis of brain perfusion parameters in dogs with idiopathic epilepsy by use of magnetic resonance imaging. *Am J Vet Res.* (2018) 79:433–42. doi: 10.2460/ajvr.79.4.433

29. Viitmaa R, Haaparanta-Solin M, Snellman M, Cizinauskas S, Orro T, Kuusela E, et al. Cerebral glucose utilization measured with high resolution positron emission tomography in epileptic Finnish Spitz dogs and healthy dogs. *Vet Radiol Ultrasound.* (2014) 55:453–61. doi: 10.1111/vru.12147

30. Beckmann KM, Wang-Leandro A, Richter H, Bektas RN, Steffen F, Dennler M, et al. Increased resting state connectivity in the anterior default mode network of idiopathic epileptic dogs. *Sci Rep.* (2021) 11:23854. doi: 10.1038/s41598-021-03349-x

31. Mauri N, Richter H, Steffen F, Zölch N, Beckmann KM. Single-voxel proton magnetic resonance spectroscopy of the thalamus in idiopathic epileptic dogs and in healthy control dogs. *Front Vet Sci.* (2022) 9:885044. doi: 10.3389/fvets.2022.885044

32. Schmidt T, Meller S, Talbot SR, Berk BA, Law TH, Hobbs SL, et al. Urinary neurotransmitter patterns are altered in canine epilepsy. *Front Vet Sci.* (2022) 9:893013. doi: 10.3389/fvets.2022.893013

33. Rodriguez CI, Kegeles LS, Levinson A, Ogden RT, Mao X, Milak MS, et al. *In vivo* effects of ketamine on glutamate-glutamine and gamma-aminobutyric acid in obsessive-compulsive disorder: Proof of concept. *Psychiatry Res.* (2015) 233:141–7. doi: 10.1016/j.pscychresns.2015.06.001

34. Milak MS, Proper CJ, Mulhern ST, Parter AL, Kegeles LS, Ogden RT, et al. A pilot *in vivo* proton magnetic resonance spectroscopy study of amino acid neurotransmitter response to ketamine treatment of major depressive disorder. *Mol Psychiatry.* (2016) 21:320–7. doi: 10.1038/mp.2015.83

35. Milak MS, Rashid R, Dong Z, Kegeles LS, Grunebaum MF, Ogden RT, et al. Assessment of relationship of ketamine dose with magnetic resonance spectroscopy of Glx and GABA responses in adults with major depression: a randomized clinical trial. *JAMA Netw Open.* (2020) 3:e2013211-e. doi: 10.1001/jamanetworkopen.2020.13211

36. Egerton A. The potential of 1H-MRS in CNS drug development. *Psychopharmacology.* (2019) 238:1241–54. doi: 10.1007/s00213-019-05344-7

37. Soares DP, Law M. Magnetic resonance spectroscopy of the brain: review of metabolites and clinical applications. *Clin Radiol.* (2009) 64:12–21. doi: 10.1016/j.crad.2008.07.002

38. Ramadan S, Lin A, Stanwell P. Glutamate and glutamine: a review of *in vivo* MRS in the human brain. *NMR Biomed.* (2013) 26:1630–46. doi: 10.1002/nbm.3045

39. Provencher SW. Estimation of metabolite concentrations from localized *in vivo* proton NMR spectra. *Magn Reson Med.* (1993) 30:672–9. doi: 10.1002/mrm.1910300604

40. Puts NA, Edden RA. *In vivo* magnetic resonance spectroscopy of GABA: a methodological review. *Prog Nucl Magn Reson Spectrosc.* (2012) 60:29–41. doi: 10.1016/j.pnmrs.2011.06.001

41. Doelken MT, Hammen T, Bogner W, Mennecke A, Stadlbauer A, Boettcher U, et al. Alterations of intracerebral γ-aminobutyric acid (GABA) levels by titration with levetiracetam in patients with focal epilepsies. *Epilepsia.* (2010) 51:1477–82. doi: 10.1111/j.1528-1167.2010.02544.x

42. Pollack MH, Jensen JE, Simon NM, Kaufman RE, Renshaw PF. High-field MRS study of GABA, glutamate and glutamine in social anxiety disorder: Response to treatment with levetiracetam. *Progr Neuro-Psychopharmacol Biol Psychiatry.* (2008) 32:739–43. doi: 10.1016/j.pnpbp.2007.11.023

43. Henry ME, Jensen JE, Licata SC, Ravichandran C, Butman ML, Shanahan M, et al. The acute and late CNS glutamine response to benzodiazepine challenge: a pilot pharmacokinetic study using proton magnetic resonance spectroscopy. *Psychiatry Res Neuroimag.* (2010) 184:171–6. doi: 10.1016/j.pscychresns.2010.08.003

44. Olszewska A, Schmidt MJ, Failing K, Nicpoń J, Podgórski P, Wrzosek MA. Interictal single-voxel proton magnetic resonance spectroscopy of the temporal lobe in dogs with idiopathic epilepsy. *Front Vet Sci.* (2020) 7:644. doi: 10.3389/fvets.2020.00644

45. Söbbeler FJ, Carrera I, Pasloske K, Ranasinghe MG, Kircher P, Kästner SBR. Effects of isoflurane, sevoflurane, propofol and alfaxalone on brain metabolism in dogs assessed by proton magnetic resonance spectroscopy (1H MRS). *BMC Vet Res.* (2018) 14:69. doi: 10.1186/s12917-018-1396-1

46. Lee SH, Kim SY, Woo DC, Choe BY Ryu KN, Choi WS, et al. Differential neurochemical responses of the canine striatum with pentobarbital or ketamine anesthesia: a 3T proton MRS study. *J Vet Med Sci.* (2010) 72:583–7. doi: 10.1292/jvms.09-0103

47. De Risio L, Bhatti S, Muñana K, Penderis J, Stein V, Tipold A, et al. International veterinary epilepsy task force consensus proposal: diagnostic approach to epilepsy in dogs. *BMC Vet Res.* (2015) 11:148. doi: 10.1186/s12917-015-0462-1

48. Alger JR. Quantitative proton magnetic resonance spectroscopy and spectroscopic imaging of the brain: a didactic review. *Top Magn Reson Imag.* (2010) 21:115–28. doi: 10.1097/RMR.0b013e31821e568f

49. Kreis R. The trouble with quality filtering based on relative Cramér-Rao lower bounds. *Magn Reson Med.* (2016) 75:15–8. doi: 10.1002/mrm.25568

50. Sarlo GL, Holton KF. Brain concentrations of glutamate and GABA in human epilepsy: a review. *Seizure.* (2021) 91:213–27. doi: 10.1016/j.seizure.2021.06.028

51. Silberbauer LR, Spurny B, Handschuh P, Klöbl M, Bednarik P, Reiter B, et al. Effect of ketamine on limbic gaba and glutamate: a human *in vivo* multivoxel magnetic resonance spectroscopy study. *Front Psychiatry.* (2020) 11:920. doi: 10.3389/fpsyt.2020.549903

52. Kim SY, Lee H, Kim HJ, Bang E, Lee SH, Lee DW, et al. *In vivo* and ex vivo evidence for ketamine-induced hyperglutamatergic activity in the cerebral cortex of the rat: potential relevance to schizophrenia. *NMR Biomed.* (2011) 24:1235–42. doi: 10.1002/nbm.1681

53. Rowland LM, Bustillo JR, Mullins PG, Jung RE, Lenroot R, Landgraf E, et al. Effects of ketamine on anterior cingulate glutamate metabolism in healthy humans: a 4-T proton MRS study. *Am J Psychiatry.* (2005) 162:394–6. doi: 10.1176/appi.ajp.162.2.394

54. Hertz L, Chen Y. Integration between glycolysis and glutamate-glutamine cycle flux may explain preferential glycolytic increase during brain activation, requiring glutamate. *Front Integr Neurosci.* (2017) 11:18. doi: 10.3389/fnint.2017.00018

55. Iltis I, Koski DM, Eberly LE, Nelson CD, Deelchand DK, Valette J, et al. Neurochemical changes in the rat prefrontal cortex following acute phencyclidine treatment: an *in vivo* localized (1)H MRS study. *NMR Biomed.* (2009) 22:737–44. doi: 10.1002/nbm.1385

56. Nicolo J-P, O'Brien TJ, Kwan P. Role of cerebral glutamate in post-stroke epileptogenesis. *NeuroImage Clin.* (2019) 24:102069. doi: 10.1016/j.nicl.2019.102069

57. Moghaddam B, Adams B, Verma A, Daly D. Activation of glutamatergic neurotransmission by ketamine: a novel step in the pathway from NMDA receptor blockade to dopaminergic and cognitive disruptions associated with the prefrontal cortex. *J Neurosci.* (1997) 17:2921–7. doi: 10.1523/JNEUROSCI.17-08-02921.1997

58. Meldrum BS. Glutamate as a neurotransmitter in the brain: review of physiology and pathology. *J Nutr.* (2000) 130:1007S–15S. doi: 10.1093/jn/130.4.1007S

59. Miyamoto S, Leipzig JN, Lieberman JA, Duncan GE. Effects of ketamine, MK-801, and amphetamine on regional brain 2-deoxyglucose uptake in freely moving mice. *Neuropsychopharmacology.* (2000) 22:400–12. doi: 10.1016/S0893-133X(99)00127-X

60. Rae CD, A. guide to the metabolic pathways and function of metabolites observed in human brain 1H magnetic resonance spectra. *Neurochem Res.* (2014) 39:1–36. doi: 10.1007/s11064-013-1199-5

61. Hertz L, Rothman DL. Glutamine-glutamate cycle flux is similar in cultured astrocytes and brain and both glutamate production and oxidation are mainly catalyzed by aspartate aminotransferase. *Biology.* (2017) 6:17. doi: 10.3390/biology6010017

62. Stephan H, Sonntag H, Lange H, Rieke H. Cerebral effects of anaesthesia and hypothermia. *Anaesthesia.* (1989) 44:310–6. doi: 10.1111/j.1365-2044.1989.tb11284.x

63. Noel-Morgan J, Muir WW. Anesthesia-associated relative hypovolemia: mechanisms, monitoring, and treatment considerations. *Front Vet Sci.* (2018) 5:53. doi: 10.3389/fvets.2018.00053

64. Nugent AC, Diazgranados N, Carlson PJ, Ibrahim L, Luckenbaugh DA, Brutsche N, et al. Neural correlates of rapid antidepressant response to ketamine in bipolar disorder. *Bipolar Disorder.* (2014) 16:119–28. doi: 10.1111/bdi.12118

65. Långsjö Jaakko W, Salmi E, Kaisti Kaike K, Aalto S, Hinkka S, Aantaa R, et al. Effects of subanesthetic ketamine on regional cerebral glucose metabolism in humans. Anesthesiology. (2004) 100:1065–71. doi: 10.1097/00000542-200405000-00006

66. Laaksonen L, Kallioinen M, Långsjö J, Laitio T, Scheinin A, Scheinin J, et al. Comparative effects of dexmedetomidine, propofol, sevoflurane, and S-ketamine on regional cerebral glucose metabolism in humans: a positron emission tomography study. *Br J Anaesth.* (2018) 121:281–90. doi: 10.1016/j.bja.2018.04.008

67. Freo U, Ori C. Effects of anesthesia and recovery from ketamine racemate and enantiomers on regional cerebral glucose metabolism in rats. *Anesthesiology.* (2004) 100:1172–8. doi: 10.1097/00000542-200405000-00020

68. Crosby G, Crane AM, Sokoloff L. Local changes in cerebral glucose utilization during ketamine anesthesia. *Anesthesiology.* (1982) 56:437–43. doi: 10.1097/00000542-198206000-00005

69. Alvestad S, Hammer J, Qu H, Håberg A, Ottersen OP, Sonnewald U. Reduced astrocytic contribution to the turnover of glutamate, glutamine, and GABA characterizes the latent phase in the kainate model of temporal lobe epilepsy. *J Cerebral Blood Flow Metabol.* (2011) 31:1675–86. doi: 10.1038/jcbfm.2011.36

70. Patel M, A. Metabolic Paradigm for Epilepsy. *Epilepsy Curr.* (2018) 18:318–22. doi: 10.5698/1535-7597.18.5.318

71. Suleiman IS, Hanan AA. Effect of intravenous ketamine administration on blood glucose levels in conscious rabbits. *Am J Pharmacol Toxicol.* (2009) 4:38–45. doi: 10.3844/ajptsp.2009.38.45

72. Muñoz KA, Robertson SA, Wilson DV. Alfaxalone alone or combined with midazolam or ketamine in dogs: intubation dose and select physiologic effects. *Vet Anaesth Analg.* (2017) 44:766–74. doi: 10.1016/j.vaa.2017.01.004

73. Khan WA, Durrani U, Aslam S, Javeed A, Mahmood AK, Waqas M. Study on haemoglycemic effects of xylazine, diazepam and ketamine in surgically treated dogs. *IOSR J Agric Vet Sci.* (2014) 7:16–9. doi: 10.9790/2380-07911619

74. Lim S-I, Xin L. γ-aminobutyric acid measurement in the human brain at 7 T: Short echo-time or Mescher–Garwood editing. *NMR Biomed.* (2022) 35:e4706. doi: 10.1002/nbm.4706

75. Chan KL, Hock A, Edden RAE, MacMillan EL, Henning A. Improved prospective frequency correction for macromolecule-suppressed GABA editing with metabolite cycling at 3T. *Magn Reson Med.* (2021) 86:2945–56. doi: 10.1002/mrm.28950

76. Mion G, Villevieille T. Ketamine pharmacology: an update (pharmacodynamics and molecular aspects, recent findings). *CNS Neurosci Ther.* (2013) 19:370–80. doi: 10.1111/cns.12099

77. Xue J-G, Masuoka T, Gong X-D, Chen K-S, Yanagawa Y, Law SKA, et al. NMDA receptor activation enhances inhibitory GABAergic transmission onto hippocampal pyramidal neurons via presynaptic and postsynaptic mechanisms. *J Neurophysiol.* (2011) 105:2897–906. doi: 10.1152/jn.00287.2010

78. Hattingen E, Lückerath C, Pellikan S, Vronski D, Roth C, Knake S, et al. Frontal and thalamic changes of GABA concentration indicate dysfunction of thalamofrontal networks in juvenile myoclonic epilepsy. *Epilepsia.* (2014) 55:1030–7. doi: 10.1111/epi.12656

79. Kuzniecky R, Ho S, Pan J, Martin R, Gilliam F, Faught E, et al. Modulation of cerebral GABA by topiramate, lamotrigine, and gabapentin in healthy adults. *Neurology.* (2002) 58:368–72. doi: 10.1212/WNL.58.3.368

80. Wakasugi M, Hirota K, Roth SH, Ito Y. The effects of general anesthetics on excitatory and inhibitory synaptic transmission in area CA1 of the rat hippocampus in vitro. *Anesth Analg.* (1999) 88:676–80. doi: 10.1097/00000539-199903000-00039

81. Shih Y-Y, Büchert M, Chung H-W, Hennig J, von Elverfeldt D. Vitamin C estimation with standard 1H spectroscopy using a clinical 3T MR system: detectability and reliability within the human brain. *J Magn Reson Imag.* (2008) 28:351–8. doi: 10.1002/jmri.21466

82. Rice ME. Ascorbate regulation and its neuroprotective role in the brain. *Trends Neurosci.* (2000) 23:209–16. doi: 10.1016/S0166-2236(99)01543-X

83. O'Neill RD, Fillenz M, Sundstrom L, Rawlins JN. Voltammetrically monitored brain ascorbate as an index of excitatory amino acid release in the unrestrained rat. *Neurosci Lett.* (1984) 52:227–33. doi: 10.1016/0304-3940(84)90166-6

84. Cammack J, Ghasemzadeh B, Adams RN. The pharmacological profile of glutamate-evoked ascorbic acid efflux measured by *in vivo* electrochemistry. *Brain Res.* (1991) 565:17–22. doi: 10.1016/0006-8993(91)91731-F

85. Elsa A, Ubandawaki S. Ketamine anaesthesia following premedication of rabbits with vitamin C. *J Vet Sci.* (2005) 6:239–41. doi: 10.4142/jvs.2005.6.3.239

86. Sawicka-Glazer E, Czuczwar SJ. Vitamin C: a new auxiliary treatment of epilepsy? *Pharmacol Rep.* (2014) 66:529–33. doi: 10.1016/j.pharep.2014.02.016

87. Makaryus R, Lee H, Yu M, Zhang S, Smith SD, Rebecchi M, et al. The metabolomic profile during isoflurane anesthesia differs from propofol anesthesia in the live rodent brain. *J Cerebral Blood Flow Metabol.* (2011) 31:1432–42. doi: 10.1038/jcbfm.2011.1

88. Arenillas M, Canfrán S, Aguado D, Gómez de Segura IA. Sedative and analgesic effects of two subanaesthetic doses of ketamine in combination with methadone and a low dose of dexmedetomidine in healthy dogs. *Vet Anaesth Analg.* (2021) 48:545–53. doi: 10.1016/j.vaa.2020.11.010

89. Wan X, Liu L, Wang W, Tan Q, Su X, Zhang S, et al. 1H-MRS reveals metabolic alterations in generalized tonic-clonic seizures before and after treatment. *Acta Neurol Scand.* (2022) 145:200–7. doi: 10.1111/ane.13534

90. Petroff OAC, Rothman DL, Behar KL, Hyder F, Mattson RH. Effects of valproate and other antiepileptic drugs on brain glutamate, glutamine, and GABA in patients with refractory complex partial seizures. *Seizure.* (1999) 8:120–7. doi: 10.1053/seiz.1999.0267

91. Bernasconi A, Bernasconi N, Natsume J, Antel SB, Andermann F, Arnold DL. Magnetic resonance spectroscopy and imaging of the thalamus in idiopathic generalized epilepsy. *Brain.* (2003) 126:2447–54. doi: 10.1093/brain/awg249

92. Nagendran A, McConnell JF, De Risio L, José-López R, Quintana RG, Robinson K, et al. Peri-ictal *Magn Reson* imaging characteristics in dogs with suspected idiopathic epilepsy. *J Vet Intern Med.* (2021) 35:1008–17. doi: 10.1111/jvim.16058

93. Sauer-Delhées S, Steffen F, Reichler I, Beckmann K. [Clinical characteristics of Idiopathic Epilepsy in Greater Swiss Mountain Dogs in Switzerland]. *Schweizer Archiv für Tierheilkunde.* (2020) 162:697–706. doi: 10.17236/sat00279

94. Santifort KM, Bertijn E, Bhatti SFM, Leegwater P, Fischer A, Mandigers PJJ. Phenotypic characterization of idiopathic epilepsy in border collies. *Front Vet Sci.* (2022) 9:455. doi: 10.3389/fvets.2022.880318

95. Hu W, Zhang M, Czéh B, Flügge G, Zhang W. Stress impairs GABAergic network function in the hippocampus by activating nongenomic glucocorticoid receptors and affecting the integrity of the parvalbumin-expressing neuronal network. *Neuropsychopharmacology.* (2010) 35:1693–707. doi: 10.1038/npp.2010.31

96. Döring D, Roscher A, Scheipl F, Küchenhoff H, Erhard MH. Fear-related behaviour of dogs in veterinary practice. *Vet J.* (2009) 182:38–43. doi: 10.1016/j.tvjl.2008.05.006